Thermodynamics and life

Past, Present and Future of the use of energy by living beings

Alfonso Delgado Bonal

Instituto de Física Fundamental y Matemáticas
Universidad de Salamanca

A thesis submitted for the degree of
Doctor of Philosophy

July 2015

Abstract

Life emerged on Earth more than 3.5 Gyr ago and it has been using energy ever since. The purpose of this thesis is to study several aspects of the relationship between energy and life. First, I start with the analysis of the nitrogen requirements of life in the Early Earth, and conclude that life was not able to produce enough biological nitrogen by itself, meaning that other sources of energy were required by the time. In the course of evolution, life developed the ability to use the solar energy that reached the surface of our planet, and its use modified not only the evolution of the living beings but also the evolution of the atmosphere. The changes in the atmosphere were followed by changes in the maximum efficiency in the energy obtainable from solar radiation. On a different aspect, it is believed that Mars was inside the so-called habitable zone once, where liquid water exists and the conditions are suitable for life, but now the environment is dry and harsh. Despite the fact that we have not found life so far in the planet, a biosphere might be living beneath the regolith and chemolithotrophic organisms could be using chemical energy to survive in the current martian environment. I analyse the energetic features of the present day near-surface martian atmosphere using the state-of-the-art knowledge of the thermodynamic variables nowadays, provided by rovers and satellites. As many of those spacecrafts are powered with solar energy, the knowledge of the maximum obtainable work of solar cells in the environment of Mars is extremely important for the future of exploration and colonization of the planet. I provide clues on the maximum efficiency of solar radiation in the planet under different conditions.

Thermodynamics and life

Past, Present and Future of the use of energy by living beings

Alfonso Delgado Bonal

Instituto de Física Fundamental y Matemáticas

Universidad de Salamanca

Advisor: F. Javier Martín Torres

Consejo Superior de Investigaciones Científicas

A thesis submitted for the degree of

Doctor of Philosophy

July 2015

To my beautiful wife.

Acknowledgements

During the time of this thesis work "I've ... seen things you people wouldn't believe ...". I have swam with sharks in the Pacific Ocean, I have being inside of meteoritic craters and I have seen the most beautiful northern lights. "All those ... moments ... will be lost in time", but the science will stay.

In this thesis work I had the chance to play in the same playground than Boltzmann, Wien and Planck, and humbly contribute to the building of science. We rediscovered forgotten ideas, prove new laws and even found new natural constants. For all of that, I am extremely grateful to my advisor, Prof. F. Javier Martín-Torres, who gave me the chance to develop ideas *in the edge of knowledge* and encouraged me to continue doing it in the future.

I am also in deep debt with my girlfriend, who became my wife in the course of this work. Her support, her blind faith in my skills and our scientific discussions have being crucial in the development of this volume.

Durante el transcurso de esta tesis, "Yo ... he visto cosas que vosotros no creeríais ...". He nadado con tiburones en el Océano Pacífico, he estado dentro de cráteres de meteoritos y he visto auroras boreales increíbles. "Todos esos ... momentos ... se perderán en el tiempo", pero la ciencia perdurará.

En esta tesis doctoral he tenido la oportunidad de trabajar con las mismas ideas que Boltzmann, Wien y Planck, y humildemente contribuir al edificio de la ciencia. Hemos redescubierto ideas olvidadas, demostrado nuevas leyes e incluso encontrado nuevas constantes de la naturaleza. Por todo ello, estoy extremadamente agradecido a mi supervisor, Prof. F. Javier Martín-Torres, quien me dio la oportunidad de desarrollar ideas *en el borde del conocimiento* y me animó a continuar haciéndolo en el futuro.

También estoy en deuda con mi novia, quien se convirtió en mi mujer en el transcurso de esta tesis. Su apoyo, su fé ciega en mis habilidades y nuestras discusiones científicas han sido cruciales para el desarrollo de este volumen.

Abstract

Life emerged on Earth more than 3.5 Gyr ago and it has been using energy ever since. The purpose of this thesis is to study several aspects of the relationship between energy and life. First, I start with the analysis of the nitrogen requirements of life in the Early Earth, and conclude that life was not able to produce enough biological nitrogen by itself, meaning that other sources of energy were required by the time. In the course of evolution, life developed the ability to use the solar energy that reached the surface of our planet, and its use modified not only the evolution of the living beings but also the evolution of the atmosphere. The changes in the atmosphere were followed by changes in the maximum efficiency in the energy obtainable from solar radiation. On a different aspect, it is believed that Mars was inside the so-called habitable zone once, where liquid water exists and the conditions are suitable for life, but now the environment is dry and harsh. Despite the fact that we have not found life so far in the planet, a biosphere might be living beneath the regolith and chemolithotrophic organisms could be using chemical energy to survive in the current martian environment. I analyse the energetic features of the present day near-surface martian atmosphere using the state-of-the-art knowledge of the thermodynamic variables nowadays, provided by rovers and satellites. As many of those spacecrafts are powered with solar energy, the knowledge of the maximum obtainable work of solar cells in the environment of Mars is extremely important for the future of exploration and colonization of the planet. I provide clues on the maximum efficiency of solar radiation in the planet under different conditions.

Contents

1 Introducción

Aunque por la natural envidia de los hombres haya sido siempre tan peligroso descubrir nuevos y originales procedimientos como mares y tierras desconocidos, por ser más fácil y pronta la censura que el aplauso para los actos ajenos, sin embargo, dominándome el deseo que siempre tuve de ejecutar sin consideración alguna lo que juzgo de común beneficio, he determinado entrar por vía que, no seguida por nadie hasta ahora, me será difícil y trabajosa; pero creo me proporcione la estimación de los que benignamente aprecien mi tarea.

Y si la pobreza de mi ingenio, mi escasa experiencia de las cosas presentes y las incompletas noticias de las antiguas hacen esta tentativa defectuosa y de no de gran utilidad, al menos enseñaré el camino a alguno que, con más talento, instrucción y juicio realice lo que ahora intento, por lo cual si no consigo elogio, tampoco mereceré censura.

Nicolás Maquiavelo

Discursos sobre la primera década de Tito Livio.

Las evidencias de vida en nuestro planeta se remontan a hace más de 3500 millones de años, aunque hay indicios de que los primeros organismos habitaban nuestro planeta incluso antes, hace unos 3800 millones de años. Teniendo en cuenta que la Tierra se formó hace aproximadamente 4500 millones de años, en escalas geológicas la vida apareció en la Tierra poco después de su formación.

Los seres vivos han evolucionado en nuestro planeta desde entonces, utilizando diferentes mecanismos para la obtención de energía y modificando el entorno en mayor o menor medida. La energía química fue la primera fuente de energía utilizada por los seres vivos en nuestro planeta (organismos quimiolitoautótrofos). Desde la aparición de la vida en nuestro planeta hasta hace aproximadamente 2500 millones de años, los organismos obtenían energía de compuestos químicos y dependían por tanto de su abundancia. La expansión de la vida estaba limitada por la composición de nuestro planeta y su atmósfera. En particular, el crecimiento y expansión de los seres vivos estaba limitado por la cantidad de nitrógeno disponible[1]. En la Tierra primitiva, la composición atmosférica era principalmente nitrógeno, en una concentración de más del 99 %, y había poca disponibilidad de compuestos nitrogenados en la litosfera. El nitrógeno disponible en la atmósfera se encuentra mayoritariamente en la forma de nitrógeno molecular, N_2. Este nitrógeno tiene que convertirse a otras formas nitrogenadas por procesos de fijación del nitrógeno, antes de poder ser utilizado directamente por los seres vivos.

Aunque hoy en día la mayor parte del nitrógeno se fija por una gran variedad de organismos, en la Tierra primitiva no era así. Los únicos seres vivos capaces de fijar nitrógeno eran organismos libres, cuya capacidad de fijación de nitrógeno era muy limitada. Hoy en día, gracias a la simbiosis entre organismos, la capacidad de fijación ha aumentado, sobrepasando la capacidad de fijación abiótica.

[1] **A Mathematic Approach to Nitrogen Fixation Through Earth History**, A. Delgado-Bonal and F. J. Martín-Torres, 2013, in: The Early Evolution of the Atmospheres of Terrestrial Planets, Springer, Vol. 35, pp. 23-31. doi: 10.1007/978-1-4614-5191-4_3

En la Tierra primitiva, los procesos abióticos de fijación de nitrógeno eran esenciales para el mantenimiento de la vida. Procesos altamente energéticos como los rayos en las tormentas o las erupciones volcánicas pueden romper la molécula de nitrógeno, que se recombina con otras especies químicas formando compuestos nitrogenados útiles para la vida.

Desde la aparición de la vida hasta la explosión del Cámbrico, hace unos 542 millones de años, la vida era microbiana. La falta de nitrógeno útil limitó considerablemente su expansión, ya que como veremos en el **Capítulo 2**, los seres vivos no eran capaces de automantenerse y eran dependientes de la fijación de nitrógeno abiótica. Esta situación cambió hace aproximadamente 2500 millones de años con la aparición de un nuevo mecanismo para utilizar la energía solar: la fotosíntesis. La capacidad de utilizar la energía solar, la mayor fuente de energía disponible en nuestro planeta, permitió la evolución de los seres vivos y su expansión en nuestro planeta. El uso de nuevos procesos de utilización de la energía dio lugar a nuevos productos liberados a la atmósfera.

El cambio en la composición atmosférica cambió la radiación que llega a la superficie de la Tierra. Durante su paso por la atmósfera, la radiación interacciona con sus componentes, disminuye su intensidad y cambia su distribución. Como cualquier otro sistema termodinámico, la radiación contiene energía y entropía. La radiación interacciona con la materia en procesos irreversibles aumentando su entropía. Cuando aumentan los procesos irreversibles, aumenta la entropía del sistema, disminuyendo la capacidad de realizar trabajo, la exergía. En el **Capítulo 3** expongo las bases termodinámicas del análisis de la entropía y la exergía de la radiación[2]. En dicho capítulo, examino las bases teóricas necesarias para el cálculo de la exergía de la radiación. El enfoque propuesto permite calcular el valor de la eficiencia de la radiación en la superficie y determinar el cambio en la atmósfera a distintas alturas. En muchos trabajos previos se considera incorrectamente que la eficiencia máxima viene determinada por

[2]**Maximum obtainable work from solar energy in the atmosphere**, A. Delgado-Bonal and F. J. Martín-Torres, 2015, Submitted to Solar Energy

un ciclo de Carnot. Sin embargo, al ser el sistema irreversible, el análisis de la eficiencia máxima debe hacerse estudiando el comportamiento de la entropía en nuestra atmósfera.

La exergía de la radiación depende de la temperatura del ambiente, y decrece conforme aumenta la longitud de onda, como consecuencia del aumento de la entropía. En este capítulo muestro que las formulaciones usadas en trabajos anteriores sobreestiman el valor de la exergía hasta en un 10 %. Los resultados obtenidos son importantes para determinar la máxima eficiencia teórica de los paneles solares en la superficie de la Tierra, y muestran el camino a seguir a la hora de determinar estas eficiencias en otros ambientes. El conocimiento de la eficiencia de la energía solar es útil para el diseño de satélites y la fabricación de paneles solares para la superficie de la Tierra. También determina el rendimiento máximo de la fotosíntesis en distintos ambientes o en otros planetas.

Las condiciones actuales de radiación de la superficie de Marte son poco propicias para la existencia de vida en la superficie del planeta. Es más probable que, de existir vida en el planeta, ésta esté en la subsuperficie y utilice energía química al igual que la vida en nuestro planeta en las primeras etapas. La atmósfera de Marte es más tenue que la atmósfera de la Tierra, aproximadamente mil veces menos densa y con menos variedad de compuestos. El análisis de la energía química disponible en la atmósfera que podría ser utilizada por seres vivos se puede determinar calculando la energía útil, mediante la energía libre de Gibbs. La energía útil - exergía en un sistema de radiación y energía libre de Gibbs en un sistema químico - determina el máximo de energía que se puede obtener del sistema desde el punto de vista termodinámico. El análisis de la energía de Gibbs de la atmósfera de Marte se detalla en el **Capítulo 4**. Aunque este tipo de análisis se ha llevado a cabo para condiciones diferentes a las condiciones estándar, es frecuente ver cálculos que no tienen en cuenta las variaciones de la presión y la temperatura. Las ecuaciones necesarias para determinar la energía libre de Gibbs se detallan en este capítulo, y posteriormente

se aplican a la atmósfera de Marte como ejemplo de aplicación[3].

Utilizando un modelo fotoquímico de la atmósfera de Marte que ha demostrado ser representativo de las condiciones actuales, he determinado la energía de Gibbs liberada por las reacciones relevantes en la atmósfera de Marte cerca de la superficie. Esta energía de Gibbs podría ser utilizada por organismos quimiolitoautótrofos, capaces de utilizar compuestos químicos para obtener energía y utilizarla en el metabolismo respiratorio. Sin embargo, para poder mantener una biosfera, no es suficiente con que exista energía en el sistema, es necesario además que el sistema no esté en equilibrio. En nuestra atmósfera, por ejemplo, la composición química no está en equilibrio como consecuencia entre otras cosas de la liberación de oxígeno por los organismos fotosintéticos. Se ha sugerido que este desequilibrio, llamado en este caso desequilibrio químico, es necesario para poder mantener organismos vivos en un sistema. En un sistema en desequilibrio es posible crear y mantener estructuras complejas emergentes. Esta línea de pensamiento, iniciada por Ilya Prigogine, se ha estudiado en relación al origen de la vida en la Tierra, y se ha concluido que el desequilibrio es una situación necesaria. En el **Capítulo 5** determino el desequilibrio de la atmósfera de Marte utilizando el modelo fotoquímico detallado en el capítulo anterior. Para calcularlo, analizo la producción de entropía por reacciones químicas en la atmósfera de Marte y lo comparo con valores obtenidos para la Tierra. Concluyo que la producción de entropía en Marte es mucho menor que la producida en la Tierra como consecuencia de la baja densidad y la pobre variedad de especies químicas de la atmósfera marciana.

Si se necesita desequilibrio para crear y mantener estructuras complejas en un sistema, en este capítulo concluyo que las reacciones químicas en la atmósfera de Marte cerca de la superficie no permiten mantener grandes estructuras

[3]**General equation of the Gibbs free energy and application to present day Mars**, A. Delgado-Bonal, P. Valentín-Serrano, M.-P. Zorzano and F. J. Martín-Torres, 2015, Submitted to Journal of Geophysical Research

físico-químicas como las creadas en Tierra[4].

Como se ha comentado antes, hoy en día se considera poco probable encontrar vida en la superficie de Marte. La atmósfera del planeta es tan tenue que la radiación no es absorbida igual que en la atmósfera de la Tierra. En la Tierra, por ejemplo, el ozono de nuestra atmósfera impide que gran parte de la radiación ultravioleta llegue a la superficie, permitiendo así la existencia de vida en la superficie. Esta radiación ultravioleta, altamente energética, puede impedir algunas funciones biológicas de organismos vivos e incluso destruirlos. La cantidad de ozono en Marte es mucho menor que la que encontramos en nuestro planeta y la radiación llega a la superficie, creando un panorama inhóspito para los posibles seres vivos.

El conocimiento de la radiación que llega a lo alto de la atmósfera es esencial para determinar la radiación que llega a la superficie del planeta o para conocer cómo se comporta la fotoquímica de la atmósfera. En la Tierra disponemos de satélites orbitando nuestra atmósfera y medidores en la superficie que nos permiten conocer los valores de la radiación día a día. Para Marte, sin embargo, éste no es el caso. Hoy en día no existen satélites midiendo la radiación que llega al planeta, limitando el conocimiento que se puede obtener sobre el planeta.

Para solventar en la medida de lo posible este problema, en el **Capítulo 6** presento una base de datos con los valores de la radiación que llega a la parte superior de la atmósfera de Marte en el rango entre 10 y 420 nm. Esta base de datos está basada en los valores de la radiación que llega a la Tierra medida desde satélite, y permite conocer una estimación de la radiación que llega a Marte día a día.

Esta base de datos es útil para análisis de la atmósfera de Marte y para estudios de habitabilidad del planeta. Por ejemplo, utilizando nuestra base de datos y conociendo la radiación que hay en la superficie medida con instrumentos in-situ, es posible determinar la opacidad de la atmósfera.

[4]**Evaluation of the Mars atmospheric chemical entropy production**, A. Delgado-Bonal and F. J. Martín-Torres, 2015, Entropy, Vol. 17, pp. 5047-5062. doi:10.3390/e17075047

Con esta base de datos se pretende proporcionar una herramienta más exacta que los medios actualmente disponibles. En general, hoy en día se recurre a espectros solares genéricos que son extrapolados geométricamente a la posición de Marte. Comparando nuestra base de datos con los espectros genéricos vemos que, si bien la forma es similar, la irradiancia en algunas longitudes de onda cambia sustancialmente con la etapa del ciclo solar[5].

La radiación ultravioleta que llega a la superficie impide que la vida tal y como la conocemos en la Tierra sobreviva en la superficie marciana. Sin embargo, dicha radiación podría ser utilizada para la exploración y colonización del planeta mediante el uso de paneles solares. Los paneles solares disponibles en la actualidad no están optimizados para el uso de la radiación ultravioleta porque esta radiación es bloqueada por la atmósfera de nuestro planeta. Sin embargo, la radiación ultravioleta (más energética que la radiación en el visible) ofrece una gran alternativa para la futura exploración y colonización de Marte.

Los paneles solares que se utilizan en la Tierra para producir energía no contaminante han sido utilizados para la exploración espacial con muy buenos resultados. En concreto para Marte, los paneles solares se han utilizado como fuente de energía desde las Vikings en los 70. Su uso ha permitido, por ejemplo, las operaciones del Spirit MER-A, prolongándose más de una década cuando esta tesis se está redactando.

A pesar de ello, el uso de paneles solares en Marte se ha visto limitado por el bajo rendimiento de la transformación de la energía. Los instrumentos que se mandan en las misiones espaciales requieren cada vez más energía y el tamaño de los paneles solares necesarios es demasiado como para poder ser considerado. Por ello, en la última misión in-situ de la NASA, Mars Science Laboratory, la fuente de energía seleccionada ha sido energía nuclear.

[5]**Martian Top of the Atmosphere 10-to 420 nm spectral irradiance database and forecast for solar cycle 24**, A. Delgado-Bonal, M.-P Zorzano and F. J. Martín-Torres, 2015, Submitted to Solar Energy

Aunque esta alternativa es viable para una misión espacial no es una solución realista si se pretende colonizar Marte. En ese caso, se necesitaría una fuente de energía no contaminante e ilimitada y la mejor opción son paneles solares. La eficiencia de un panel solar viene determinada entre otras cosas por la temperatura a la que se encuentra el panel[6]. Para determinar esta temperatura se han propuesto varias ecuaciones generales y varias simplificaciones que dependen principalmente de la radiación que llega al panel. Estas aproximaciones son útiles para la Tierra, pero pueden no serlo para otros entornos como Marte. En el **Capítulo 7** determino la temperatura de un panel solar en Marte, proporcionando una aproximación lineal que sólo depende de la radiación y de la velocidad del viento.

El principal problema del uso de paneles solares es su elevado coste y su baja eficiencia comparado con el uso de combustibles fósiles. Aunque la eficiencia de los paneles solares sigue aumentando cada día, todavía no son una alternativa completa a las energías no renovables. Una vez conocida la temperatura de operación del panel solar, el rendimiento de la transformación se determina mediante el análisis de la exergía, el trabajo máximo que podemos obtener. Este trabajo máximo depende de la radiación incidente, pero es importante tener en cuenta que también depende de las condiciones ambientales del ambiente donde se encuentra el panel. El análisis de la eficiencia se conoce como análisis de la segunda ley y se ha llevado a cabo en la Tierra para determinar qué lugares tienen las mejores condiciones meteorológicas para situar paneles solares. De este modo, algunos países donde las condiciones de radiación solar son idóneas para la transformación han conseguido aumentar la eficiencia termodinámica de la transformación.

Este análisis, realizado en numerosas ocasiones para la Tierra, no se ha llevado a cabo en Marte hasta ahora. En el **Capítulo 8** calculo el valor de la exergía en Marte utilizando datos de satélites y vehículos rover. Demuestro que

[6]**Solar Cell Temperature on Mars**, A. Delgado-Bonal and F. J. Martín-Torres, 2015, Solar Energy, Vol. 118, pp. 74-79. doi:10.1016/j.solener.2015.04.035

la eficiencia termodinámica es muy baja como consecuencia de la baja densidad de la atmósfera.

Otra energía renovable que se utiliza en la Tierra es la energía eólica. En este capítulo analizo la eficiencia de la energía eólica en Marte y comparo su producción con la de la Tierra. Una vez más como consecuencia de la baja densidad de la atmósfera, vemos que la producción de energía eólica en Marte no es una alternativa real[7].

[7] **Solar exergy and wind energy on Mars**, A. Delgado-Bonal and F. J. Martín-Torres, 2015, Submitted to Energy

1 Introduction

Although the envious nature of men, so prompt to blame and so slow to praise, makes the discovery and introduction of any new principles and systems as dangerous almost as the exploration of unknown seas and continents, yet, animated by that desire which impels me to do what may prove for the common benefit of all, I have resolved to open a new route, which has not yet been followed by any one, and may prove difficult and troublesome, but may also bring me some reward in the approbation of those who will kindly appreciate my efforts.

And if my poor talents, my little experience of the present and insufficient study of the past, should make the result of my labors defective and of little utility, I shall at least have shown the way to others, who will carry out my views with greater ability, eloquence, and judgment, so that if I do not merit praise, I ought at least not to incur censure.

Niccolo Machiavelli
Discourses on Livy.

Evidences of life on our planet date back to more than 3500 million years ago, although there are indications that the first organisms inhabited our planet even earlier, about 3800 million years ago. Given that the Earth was formed about 4500 million years ago, we can say that life appeared on Earth shortly after its formation in geological terms.

Living beings have evolved since then, using different mechanisms to obtain energy and modifying the environment. The chemical energy was the first source of energy used by organisms in our planet (chemolithotrophs organisms). Since the emergence of life in our planet until 2500 million years ago, they obtained energy from chemical compounds depending on its abundance. The expansion of life was limited by the composition of our planet and its atmosphere. In particular, the growth and expansion of the living beings was limited by the amount of available nitrogen[1]. The available nitrogen in the atmosphere is mostly in the form of molecular nitrogen, N_2. This nitrogen must be converted to other forms of nitrogen by nitrogen fixation processes before it can be used directly by living beings. In the early Earth, atmospheric composition was mostly nitrogen, at a concentration of more than 99%, and there was little availability of nitrogen compounds in the lithosphere.

Although today most of the nitrogen is fixed by a variety of organisms, on the early Earth it was not the case. The only living beings that were able to fix nitrogen were free organisms, whose nitrogen fixation capacity was very limited. Today, due to the symbiosis between organisms, the biological nitrogen fixation capacity has increased, surpassing the amount of abiotic fixation.

In the early Earth, abiotic nitrogen fixation processes were essential for the maintenance of life. Energetic processes such as lightning in storms or volcanic eruptions may break the nitrogen molecule, which was recombined with other chemical species forming nitrogen compounds useful for life.

[1] **A Mathematic Approach to Nitrogen Fixation Through Earth History**, A. Delgado-Bonal and F. J. Martín-Torres, 2013, in: The Early Evolution of the Atmospheres of Terrestrial Planets, Springer, Vol. 35, pp. 23-31. doi: 10.1007/978-1-4614-5191-4_3

Since the appearance of life to the Cambrian explosion about 542 million years ago, the only forms of life were microorganisms. The lack of usable nitrogen limited considerably its expansion of life, since as discussed in **Chapter 2**, living beings were not able to maintain itself and were dependent on the abiotic nitrogen fixation. This situation changed around 2500 million years ago with the emergence of a new mechanism that allowed the use of solar energy: the photosynthesis. The ability to use solar energy, the major source of energy available in our planet, enabled the evolution of living beings and their expansion in our planet. The use of new processes for the use of energy resulted in new products released into the atmosphere.

The change in the atmospheric composition affects the change in the radiation reaching the surface of the Earth. During its passage through the atmosphere, the radiation interacts with chemical compounds, reducing its intensity and changing its distribution. Radiation contains energy and entropy. During its interaction with matter increases its entropy in irreversible processes, reducing the ability to perform work, called exergy. In **Chapter 3**, I expose the thermodynamic basis of the analysis of entropy and exergy of radiation[2]. In this chapter, I examine the theoretical basis needed for the calculation of the availability of work from radiation. The proposed approach allows to calculate the value of the radiation efficiency on the surface and to determine its change in the atmosphere at different heights. Previous studies considered incorrectly that the maximum efficiency is determined by a Carnot cycle; however, as the processes in the system are irreversible, the maximum efficiency analysis should be done by studying the behavior of entropy in our atmosphere.

The exergy of radiation depends on the ambient temperature, and decreases with increasing wavelength, as a result of the increase of entropy. In this chapter 4 I show that the formulations used in previous studies overestimate the value of the availability up to 10%. The results are important in order to

[2]**Maximum obtainable work from solar energy in the atmosphere**, A. Delgado-Bonal and F. J. Martín-Torres, 2015, Submitted to Solar Energy

determine the theoretical maximum efficiency of solar panels on the surface of the Earth; and they are also useful to determine the efficiency of solar radiation in other environments, for the design of satellites, and for the manufacture of solar panels for the Earth's surface. It also determines the maximum yield of photosynthesis in different environments or in other planets.

The current conditions of radiation on Mars are hardly appropriate for the existence of life on the surface of the planet. It is more likely that if life exists on Mars, it is under the surface and using chemical energy, like life in our planet did in its early stages. The atmosphere of Mars is about a thousand times less dense than the atmosphere of the Earth and it contains less variety of compounds. The analysis of the chemical energy available in the atmosphere that could be used by living beings can be determined by calculating the useful energy through the available free energy. The maximum useful energy, so called exergy in a radiation system, and Gibbs free energy in a chemical system, determines the maximum power that can be obtained from the system from a thermodynamic point of view. The analysis of the Gibbs free energy of the atmosphere of Mars is detailed in **Chapter 4**, where the equations to determine the Gibbs free energy taking into account pressure and temperature dependence are described and applied to the Martian atmosphere.

Using a photochemical model of the atmosphere of Mars, we have determined the Gibbs free energy released by relevant chemical reactions in the atmosphere near the surface. This Gibbs free energy could be used by chemolithotroph organisms, capable of use chemicals to produce energy and use it in the respiratory metabolism[3]. However, to maintain a biosphere it is also necessary that the system is not in equilibrium. Our atmosphere, for example, is in chemical disequilibrium as a result of the release of oxygen by photosynthetic organisms. In **Chapter 5** I determine the disequilibrium of the

[3]**General equation of the Gibbs free energy and application to present day Mars**, A. Delgado-Bonal, P. Valentín-Serrano, M.-P. Zorzano and F. J. Martín-Torres, 2015, Submitted to Journal of Geophysical Research

atmosphere of Mars using the photochemical model detailed in the previous chapter. In order to calculate it, I analyse the entropy production by chemical reactions in the atmosphere of Mars and compare it with values obtained for the Earth. I conclude that the entropy production on Mars is much smaller than that produced on Earth as a result of the low density and small variety of species of the Martian atmosphere. If disequilibrium is a necessary condition to create and maintain complex structures in a system, the results in this chapter suggests that the chemical reactions in the atmosphere of Mars near the surface do not allow for large physicochemical structures as those created in Earth[4].

The knowledge of the radiation reaching the top of the atmosphere is essential to determine the radiation reaching the surface of the planet and to study the photochemistry of the atmosphere. On Earth, there are satellites orbiting our atmosphere and detectors on the surface that allow us to know the values of radiation every day. For Mars, however, this is not the case. Today there are no satellites measuring the radiation reaching the planet, limiting the knowledge that you can get on the planet's environment. To solve this problem as far as possible, I present in **Chapter 6** a database with the values of the radiation reaching the top of the Martian atmosphere in the range between 10 and 420 nm. This database is based on the values of the radiation reaching the Earth from satellite measurement, and provides an estimate of the radiation reaching Mars every day. This database is useful for the analysis of the Martian atmosphere and to study the habitability of the planet. For example, using our database and knowing the radiation in the surface measured with in-situ instruments, it is possible to determine the opacity of the atmosphere.

This database is intended to provide a more accurate tool than those currently available. Nowadays, generic solar spectra that are geometrically extrapolated to the position of Mars are used. Comparing our database with

[4]**Evaluation of the Mars atmospheric chemical entropy production**, A. Delgado-Bonal and F. J. Martín-Torres, 2015, Entropy, Vol. 17, pp. 5047-5062. doi:10.3390/e17075047

those generic spectra I find that although qualitatively they present a similar behaviour, the irradiance at some wavelengths changes substantially with the solar cycle[5].

The amount of ozone on Mars is much smaller than on Earth and the ultraviolet radiation reaches the surface preventing life as we know it on Earth, to survive on the Martian surface, as I mentioned before. However, this radiation could be used for the exploration and colonization of the planet by using solar panels. Solar panels currently available are not optimized for the use of ultraviolet radiation because this radiation is blocked by the atmosphere of our planet. However, the ultraviolet radiation (more energetic than visible radiation) provides a great alternative for future exploration and colonization of Mars. Solar panels are used on Earth to produce clean energy and they have been used for space exploration with very good results. Specifically for Mars, solar panels have been used as an energy source since the Vikings in the 70's. Its use has allowed, for example, the operations of the Spirit MER-A and lasted more than a decade when this thesis is written. However, the use of solar panels on Mars has been limited by the low yield of the transformation of energy. Instruments that are sent in space missions require ever more energy and the size of the required solar panels is too much to be considered. Therefore, in the last in-situ mission by NASA, the Mars Science Laboratory, the energy source selected has been nuclear energy. Although this alternative is viable for a space mission is not a realistic solution to colonize Mars. In that case, you need a source of clean and limitless energy and the best option so far is solar panels. The efficiency of a solar panel is determined among other things by the temperature of the panel. In order to determine this temperature, several general equations and simplifications have been proposed that rely primarily on the radiation reaching the panel. These approaches are useful for the Earth, but

[5]**Martian Top of the Atmosphere 10-to 420 nm spectral irradiance database and forecast for solar cycle 24**, A. Delgado-Bonal, M.-P Zorzano and F. J. Martín-Torres, 2015, Submitted to Solar Energy

may not be for other environments such as Mars. In **Chapter 7**, I determine the temperature of a solar panel on Mars, providing a linear approximation that depends only on the radiation flux and wind speed[6].

The main problem with the use of solar panels is their high cost and low efficiency compared to the use of fossil fuels. Although the efficiency of solar panels continues to increase every day, they are not yet a complete alternative to non-renewable energy. Once the operating temperature of the solar panel is known, the performance of the transformation is determined by analysing the exergy, the maximum work that we can get. This maximum work depends on the incident radiation, but it is important to note that it also depends on the environmental conditions where the panel is located. The efficiency analysis is known as the second law analysis and was carried out on Earth to determine which places have the best weather conditions to locate solar panels. Thus, some countries where solar radiation conditions are suitable for transformation, have managed to increase the thermodynamic efficiency of the transformation.

This analysis, carried out on numerous occasions to Earth, has not been done so far on Mars. In **Chapter 8**, I calculate the value of the exergy of radiation on Mars using data from satellites and rovers. I show that the thermodynamic efficiency is very low due to the low density of the atmosphere.

Another renewable energy used on Earth is wind energy. This chapter examines the efficiency and production of wind energy on Mars and compare it with that on Earth. Again due to the low density of the atmosphere, I show that the production of wind energy on Mars is not a real alternative[7].

[6]**Solar Cell Temperature on Mars**, A. Delgado-Bonal and F. J. Martín-Torres, 2015, Solar Energy, Vol. 118, pp. 74-79. doi:10.1016/j.solener.2015.04.035

[7]**Solar exergy and wind energy on Mars**, A. Delgado-Bonal and F. J. Martín-Torres, 2015, Submitted to Energy

2

A mathematic approach to nitrogen fixation through Earth history

El nitrógeno es esencial para la vida tal como la conocemos. La inmensa mayoría del nitrógeno en nuestro planeta se encuentra en forma de nitrógeno molecular, N_2, en la atmósfera, y no puede ser utilizado directamente por la mayor parte de los seres vivos. Para ser biológicamente útil ha de convertirse en otras formas nitrogenadas como NO_2 o NO_3 mediante procesos de fijación de nitrógeno. Dichos procesos pueden ser abióticos, mediante descargas eléctricas en la atmósfera por ejemplo, o biológicos, pero no todos los organismos tienen la capacidad de fijar nitrógeno.

Según los estudios filogenéticos, todos los organismos capaces de fijar nitrógeno son procariotas (bacterias y arqueas), lo que sugiere que la fijación de nitrógeno y la asimilación de amonio fueron características metabólicas del Ultimo Ancestro Común Universal (LUCA por sus siglas en inglés).

En la actualidad la cantidad de nitrógeno fijado biológicamente es de alrededor de 2×10^{13} g/año, una cantidad mucho mayor que la correspondiente a la de nitrógeno fijado abióticamente (entre 2.6×10^{9} y 3×10^{11} g/año). La cantidad actual de nitrógeno fijado es mucho mayor de lo que era en la Tierra antes de la explosión del Cámbrico, donde las asociaciones simbióticas con plantas leguminosas (la principal forma de fijación de nitrógeno en la actualidad) no existían y el nitrógeno se fijaba únicamente por los organismos libres como cianobacterias. Dado que el nitrógeno es esencial para la vida, estudios previos han sugerido que las fuentes abióticas de fijación de nitrógeno pudieron tener un papel importante en los primeros estadios de la evolución biológica, que provocó una presión de selección a favor de la evolución de nitrogenasa y un aumento en la tasa de fijación de nitrógeno. En el capítulo 2 se presenta un método para analizar la cantidad de nitrógeno fijado, tanto biótico y abiótico, a lo largo de la historia de la Tierra, y se concluye que las fuentes de fijación abióticas eran necesarias para poder mantener una biosfera como la que existía antes de la explosión del Cámbrico.

3

Maximum obtainable work from solar energy in the atmosphere

La radiación electromagnética contiene energía y entropía. Durante su viaje desde el Sol a la superficie de la Tierra la entropía del haz de radiación solar aumenta debido a procesos irreversibles en la atmósfera, tales como la dispersión y absorción. Este aumento de la entropía produce una disminución de la capacidad de producir trabajo.

La cantidad de energía que es útil para hacer trabajo se llama *exergía*. La evaluación de la exergía nos permite conocer el rendimiento máximo teórico de la transformación de energía solar por células fotovoltaicas por ejemplo. La revisión de los trabajos previos sobre el máximo rendimiento de la energía solar y el efecto del medio ambiente que he realizado durante el transcurso de esta tésis me han permitido constatar que se han venido utilizando conceptos erróneos y formulaciones incorrectas en el cálculo de la exergía. Aunque la exergía es un concepto que recuerda a la eficiencia de Carnot, la evaluación de la exergía de la radiación requiere la comprensión de la interacción entre la radiación y la materia en la atmósfera y no depende de la caracterización de la propia fuente.

En este capítulo calculo la exergía de la radiación siguiendo un procedimiento diferente al usado habitualmente. En lugar de determinar la exergía suponiendo una temperatura efectiva para el Sol, se calcula la radiación resolviendo la ecuación de transporte radiativo y usando datos de satélites. De este modo se obtienen valores de la exergía de la radiación a través de las diferentes capas de la atmósfera de la Tierra así como en la superficie mediante la integración línea a línea de la ecuación de la ecuación de transporte radiativo, y comparamos con los resultados anteriores. Para estimar el límite superior de la exergía de radiación calculamos la exergía en condiciones de cielo despejado. Los resultados muestran que los cálculos anteriores sobreestiman el valor de la exergía de la atmósfera entre un 2% y 10%. Esto tiene implicaciones para el estudio de las células solares y procesos atmosféricos.

Maximum obtainable work from solar energy in the atmosphere

Alfonso Delgado-Bonal[a,b,*], F. Javier Martín-Torres[b,c]

[a] *Institute of Fundamental Physics and Mathematics, University of Salamanca, Casas del Parque, 37008, Spain*
[b] *Division of Space Technology, Department of Computer Science, Electrical and Space Engineering, Luleå University of Technology, Kiruna, Sweden*
[c] *Instituto Andaluz de Ciencias de la Tierra (CSIC-UGR), Avda. de Las Palmeras n 4, Armilla, 18100, Granada, Spain*

Abstract

The electromagnetic radiation reaching our atmosphere carries out energy and entropy. During its travel from the Sun to the surface of the Earth the entropy of the radiation beam increases due to irreversible processes in the atmosphere such as scattering and absorption, and then decreases its availability to produce work. The amount of energy which is useful to do work is called exergy. In previous works about solar energy and its environmental effect, there are misconceptions and incorrect formulations regarding the calculation of exergy. Although exergy is a concept that reminds the Carnot efficiency idea, the evaluation of the exergy of radiation requires the understanding of the interaction between radiation and matter in the atmosphere and not the characterization of the source itself. We calculate the exergy of radiation through the different layers of the Earth's atmosphere by integrating line-by-line the radiative transfer equation, and compare with previous results. Here, we present calculations under clear sky conditions in order to estimate the maximum value of the exergy of radiation. Our results show that previous calculations overestimate the value of the exergy of the atmosphere between 2% and 10%. This has implications for the study of solar cells and atmospheric processes.

Keywords:
Spectral Exergy, Radiative transfer exergy, Exergy of radiation, Greenhouse

1. Introduction

The solar photons reaching the Earth carry out energy and entropy [1]. This idea was first proposed by the italian researcher Bartoli [2] when he was investigating the radiation pressure in vacuum. It was continued by Boltzmann and demonstrated by Planck, described in his classical work "The Theory of Heat Radiation" [3]. The increase in the entropy content of the radiation is directly correlated with an increase of the heat exchange with the environment, and then in a degradation of the energy to produce work. This availability is described by the concept of exergy (from the greek exo - $\varepsilon\xi o$ - and energia -$\varepsilon\nu\varepsilon\rho\gamma\iota\alpha$-). The exergy of a thermodynamic system is a measure of the potential work of the system [4]. For a detailed historic description of the exergy concept, refer to [Rezac and Metghalchi, 2004] [5].

It has been applied mainly in engineering thermodynamics, and resulted in a more effective method to analyze heat transfer than energy analysis [6]. In particular, the idea of exergy was also investigated in relation with solar radiation, proving to be a very successful area with theoretical and engineer applications. The early ideas of Petela and Spanner in 1964 [7] [8] started an ongoing research on the exergy of radiation, providing methods to evaluate the maximum conversion efficiency of solar radiation with different approaches, including direct and diffuse radiation, blackbody approximations, dilute radiation or semi transparent medium [9] [10] [11] [12]. Although Planck derived originally the expression for the radiation intensity for a monochromatic radiation beam at thermodynamic equilibrium, it has been demonstrated to hold for non blackbody radiation at a non equilibrium condition as well [13] [14] [15] [16].

Most of these works deal with the maximum of "useful" energy that can be obtained from solar radiation considering Carnot efficiencies or ideal reversible machines, determining the efficiency by the ambient temperature. However, the evaluation of the exergy of solar radiation using the temperature of the surface of our planet is an approach that completely ignores the environment and all the processes in the atmosphere. The assumption that the temperature of a particular location is only determined by the radiation field is incorrect and completely ignores the irreversible processes which could increase the entropy of the radiation. Environments at the same temperature could have different values of the exergy of radiation. Although the determination of the efficiency using simplified formulations can be useful in determinate circumstances, it is not realistic in the determination of the exergy of radiation in the atmosphere. For example, clouds in the atmosphere could be blocking the direct solar radiation, independently of the surface temperature. Also, greenhouse effects caused by certain gases in the atmosphere create an increase of the temperature of the surface which is independent on the direct radiation beam.

In order to account for all these effects in the calculation of the exergy of radiation on Earth's atmosphere, some researchers have incorporated on their calculations some factors which include non blackbody radiation or diffuse beams. Nevertheless their calculation of the Earths radiation entropy flux was wrong,

*Phone: 0034958230000 - ext: 190209
Email address: alfonso.delgado-bonal@ltu.se (Alfonso Delgado-Bonal)

Nomenclature

c	speed of light in vacuum, ($\approx 2.99792458 \times 10^8$ m s^{-1})
Ex_ν	spectral radiation exergy intensity (W m^{-2} sr^{-1}Hz^{-1})
Ex_λ	spectral radiation exergy intensity (W m^{-2} nm^{-1})
h	Planck's constant ($\approx 6.626176 \times 10^{-34}$ J s)
k	Boltzmann constant ($\approx 1.3806488 \times 10^{-23}$ J K^{-1})
L_ν	spectral radiative intensity (W m^{-2} sr^{-1}Hz^{-1})
L_λ	spectral radiative intensity (W m^{-2} nm^{-1})
T	temperature (K)
T_0	temperature of the environment (K)
T_λ	spectral radiation temperature (K)
T_ν	spectral radiation temperature (K)
Tra_λ	transmission spectra (%)
S_ν	spectral entropy intensity (W m^{-2} sr^{-1}Hz^{-1} K^{-1})
S_λ	spectral entropy intensity (W m^{-2} nm^{-1} K^{-1})
W	work flux density (W m^{-2} sr)

Greek Symbols

η_ν	spectral quality factor
η	total quality factor
λ	wavelength (nm)
σ	Stefan constant ($\approx 5.670373 \times 10^{-8}$ W m^{-2} K^4)
ν	frequency (Hz)

as we explain in Section 3, and therefore the exergy of radiation.

In order ro compute the exergy of radiation in the atmosphere, instead of using the Carnot cycle approach, it is needed the the use of radiative transfer models and take into account the atmospheric composition and distribution [17]. With this in mind, we have determined which bands are carrying more exergy (or equivalently less entropy of radiation), and then the ability to obtain more useful work from a particular wavelength.

The Earth's atmosphere is a complex mixture of gases with characteristic temperature vertical profiles and molecular compositions that determine the intensity of the radiation that reaches the surface at each wavelength. The existence of ozone, for example, prevents high levels of UV radiation in the surface, but at the same time decreases the exergy of the total radiation. CO_2 in our atmosphere is believed to cause greenhouse effect, trapping the infrared radiation and heating the surface of our planet but is also responsible of the cooling rate in the mesosphere. It is well known that the temperature increase in the surface is not only determined by the incident radiation and, as a consequence, the estimations of solar exergy based on the temperature of a particular location can lead to wrong conclusions.

In this paper, we evaluate the exergy of radiation of the atmosphere at every altitude using a line-by-line radiative transfer code [18] [19] and considering clear sky conditions (and then the maximum obtainable work). The inclusion of other processes such as the existence of clouds will decrease the exergy of radiation. Then, in this paper, we estimate the upper level of obtainable exergy. Previous attempts to calculate the exergy of radiation in the atmosphere have been carried out considering the temperature profile of the atmosphere, without accounting for the spectral distribution of the exergy [20]. We will compare the exergy values considering the system as a Carnot cycle or reversible machine versus the accurate line-by-line radiative transfer approach, taking into account the spectral distribution of the radiation field in each layer of the atmosphere. In a recent manuscript the exergy of radiation is determined at surface [17], using generic spectra for the top of the atmosphere and surface, but this work is unable to determine the exergy of the atmosphere as function of altitude.

The knowledge of the exergy of radiation is nowadays a field of research for the improvement of photovoltaic cells design and estimate the maximum usable solar irradiation [20] [21]. Its determination for the different layers of the atmosphere will be of importance on the development of solar powered satellites for example or to obtain information about the irreversible processes in the atmosphere.

In Section 2, we explain the formalism used in this work to determine the exergy of radiation applying it to the particular case of the Earth's atmosphere. Currently, the value used in science and engineering studies to determine the availability of energy is the intensity of radiation. However, as it is clearly explained in the first law of thermodynamics, energy is divided into heat and work, and therefore the use of the intensity might not be accurate. The obtainable work is determined by the exergy of radiation [4]. The explanation of the formulation will make clear the concept of exergy and its usefulness. The logical path is: we determine the entropy of radiation, then the exergy of radiation via Legendre transformation; and the quality factor of the radiation. The explanation of the quality factor calculation is done in Section 3 in terms of obtainable work from a radiation field, using the most basic thermodynamic principles to clarify its meaning. Previous published calculations are sometimes not correct and/or unclear [17].

The evaluation of the exergy of radiation at each layer of the atmosphere is done in Section 4. Using a radiative transfer code [18] and an atmospheric profile [22] containing temperature, pressure and molecular composition, we can estimate the effect of molecular absorption in the atmosphere. We show the effect of the different molecules and layers and provide values of the quality factor of radiation for different altitudes.

In Section 5, we compare our results with those obtained using different formulations. The determination of the exergy with only the temperature is an oversimplification that might not be correct in some cases. We will show the differences in the calculations by considering a line-by-line radiative trans-

fer formalism for the determination of energy and entropy of radiation and considering only the environmental temperature without considerations of the processes involved.

Finally, in Section 6, we explain the differences in the various approaches by appealing to the irreversible processes and discuss the possibility of exergy lost by other interactions in the atmosphere. The importance of the atmospheric density or composition of a planetary atmosphere is discussed in terms of thermodynamics. The discussion is not limited to planetary atmospheres, and we expand it to other environments and provide some insights for the future work. In Section 7 we summarize the highlights of this investigation and future work.

2. Exergy of radiation calculations

Planck presented the expression of a blackbody and the entropy content of radiation as a function of frequency (or wavelength):

$$S_\nu = \frac{k\nu^2}{c^2}\left\{\left(1+\frac{c^2L_\nu}{h\nu^3}\right)\log\left(1+\frac{c^2L_\nu}{h\nu^3}\right)-\frac{c^2L_\nu}{h\nu^3}\log\frac{c^2L_\nu}{h\nu^3}\right\} \quad (1)$$

where L_ν is the so-called Planck's law:

$$L_\nu = \frac{h\nu^3}{c^2}\frac{1}{e^{\frac{h\nu}{kT}}-1} \quad (2)$$

Using these definitions, Candau [23] defined the spectral radiative exergy intensity (exergy of radiation) as:

$$Ex_\nu = L_\nu(T_\nu) - L_\nu(T_0) - T_0[S_\nu(T_\nu) - S_\nu(T_0)] \quad (3)$$

It is worth notice that in the original formulation by Planck, the intensity was denoted by the letter I instead of L, and entropy with letter L instead of S (other authors call K to the entropy). Their meanings should not be confused for the correct understanding of this paper. Exergy was recently used to analyze the terrestrial spectra by Chu and Liu [17] using a standard profile for atmospheric conditions and the radiative transfer code SMARTS (Simple Model of the Atmospheric Radiative Transfer of Sunshine), developed by Gueymard [24]. Liu and Chu [25] presented the radiative transfer equation for the exergy of radiation, although, to our knowledge, no attempts to solve it numerically have been made. The total exergy can be obtained by integrating Eq. 3 in wavelength:

$$\begin{aligned} Ex &= \int_0^{\inf} L_\nu(T_\nu) - L_\nu(T_0) - T_0[S_\nu(T_\nu) - S_\nu(T_0)]d\nu \\ &= \int_0^{\inf} Ex_\nu d\nu \end{aligned} \quad (4)$$

which, as was noticed by Candau, depends only on the spectral distribution of the radiating flux.

In Equation 4, some terms depends on the incident radiation (T_ν) and others on the environment radiation (T_0). The exergy is the obtainable work from the radiating flux emitted by a blackbody at temperature T_ν reaching a system at temperature T_0. In our atmosphere every layer has a temperature as well as the radiation beam that reaches them. It is important to notice that we are dealing with the radiating flux reaching the environment, and not with the temperature of the source, and considering the atmospheric emission as well.

To analyze the interaction of radiation-matter in the atmosphere, we have used the radiative transfer code FUTBOLIN (Full Transfer By Optimized LINe-by-line) [19] [18]. With this code we have determined the energy and entropy of radiation, and we have applied it to a clear sky CIRA (COSPAR International Reference Atmosphere) 30°N standard atmosphere[22]. FUTBOLIN solves the radiative transfer equation for each layer of the atmosphere and we can determine both the incoming radiation (downwelling) ($L_\nu(T_\nu)$ and $S_\nu(T_\nu)$) and the outgoing radiation (upwelling) values ($L_\nu(T_0)$ and $S_\nu(T_0)$).

In order to determine the downwelling radiation reaching the different layers of the atmosphere and the surface, we have calculated the transmittance spectra at different altitudes. The transmittance computed with FUTBOLIN is determined by the molecular absorption at each layer. FUTBOLIN uses the HITRAN [26] and GEISA [27] molecular databases for each molecule, providing very accurate values for the transmittance spectra.

The values of the transmittance at a given altitude depend on the atmospheric species at every wavelength in that particular altitude. It is defined as the fraction of incident radiation at an specific wavelength that passes through a media, in our case the atmosphere:

$$Tra_\lambda = \frac{L_\lambda}{L_{0,\lambda}} \quad (5)$$

From which we can obtain the downwelling radiation field reaching each layer of the atmosphere knowing the radiation field on the Top of the Atmosphere (TOA), as $L_\lambda = Tra_\lambda\, L_{0,\lambda}$.

The radiation field reaching the TOA changes every day, as depends on the Sun's atmosphere evolution. In this paper, we use the standard spectra 2000 ASTM (American Society for Testing and Materials) Standard Extraterrestrial Spectrum Reference E-490-00 [28] [17] [29], which provides the intensity values in the range [119.5 - 1000000] nm. ASTM E490 Air Mass Zero solar spectral irradiance is based on data from satellites, space shuttle missions, high-altitude aircraft, rocket soundings, ground-based solar telescopes, and modeled spectral irradiance.

Figure 1 shows the transmission spectra calculated with FUTBOLIN at the surface of the Earth. We have used most of the main radiatively active molecules in our atmosphere distributed in different concentrations and layers (CO_2, H_2O, O_3, CH_4, N_2O, CO, NO, NO_2 and HNO_3).

The radiation passes through the atmosphere and interacts with the atmospheric species (with different concentrations at every altitude). In the upper thermosphere, the density (ρ) is extremely low and the temperature (T) very high, being atomic oxygen, helium and hydrogen the dominant species. In the lower thermosphere, the turbulences mix nitrogen and oxygen, and below this layer is the mesosphere, the coldest region of the atmosphere. At the bottom of the mesosphere is the mesopause,

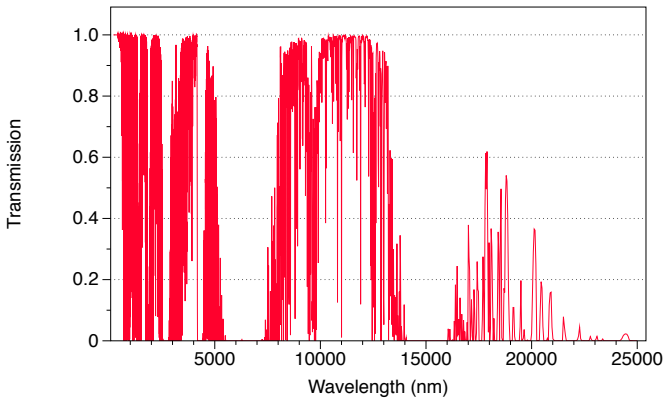

Figure 1: Simulated transmission spectra of Earth atmosphere

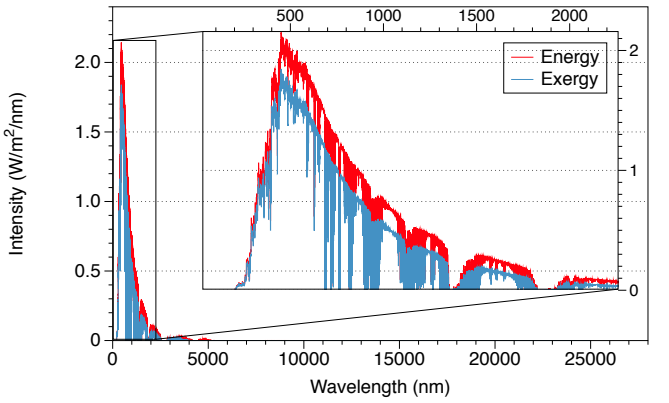

Figure 2: Simulated energy and exergy spectra at Earth's surface

and below is the stratosphere, where the ozone layer is located and most of the UV light is blocked. The lower part of the atmosphere, the troposphere, contains about 80% of the total density of the atmosphere, and its temperature in the lower part, the boundary layer, increases until 298 K approximately.

The interactions with matter increase the entropy of radiation and the environment properties have a capital effect on the exergy of radiation.

The energy and exergy spectra reaching the Earth's surface are shown in Figure 2. The entropy content is increasing in the atmosphere due to irreversible processes (molecular emission and absorption), becoming the exergetic potential less intense. The increase in entropy and the equivalent decrease in exergy is not distributed equally between all wavelengths. For engineer purposes, it might be important to know which bands are more exergetic instead of which bands are more energetic.

3. The Quality Factor

For the design of photovoltaic (PV) cells, researchers use generic spectra such as Guymard [28] to analyze the performance of the device, which provides the intensity of the band. However, the use of the exergy spectra should provide better results in the simulation of real processes.

The spectral energy quality factor can be defined as [17]:

$$\eta_\nu = \frac{Ex_\nu}{L_\nu(T_\nu)} \tag{6}$$

adn the total energy quality factor is given by $\eta = \frac{Ex}{L}$.

Using Equations 4 and 6 we can compute the exergy content of the radiation reaching the Earth surface. For the sake of simplicity we have compute η for clear sky conditions. Cloudy/aerosoles conditions will be the purpose of a future paper by the authors, although with the calculations provided in this work we give a value for the maximum efficiency. With our calculations, the exergy of radiation reaching the Earth's surface has a quality factor of $\eta = 0.869$, which means that the 86.9% of the downwelling radiation could be used to produce work.

These values are smaller than previous reported values, as we will see in Section 5. The reason is that for the first time we are quantifying the effect of irreversibilities in the atmosphere as a consequence of radiation-matter interaction. In our study, we are not considering scattering, which in any case will reduce the quality factor even more.

η is the quality factor in the downwelling radiation. Note that the denominator of Equation 6 is the downwelling radiation, i.e., for a situation where the source is at a higher temperature than the environment, $T > T_0$, it is constrained in the range [0-1]. At lower temperatures, when $T = T_0$, the value is zero, meaning that is not possible to obtain work from a source at the same temperature than the body, and for those cases when $T < T_0$, the values are bigger than one.

Note that the explanation in the last paragraph is refereed to the temperature of the source and we are dealing with the energy flux instead of the source.

In radiative transfer, is common to define the brightness temperature, the temperature that a blackbody should have to reproduce the observed intensity:

$$T_\lambda = \frac{hc}{k\lambda} \ln^{-1}\left(1 + \frac{2hc^2}{I_\lambda \lambda^5}\right) \tag{7}$$

This brightness temperature is dependent on wavelength. At some wavelengths, the equivalent source temperature will be greater than the environment temperature, but beyond some point, the temperature will be lower. In Figure 3 we represent the brightness temperature of the radiation after its pass through the atmosphere. For wavelengths greater than approximately 4150 nm, the temperature of the equivalent blackbody is lower than the temperature of the environment. Is therefore not possible to obtain work from those wavelengths, since our own environment is radiating more intensely at that wavelength. This is well known in engineering; when someone is dealing with infrared radiation measurements, it is necessary to refrigerate the detector in order to measure correctly.

There are some misconceptions about the exergy of radiation and the quality factor [11] [17]. It is clear from the expressions in Section 2 that the obtainable work depends on both the downwelling radiative flux and the upwelling radiation. The fact that we are trying to obtain work in an environment at temperature

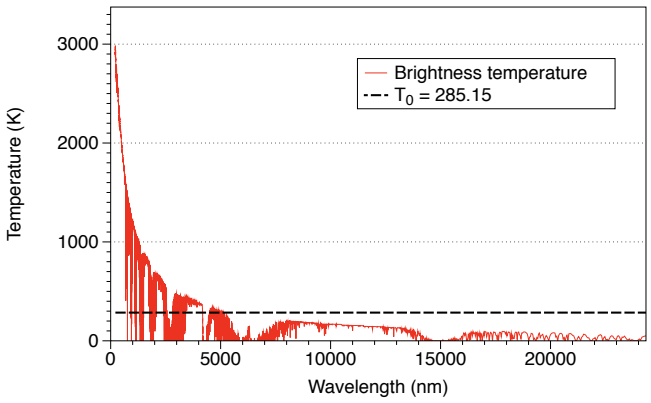

Figure 3: Brightness temperature of the radiation after its passage through the atmosphere. We have selected T_0 = 285.15 K as the Earth's temperature.

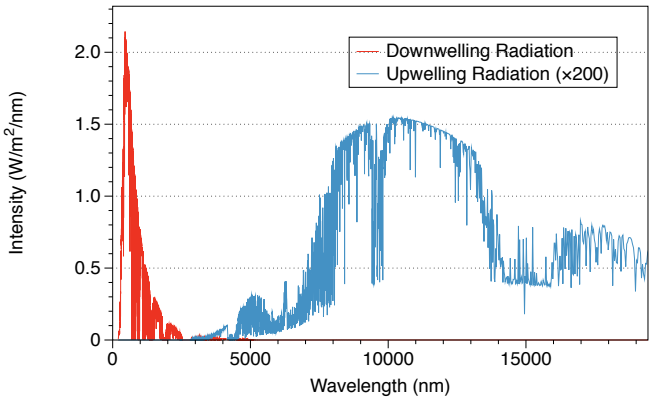

Figure 4: Downwelling and upwelling radiative fluxes. The upwelling flux is magnified 200 times for ilustrative purposes.

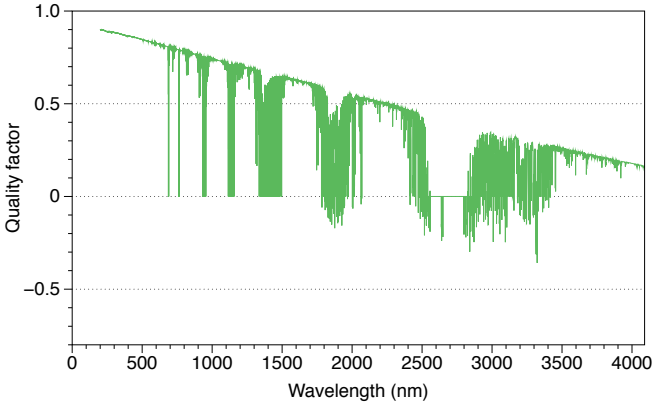

Figure 5: Wavelength dependence of the quality factor for the Earth environment at 285.15 K for [0-4000] nm.

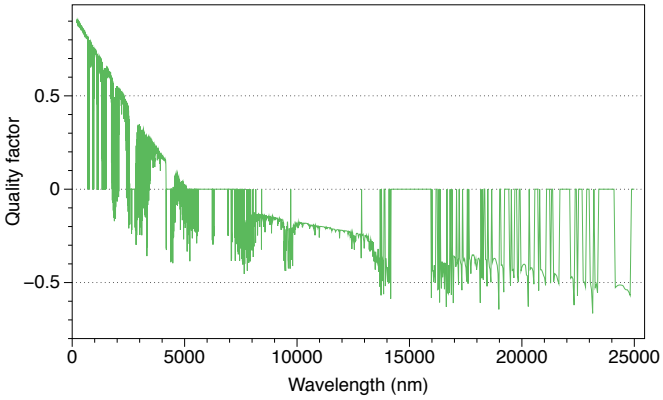

Figure 6: Wavelength dependence of the quality factor for the Earth environment at 285.15 K for [0-25000] nm.

T_0 from a body at temperature T (where T_0 < T) should not be forgiven. The Earth is emitting radiation itself as a consequence of its temperature. Therefore, in some bands that are completely blocked in our atmosphere, the only radiation that exists is the one from the planet. This means that the radiative downwelling flux is zero, but there is an existing radiative upwelling flux which is different to zero. In those cases, the total exergy as defined in Equation 3 is negative: we cannot obtain work in that wavelength, the Earth is giving out energy which could be used by a colder body to obtain work. The existence of negative values for the exergy of radiation is nothing else but thermodynamics. This situation mainly occurs in the infrared. As shown in Figure 4, the downwelling radiation is mainly distributed in ultraviolet and visible wavelengths, and the upwelling radiation lies in the infrared part of the spectra, with little mixing [30].

It is interesting to compute the quality factor for the total flux instead for the downwelling radiation. In early attempts [11] the conversion efficiency was calculated as the variation of work over the change in energy. In the atmospheric system the energy is determined by the downwelling and upwelling radiation, and the expression for the net quality factor is:

$$\eta = \frac{\Delta W}{\Delta U} = \frac{Exergy}{L_{downwelling} - L_{upwelling}} \tag{8}$$

In this case, the quality factor is restricted to the [-1,1] interval. Positive values determine the efficiency of the conversion of the downwelling radiation, and negative values express the fact that at those wavelengths is the environment who is giving out energy in the form of radiation, due to the fact that downwelling radiation is blocked in those wavelengths or because it is very low intense, as in the case of infrared radiation.

In Figure 5 we show the quality factor as a function of wavelength for the interval [0-4000] nm. In Figure 6, the same quality factor is represented in the [0-25000] nm range.

In both cases is possible to see a trend to the zero. The explanations in terms of thermodynamics is easy if we consider the origin of the radiation. The maximum of the solar radiation is in the visible spectral region, around 500 nm, where the value of the quality factor is near the unity. At higher wavelengths, in the infrared range, the emission from the Sun is not so high, and the obtainable work is less since that radiation is highly entropic. In Figure 3 is possible to see that about 4180 nm the brightness temperature is almost equal to the environment temperature, and therefore the quality factor should be zero, which

is verified in Figure 6.

In Chu and Liu [17], the quality factor of downwelling radiation is near the unity in all the spectra, and non-negative values are reported. However, using the same solar spectra, we find very different values. As an example of the inconsistency of previously published data, we explicitly evaluate the quality factor of solar radiation in the near infrared. Considering the very best case scenario, where all the radiation reaching the top of our atmosphere reaches the surface of the Earth (10.57 W m^{-2} μm^{-1} at 3.8 μm), and that the Earth is emitting at 288.1 K (which is the reference value in their paper), the quality factor of the downwelling radiation should be:

$$\begin{aligned}\eta_{3.8\mu m} =& \frac{L_\nu(T_\nu) - L_\nu(T_0) - T_0[S_\nu(T_\nu) - S_\nu(T_0)]}{L_\nu(T_\nu)} \\ =& \frac{10.57 - 0.257 - 288.1 \cdot (0.029471 - 0.000969)}{10.57} \\ =& 0.1988\end{aligned} \quad (9)$$

Which is very different to the value (0.92) of Chu and Liu [17]. The brightness temperature corresponding to that wavelength is about 300K, which is very close to the Earth temperature, and the quality factor is close to zero. At the environment temperature, the quality factor becomes zero as seen in the previous figures.

Due to the definition of exergy, it is not possible to quantify the exergy quality factor of the radiation that reaches the top of the atmosphere. The exergy concept is indeed the transfer of work between a source and an environment. Outside of our atmosphere, we cannot apply the concept of exergy, because the system is not properly defined by thermodynamics (absence of molecules). It is necessary an environment to be able to define the exergy. Chu and Liu [17] evaluate the exergy content of the Extraterrestrial radiation, and in the view of the authors, they refer with that to the exergy content that the radiation would have if it reaches the Earth's surface without passing through the atmosphere. However, the quality factor of that radiation also depends on the Earth's temperature and is not near to the unity for the whole spectra.

4. Degradation of radiation in the atmosphere

Solving the radiative transfer equation we are able to determine the exergy of radiation of the atmosphere at different altitudes and we can estimate the effect of the different atmospheric layers in the exergy of radiation.

When the radiation field interacts with the environment by molecular absorption, it suffers a "degradation", in the sense that the entropy of radiation increases in the process and the resulting radiation has less potential to do work.

The knowledge of the exergy of radiation at the surface is important for the future of the design of PV cells, but we should not forget that several satellites and spacecrafts are orbiting our Earth are using solar power, and the correct characterization of the exergy at different altitudes can help in the improvement of those areas of research.

The atmosphere is usually divided into different layers as a function of the sign of the temperature gradient. The thermosphere begins around 100 km above the Earth's surface, above the mesosphere and directly below the exosphere. Ultraviolet radiation ionize the molecules, and atmospheric particles become electrically charged. This layer is extremely dependent on solar activity, and the temperature in the thermosphere increases with altitude as a consequence of highly energetic solar radiation absorption. In the lower thermosphere, turbulences mixes the gases and the composition is mainly molecular oxygen (O_2) and nitrogen (N_2). At higher altitudes, the composition is dominated by atomic oxygen (O), helium (He), hydrogen (H), nitric oxide (NO) and carbon dioxide (CO_2). The quality factor of the downwelling radiation, i.e., exergy over downwelling intensity, at 100 km is $\eta = 0.8926 = 89.26\%$.

The mesosphere is located at heights between 50-100 km. The separation between thermosphere and mesosphere is called mesopause. In this region, due to the lack of solar heating and very strong radiative cooling from carbon dioxide, the temperature is as low as 130 K. In the mesosphere, temperature decreases with increasing altitude. The quality factor in this layer calculated at 50 km is $\eta = 0.8873 = 88.73\%$.

The stratosphere is situated between about 10-13 km and 50 km altitude above the surface. It is stratified in temperature, with warmer layers higher up and cooler layers farther down, in contrast to the troposphere. The border of the troposphere and stratosphere, the tropopause, is marked by where this inversion begins. The stratosphere is layered in temperature because ozone (O_3) in this layer absorbs UVB and UVC energy from the Sun and is broken down into atomic oxygen (O) and diatomic oxygen (O_2). The mid stratosphere has less UV light passing through it and O and O_2 are able to combine, and here is where the majority of natural ozone is produced. The lower stratosphere receives very low amounts of UVC, thus atomic oxygen is not found here and ozone is not formed. In this layer, the quality factor at 15 km is $\eta = 0.8828 = 88.28\%$.

The troposphere is the lowest portion of Earth's atmosphere. It contains approximately 80% of the atmosphere's mass and 99% of it is water vapor and aerosols. The average depth of the troposphere is approximately 17 km in the middle latitudes. The lowest part of the troposphere, where friction with the Earth's surface influences air flow, is called planetary boundary layer. This layer is typically a few hundred meters to 2 km deep. In the troposphere, temperature decreases with altitude until the tropopause. The chemical composition of the troposphere is essentially uniform, with the exception of water vapor. The proportion of water vapor is normally greatest near the surface and decreases with height. Nearly all of the water vapor and dust particles in the atmosphere are in the troposphere, and most clouds are found in this lowest layer. The troposphere is heated from below. Sunlight warms the ground and oceans which in turn radiates the heat into the atmosphere above it. The quality factor of the downwelling radiation at 5 km is $\eta = 0.8758 = 87.58\%$, and in the surface is $\eta = 0.8688 = 86.88\%$.

The effect of water vapor is the responsible of the large decrease in the efficiency. In Figure 7 we represent the tempera-

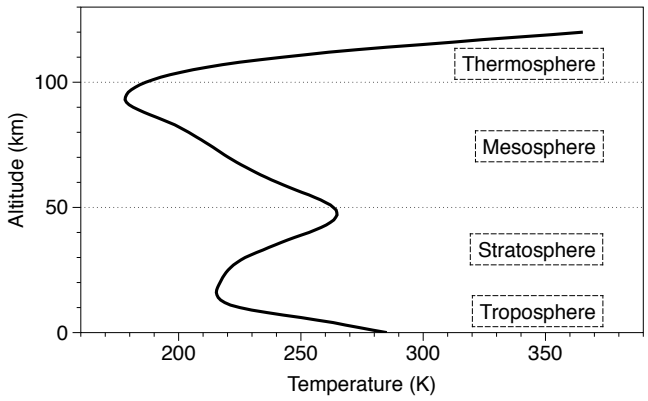

Figure 7: Temperature profile for Earth's atmosphere used in this study.

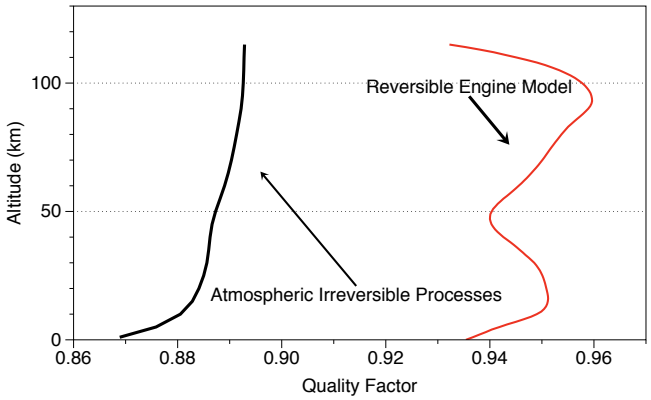

Figure 8: Radiation quality factor using a line-by-line radiative transfer code (black line) and using a reversible engine model (red line). The equation used to determine the reversible machine is the one proposed by Petela [7], listed in Table 1.

ture profile of the atmosphere and the different layers.

In Figure 8 we show the quality factor in the atmosphere using a radiative line-by-line code to calculate the exergy of radiation (black line) or using the equation that determines the exergy for a reversible engine that considers only the environment temperature (red line).

It is clear from the figure and the calculations that the exergy of radiation with the reversible engine model is only determined by the atmospheric temperature profile (see Figure 7), but the loss of exergy in the case of line-by-line radiative transfer is not. In that case, is the molecular composition of the environment along with the temperature that determines the quality factor. We conclude that it is the radiation-matter interaction, i.e., the irreversible processes, what determines the quality factor of the downwelling radiation and that the determination of the exergy by reversible approximations (only accounting for the temperature dependence) is not realistic.

5. Comparison with previous works

Several equations have been proposed to define the optimal efficiency for the conversion of radiation to work. They are summarized in Table 1, along with the related quality factor in the surface of Earth .

These previous attempts consider the atmospheric processes either as a reversible machine or proposes the exergy as the maximum efficiency, i.e., a Carnot cycle. Those approaches are dependent on the temperature of the source instead of the radiation flux, and consequently, a previous knowledge of the properties of the source is needed.

We have determined the exergy of radiation using a line-by-line radiative transfer code and compared our results with previous calculations and. Our calculations allows to determine the radiation degradation due to the atmospheric processes of radiation-matter interaction.

From the previous works, the better known equation is the proposed by Petela [7] [31], consisting in the ratio between the relative potential of the maximum energy available from thermal radiation and the total energy emitted by the source:

$$\eta = \frac{W}{\sigma T^4/\pi} = 1 - \frac{4}{3}\frac{T_0}{T} + \frac{1}{3}\left(\frac{T_0}{T}\right)^4 \tag{10}$$

which comes from the definition of work for the blackbody radiation considering reversible steps [23]:

$$W = \frac{\sigma}{\pi}(T^4 - T_0^4) - T_0\frac{4\sigma}{3\pi}(T^3 - T_0^3) \tag{11}$$

The Earth atmosphere is not a blackbody from the perspectives of both downwelling solar and upwelling terrestrial radiations, and therefore the last equation is not exact for our environment, although it could provide a fair approximation in certain cases.

His results where also obtained by other authors for the case of direct sunlight, such as the case of Press [32] and Landsberg and Tonge [10]. Using the availability concept [4], Parrot [33] reached the same equation, as well as Spanner [8] using the idea of absolute work, although he did not consider the emission of radiation by the source.

Beyond the idea of available work also some researches argue that the Carnot efficiency is applicable to the calculations of the exergy of radiation, basing their results on the analysis of the heat engine. This line of thinking is usually attributed to Jeter [11], although Castañs [34] derived the same equation than Jeter independently and using a different interpretation, considering the exergy as an upper limit. Assuming the Carnot efficiency as the maximum efficiency of solar radiation, Kabelac [35] and Millan et al. [36] also proposed the same equation.

All these formulations (either based or Petela's or Castañs' works) are simplifications of the problem. In all cases, the system is considered as reversible and neglects completely the effect of the environment. As a consequence, the formulations deal with the sources of the energy instead of the received energy flux. In order to solve this problem and obtain more accurate values, Chu and Liu [17] determined the exergy using the spectral intensity reaching the surface, although some misconceptions arises in the calculation of the quality factor, as explained in Section 3. In our calculations using a line-by-line radiative transfer model, the obtained quality factor is lower

Table 1: Comparision of the application of this and previous works at surface level conditions (T_0 = 285.14 K; T = 5885 K).

Reference	Formulae	Quality Factor	Observations
Spanner (1964)	$1 - \frac{4}{3}\frac{T_0}{T}$	93.54%	Absolute work without emission
Petela (1964)	$1 - \frac{4}{3}\frac{T_0}{T} + \frac{1}{3}\left(\frac{T_0}{T}\right)^4$	93.54%	Black Body with emission
Castañs (1976)	$\left(1 - \frac{T^4}{T_s^4}\right) \cdot \eta_\infty(T)$	85.40%	Infinite number of absorbers (T=300K and T_{sun}=6000 K)
Jeter (1981)	$1 - \frac{T_0}{T}$	95.15%	Carnot efficiency
Chu and Liu (2009)	$Ex = \int_0^{\inf} Ex_\nu d\nu$	91.71%	Generic spectra
This work	$Ex = \int_0^{\inf} Ex_\nu d\nu$	86.86%	Line-by-line integration

than previously obtained values, as could be expected, due to the inclusion of irreversible processes such as radiation-matter interaction.

6. Discussion

The entropy is directly related with irreversibilities in a system. For the case of a thin atmosphere (without absorptions or scattering), the assumption of the Planck's law for the entropy could be correct. The main difference between energy and entropy is that while energy must remain constant as a consequence of the first law, the entropy does not have the same constrain and it tends to increase. The assumption that the entropy of radiation can be obtained from the intensity of radiation as proposed by Planck might not be correct in the case of a dense atmosphere where the amount of irreversibile processes is extremely high, as it could be the case of Venus. The determination of its importance cannot be quantify until line-by-line radiative transfer equation for the entropy of radiation is solved [37] [38] [39] [40]. Also, the radiative transfer equation for the exergy has been proposed [25], but to our knowledge there is not a numerical code to solve it yet.

We have used FUTBOLIN, a line-by-line radiative transfer code, to determine the transmittance spectra under clear sky conditions. We are not considering scattering processes or clouds. The importance of those physical processes lies in the fact that they could increase the entropy content of radiation. In this work, we have determined the best case scenario of clear sky where no such interactions have been considered, just absorption and emission. The irreversible processes will increase the entropy of radiation and will limit the exergy of it, although it is unclear if they do it [23]. The characterization of these effects and the inclusion of scattering and other irreversible processes into numerical calculations will be taken into account in future works, to provide a determination of the exergy of radiation spectra under different circumstances. The calculations performed in this work show the maximum obtainable work from solar radiation at different layers in the atmosphere considering the radiation-matter interactions, which certainly increases the entropy of radiation, providing the most accurate value nowadays.

7. Conclusions

The exergy of radiation describes the obtainable work from radiation. The determination of the exergy has been done usually by considering reversible processes in the atmosphere. In this work, we determine the exergy of radiation focusing on the atmospheric fluxes instead of the source of the radiation and considering the atmospheric processes as irreversible. The increase of entropy in the atmosphere is related with the increase of heat, and therefore with a diminution of the ability to perform work.

In this paper, we discuss and clarify the meaning of the exergy of radiation, solving the debate of the last half century, and characterizing for the first time the effect of the irreversibilities of our atmosphere in the exergy values. It is clear from our treatment that it is the environment and chemical composition what finally determines the exergy of radiation, not only the temperature of the location. Different locations at the same temperature could have different values of the quality factor.

Previous attempts to determine the exergy of radiation used only the temperature to obtain the quality coefficient, without any physical or chemical considerations. It is well know however that our environment is maintained warm by atmospheric greenhouse among others, and therefore is not only a consequence of direct radiation. It is the interaction of light with chemical compounds what determines the exergy of radiation. We have focused on the effect of light-matter interactions, in

the form of molecular emission and absorption, and we have not considered other atmospheric processes that could decrease the exergy such as the existence of clouds or dust aerosols. For that we solve the radiative transfer equation in clear sky atmosphere and calculate and quantify the effect of each layer in the quality factor of the radiation.

To characterize the importance of the different layers and atmospheric compounds in the increase of the entropy content in radiation. From our analysis is concluded that the most important decrease in the quality factor occurs in the troposphere, where the 80% of the atmosphere is concentrated.

Using a line-by-line radiative transfer code it is possible to analyze the exergy quality factor at different wavelengths. In this paper we provide data and figures that might help in the development of future solar cells by knowing the bands that are carrying more potential to do work. The determination of those bands is not possible with previous approaches, and in this way is possible to expand more the thermodynamic analysis to engineer studies.

8. Acknowledgements

A.D-B. wants to acknowledge to the Luleå University of Technology in Kiruna, Sweden, for the scholarship that partially funded this investigation.

References

[1] G. Beretta, E. P. Gyftopoulos, Electromagnetic radiation: a carrier of energy and entropy, Proceedings of the 1990 Winter Annual Meeting of the ASME 19 (1990) 1–6.

[2] A. Bartoli, Soprai movimenti prodotti dalla luce e dal calore, 1st Edition, Le Monnier, Firenze, 1876.

[3] M. Planck, The Theory of Heat radiation, 1st Edition, P. Blakiston's Son & Co., Philadelphia, 1913.

[4] R. Evans, A proof that essergy is the only consistent measure of potential work, Doctoral Thesis, Dartmouth College.

[5] P. Rezac, H. Metghalchi, A brief note on the historical evolution and present state of exergy analysis, Int. J. of Exergy 1 (4) (2000) 426–427.

[6] A. Sahin, E. Mokheimer, H. Bahaidarah, M. Antar, P. Gandhidasan, R. Ben-Mansour, S. Al-Dini, S. Rehman, A. Bejan, M. Al-Nimr, H. Oztop, L. Chen, A. Midilli, J. Lawrence, Special issue: Thermodynamic optimization, exergy analysis, and constructal design, Arabian Journal for Science and Engineering Section B: Engineering 38 (2) (2013) 219.

[7] R. Petela, Exergy of heat radiation, J. Heat Transfer 86 (2) (1964) 187–192.

[8] D. Spanner, Introduction to Thermodynamics, Academic Press, New York, 1964.

[9] P. Landsberg, A note on the thermodynamcis of energy conversion in plants, Photochem. and Photobiol. 26 (1977) 572–573.

[10] P. Landsberg, G. Tongue, Thermodynamics of the conversion of diluted radiation, J. Phys.A: Math.Gen. 12 (1979) 551–562.

[11] S. Jeter, Maximum conversion efficiency for the utilization of direct solar radiation, Solar Energy 26 (1981) 231–236.

[12] A. Joshi, I. Dincer, B. Reddy, Development of new solar exergy maps, Int. J. of Energy Research 33 (8) (2009) 709–718.

[13] P. Rose, Entropy of radiation, Physical Review 96 (1954) 555. doi:10.1103/PhysRev.96.555.

[14] A. Ore, Entropy of radiation, Physical Review 98 (1955) 887–888. doi:10.1103/PhysRev.98.887.

[15] P. Landsberg, G. Tongue, Thermodynamics energy conversion efficiencies, J. Appl. Phys. 51 (1980) R1–R20.

[16] T. Pujol, G. North, Analytical investigation of the atmospheric radiation limits in semigray atmospheres in radiative equilibrium, Telus A. 55 (2003) 328–337. doi:10.1034/j.1600-0870.2003.00023.x.

[17] S. Chu, L. Liu, Analysis of terrestrial solar radiation exergy, Solar Energy 83 (8) (2009) 1390–1404.

[18] M. Mlynczak, F. Martín-Torres, D. Johnson, D. Kratz, W. Traub, K. Jucks, Observations of the o(3p) fine structure line at 63 m in the upper mesosphere and lower thermosphere, J. of Geophysical Research: Space Physics 109 (CiteID A12306) (2004) A12.

[19] F. J. Martín-Torres, M. G. Mlynczak, Futbolin (full transfer by ordinary line-by-line methods): a new radiative transfer code for atmospheric calculations in the visible and infrared, American Geophysical Union, Spring Meeting abstract A21 (2005) A–05.

[20] M. Kaymak, A. Sahin, Vertically solar irradiation exergy changes in the different layers of atmosphere, Int. J. of Exergy 9 (4) (2011) 389–398. doi:Int. J. of Exergy.

[21] O. Le Corre, J. Broc, I. Dincer, Energetic and exergetic assessment of solar and wind potentials in europe, Int. J. of Exergy 13 (2) (2013) 175–200.

[22] E. G. Fontheim, L. H. Brace, Venus bowshock precursor, Advances in Space Research 10 (1990) 11–14. doi:10.1016/0273-1177(90)90386-E.

[23] Y. Candau, On the exergy of radiation, Solar Energy 75 (2003) 241–247.

[24] C. Gueymard, Smarts, User's manual of SMARTS code Version 2.9.5.

[25] L. Liu, S. X. Chu., Radiative exergy transfer equation, Journal of Thermophysics and Heat Transfer 21 (4) (2007) 819–822.

[26] L. Rothman, I. Gordon, Y. Babikov, A. Barbe, D. C. Benner, P. Bernath, et al., The hitran 2012 molecular spectroscopic database, JQSRT 130 (2013) 4–50.

[27] N. e. a. Jacquinet-Husson, The 2009 edition of the geisa spectroscopic database, JQSRT 112 (2011) 2395–2445. doi:10.1016/j.jqsrt.2011.06.004.

[28] A. E. 00a(2014), Standard solar constant and zero air mass solar spectral irradiance tables, available at http://www.astm.org/Standards/E490.htm.

[29] D. R. Myers, E. Keith, C. Gueymard, Revising and validating spectral irradiance reference standards for photovoltaic performance evaluation, J. Sol. Energy Eng. 126 (1) (2004) 567–574. doi:10.1115/1.1638784.

[30] J. Peixoto, M. d. A. Oort, A. Tomé, Entropy budget of the atmosphere, J. Geophys. Res. 96 (10) (1991) 981–988. doi:10.1029/91JD00721.

[31] R. Petela, Exergy of undiluted thermal radiation, Solar Energy 74 (2003) 469–488. doi:10.1016/S0038-092X(03)00226-3.

[32] W. Press, Theoretical maximum for energy from direct and diffuse sunlight, Nature 264 (1976) 735.

[33] J. Parrot, Theoretical upper limit to the conversion efficiency of solar energy, Solar Energy 21 (1978) 227.

[34] M. Castañs, Bases físicas del aprovechamiento de la energía solar, Revista de Geofísica XXXV (227) (1976) 3–4.

[35] S. Kabelac, A new look at the maximum conversion efficiency of blackbody radiation, Solar Energy 46 (4) (1991) 231–236. doi:10.1016/0038-092X(91)90067-7.

[36] M. Millán, F. Hernández, E. Martín, Available solar exergy in an absorption cooling process, Solar Energy 56 (6) (1996) 505–511. doi:10.1016/0038-092X(96)00027-8.

[37] R. Wildt, Thermodynamics of the gray atmosphere. i. reversible adiabatic processes, Astrophysical Journal 140 (1964) 1343. doi:10.1086/148041.

[38] R. Wildt, Thermodynamics of the gray atmosphere. ii. unattainability of detailed balancing, Astrophysical Journal 143 (1966) 363. doi:10.1086/148520.

[39] R. Wildt, Thermodynamics of the gray atmosphere. iii. entropy defect and source function, Astrophysical Journal 146 (1966) 418. doi:10.1086/148906.

[40] R. Wildt, Thermodynamics of the gray atmosphere.iv. entropy transfer and production, Astrophysical Journal 174 (1972) 69. doi:10.1086/151469.

4

General equation of the Gibbs free energy and application to present day Mars

Carl Sagan demostró, analizando datos de la sonda Galileo de la NASA, que es posible detectar el desequilibrio químico de la atmósfera desde el espacio. Algunos investigadores han propuesto que la existencia de desequilibrio en la atmósfera de un planeta podría ser indicador de la existencia de vida en él.

Para calcular este desequilibrio químico se recurre a la energía libre de Gibbs. Una revisión de los trabajos previos me ha llevado a la conclusión de que el cálculo de la energía de Gibbs es incorrecto en algunas situaciones porque no tiene en cuenta su dependencia en la temperatura.

En este capítulo determino las ecuaciones generales para calcular la energía libre de Gibbs en función de la presión y la temperatura. Con el fin de ilustrar el uso de estas ecuaciones las he aplicado a un modelo fotoquímico de la atmósfera de Marte y, utilizando datos in-situ de temperatura y presión, he determinado la energía libre de Gibbs de las reacciones más importantes de la atmósfera, y con ello su grado de desequilibrio.

Del mismo modo, he determinado la entalpía de la atmósfera cerca de la superficie de Marte, y el flujo de entalpía en la superficie de Marte a través del regolito al subsuelo. A partir de argumentos puramente termodinámicos llego a la conclusión de que hay suficiente energía en la superficie de Marte para mantener posibles quimiolitoautótrofos debajo de su superficie.

JOURNAL OF GEOPHYSICAL RESEARCH, VOL. ???, XXXX, DOI:10.1002/,

General equation of the Gibbs free energy and application to present day Mars

Alfonso Delgado-Bonal[1,2] , Patricia Valentín-Serrano[1], María-Paz Zorzano[1], and F. Javier Martín-Torres[3,4]

Abstract. The analysis of the disequilibrium of an atmosphere can be carried out computing its Gibbs free energy. Here we determine the general equations to determine the Gibbs free energy for any kind of atmosphere (i.e., from Earth and terrestrial rocky planets to hot exoplanets). In order to illustrate the use of these equations we have applied them to a photochemical model of the Martian atmosphere, and we have determined its Gibbs free energy, and then its degree of disequilibrium, as well as the enthalpy of the near-surface Martian atmosphere. The enthalpy flux at the surface level on Mars should be suitable to propagate through the regolith to the subsurface, and we conclude that, from purely thermodynamic arguments, there is enough energy on Mars to support hypothetical chemolithoautotrophs beneath its surface.

1. Introduction

Thermodynamic disequilibrium analysis has been applied to study planetary atmospheres, from remote hot Neptunes, hot Jupiters (*Stevenson et al.* [2010],*Moses et al.* [2011]) and brown dwarfs (*Griffith and Yelle* [1999]), to closer rocky bodies such as Mars (*Jakosky and Shock* [1998], *Levine and Summers* [2003]), Europe (*McCollom* [1999]) and Titan (*McKay and Smith* [2005]) or even to study our own planet (*Kleidon* [2012]). This thermodynamic disequilibrium can be produced by biotic or abiotic processes (geological, solar or atmospheric processes in the atmosphere), and the analysis of the sources of disequilibrium is nowadays a promising ongoing field of research.

Thermodynamic disequilibrium is the first requirement for supporting life (*Most et al.* [2010], *Baross et al.* [2007]), and a far-from-equilibrium atmosphere could be an indicator of life (biomarker) in a planet (*Lovelock* [1965], *Krissansen-Totton et al.* [2015], *Catling and Bergsman* [2010]). On the other hand, a situation of non thermodynamical equilibrium can lead a system to create and maintain complex structures such as life (*Nicholls and Prigogine* [1977], *Schneider and Kay* [1995]).

Many biomarkers have been proposed from atmospheric analysis, for Earth or Mars (*Catling and Bergsman* [2010], *Summers et al.* [2002]), but none of them is as general as studying the thermodynamic disequilibrium of the atmosphere (*Catling and Bergsman* [2010], *Pilcher* [2003]). *Hitchcock and Lovelock* [1967] proposed that the "evidence of a large chemical free energy gradient between surface matter and the atmosphere in contact with it is evidence of life". From the analysis of the Earth's spectra provided by the Galileo spacecraft it was concluded that Earth's atmosphere is out of thermodynamic equilibrium (*Sagan et al.* [1993]).

The analysis of the disequilibrium of a thermodynamic system can be carried out using the Gibbs free energy, a thermodynamic potential that measures the obtainable work from a system at constant temperature and pressure. Although the atmospheric temperature and pressure in an atmosphere are not constant, we can assume that the atmospheric reactions are much faster than the variations of the thermodynamic variables, and then the use of the thermodynamic potential in atmospheric sciences is justified (*Goody* [1995]). Previous calculations of the Gibbs free energy for Mars rely in the expression used for Earth conditions, where the pressure dependence can be neglected (*Jakosky and Shock* [1998], *Boxe et al.* [2012], *Tierney et al.* [2008]). However, a proper dependence of the pressure and temperature needs to be taken into account for more general atmospheric conditions, like the case of exoplanet atmospheres. Even in the case of Mars, the inclusion of the complete formulation of the Gibbs free energy is important in the calculation of individual reactions, as we will show in this paper. In Section 2 we present the general equation for the calculation of the Gibbs free energy for every pressure and temperature conditions. In addition to the complete equation, we have developed an useful approximation for those situations where the temperature variations are small, and explain the range of validity of each one.

From the Gibbs free energy of each compound the Gibbs free energy of a system of reactions can be computed. We have developed a photochemical model to calculate the Gibbs free energy at each altitude of the Martian atmosphere and we present the results in Section 3. Our model uses the initial concentrations calculated with the Laboratoire de Météorologie Dynamique (LMD) General Circulation Model (*Forget et al.* [2013], *Lefevre and Forget* [2009]) and the in-situ measurements by the Rover Environmental Monitoring Station (REMS) (*Gómez-Elvira et al.* [2012], *Gómez-Elvira et al.* [2014]) on board the Curiosity rover (*Grotzinger et al.* [2012]).

In Section 4 we determine the enthalpy flux in the near-surface Martian atmosphere. Although estimations of this value has been done before (*Weiss et al.* [2000]), only a couple of non interacting reactions were considered. In this work, we determine the total enthalpy available in Mars' surface with a complete photochemical model. Finally, in Section 5 we summarize the main results of this work.

[1]Centro de Astrobiología (INTA-CSIC), Ctra. Ajalvir km.4, Torrejón de Ardoz, 28850, Madrid, Spain.

[2]Instituto Universitario de Física Fundamental y Matemáticas, Universidad de Salamanca, Casas del Parque, 37007, Spain.

[3]Division of Space Technology, Department of Computer Science, Electrical and Space Engineering, LuleåUniversity of Technology, Kiruna, Sweden

[4]Instituto Andaluz de Ciencias de la Tierra (CSIC-UGR), Avda. de Las Palmeras n 4, Armilla, 18100, Granada, Spain

0148-0227/15/$9.00

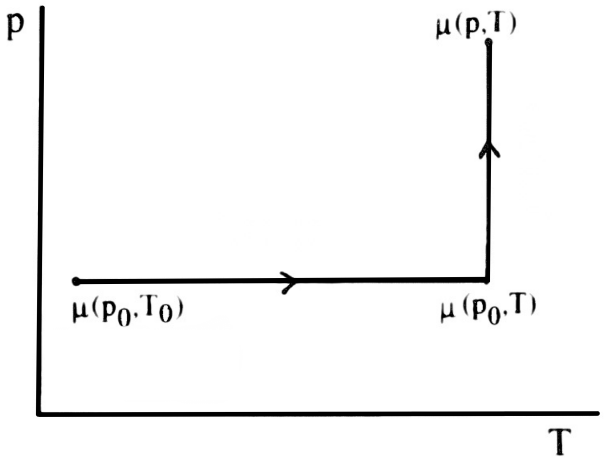

Figure 1. Chemical potential determination diagram for any pressure and temperature. Adapted from Kondepudi and Prigogine (*Kodepudi and Prigogine* [1998]).

2. Available Gibbs free energy

The Gibbs free energy potential describes the obtainable work from a system at constant temperature and pressure. Its value determines the direction of the reactions. The total Gibbs free energy in a system can be calculated as the sum of the Gibbs free energy of the individual reactions, which depends on the Gibbs free energy of formation of each compound.

For a pure compound, the chemical potential is defined as the Gibbs free energy of one mole of that compound, i.e., is the partial molar Gibbs free energy. The correct pathway to determine the chemical potential for arbitrary values of pressure and temperature is shown in Figure 1. The first step (horizontal line) is omitted in most of the works (*Line et al.* [2011], *McCollom and Shock* [1997]) and therefore the calculation of the chemical potential is not accurate. This might be not important for Earth's atmospheric conditions, since the pressure and temperature are close to standard conditions, but it is very relevant for other environments with high pressure and temperatures. On the other hand it should be noted that some works make wrong assumptions about the temperature dependence of the enthalpy (*Simoncini et al.* [2013]).

The expression that is commonly used in planetary atmospheres [Eq. 4.10 in (*Seager* [2010])], is usually written as:

$$\mu(p,T) = \mu_0 + RT\ln p \quad (1)$$

Where μ_0 is the chemical potential at unit pressure (1 atm). This expression is a particularization for a more complete equation (*Kodepudi and Prigogine* [1998]):

$$\mu(p,T) = \mu(p_0,T) + RT\ln(p/p_0) \quad (2)$$

where p_0 is the pressure at standard conditions and R the gas constant.

In order to calculate the chemical potential for arbitrary p and T, the knowledge of the chemical potential at (p_0,T) is needed. This previous step, usually omitted, can be performed as (eq. (5.5.3) in (*Kodepudi and Prigogine* [1998])):

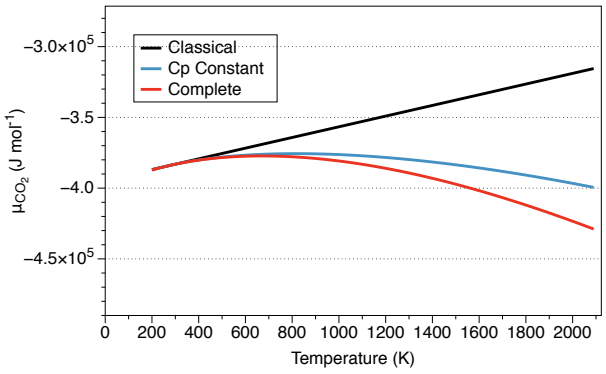

Figure 2. Chemical potential (μ(p,T)) of CO_2 formation at 95 bar as a function of temperature.

Table 1. Chemical potential calculated with Eq. 1 (classical), Eq. 5, and Eq. 6, and relative differences between Eq. 1 and Eq. 6.

T	Classical	C_p constant	Complete	Diff. (%)
200	-386849.7	-387191.0	-387231.9	-0.1
400	-379299.4	-380143.7	-380214.8	-0.2
600	-371749.1	-376710.1	-377449.1	-1.5
800	-364198.8	-375623.2	-377843.1	-3.7
1000	-356648.5	-376281.4	-380818.6	-6.8
1200	-349098.2	-378330.0	-385987.8	-10.6
1400	-341547.9	-381534.9	-393056.7	-15.1
1600	-333997.6	-385730.0	-401782.3	-20.3
1800	-326447.3	-390790.6	-411955.2	-26.2
2000	-318897.0	-396620.4	-423387.0	-32.8

$$\mu(p_0,T) = \frac{T}{T_0}\mu(p_0,T_0) + T\cdot\int_{T_0}^{T}\frac{-H_m(p_0,T')}{T'^2}dT' \quad (3)$$

Using (1) - (3) for an ideal gas, the chemical potential at a particular pressure and temperature can be written as:

$$\mu(p,T) = \mu(p_0,T) + RT\ln(p/p_0) =$$

$$\frac{T}{T_0}\mu(p_0,T_0) + T\cdot\int_{T_0}^{T}\frac{-H_m(p_0,T')}{T'^2}dT' + RT\ln(p/p_0) \quad (4)$$

where T_0 is the temperature at standard conditions and H_m is the molar enthalpy of the compound.

In those situations where the temperature variations are small, we can consider that the heat capacity at constant pressure, C_p, is not temperature dependent, and then obtain an approximation for the chemical potential of formation as (see A for the derivation):

$$\mu(p,T) = \frac{T}{T_0}\mu(p_0,T_0) + T\cdot(H_m(p_0,T_0) - C_pT_0)\left[\frac{1}{T} - \frac{1}{T_0}\right]$$

$$-C_pT\ln\frac{T}{T_0} + RT\ln(p/p_0) \quad (5)$$

In the situations where the temperature is high (above 700 K), the assumption that the heat capacity C_p is constant might not be correct. Considering a polynomial dependence on the temperature for the heat capacity, as is usually do, the chemical potential reads:

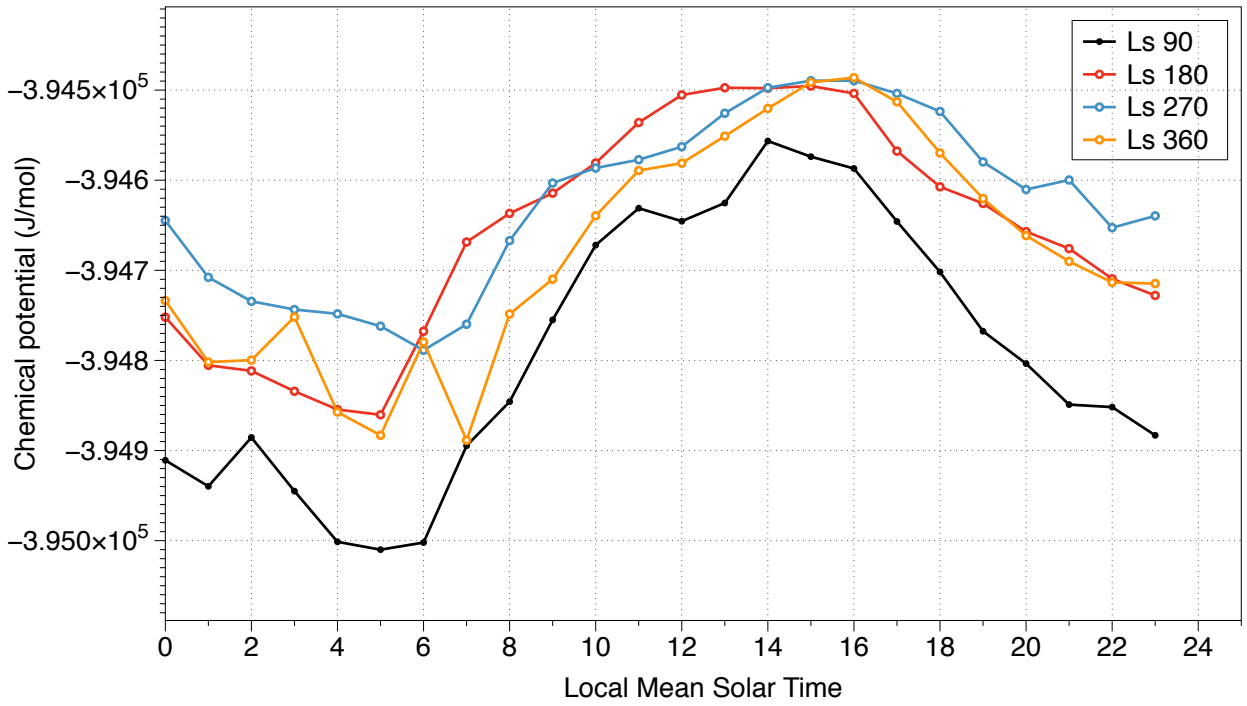

Figure 3. Chemical potential (μ(p,T)) of CO_2 formation on Mars as a function of season.

$$\mu(p,T) = \frac{T}{T_0}\mu(p_0,T_0) + RT\ln(p/p_0) + \\ + T\left(H(p_0,T_0) - (aT_0 + \frac{b}{2}T_0^2 + \frac{c}{3}T_0^3)\right)\left[\frac{1}{T} - \frac{1}{T_0}\right] \\ - aT\ln\left(\frac{T}{T_0}\right) - \frac{b}{2}T(T-T_0) - \frac{c}{6}T(T^2 - T_0^2) \quad (6)$$

Note that when we consider C_p as a constant, i.e., b and c = 0, and a =C_p, the expression (6) is reduced to (5).

In order to show the importance of the complete formulation of the Gibbs free energy, we show in Figure 2 the value of the chemical potential of CO_2 using Eq. 1, Eq. 5, and Eq. 6, at the Venus surface pressure (95 bar) and a temperature range between 200-2200 K. The relative differences between the different formulations are shown in Table 1, being as big as 32% for 2000 K.

Figure 2 shows that: i) the calculation of the chemical potential without the correct treatment of the temperature variation gives incorrect values at high temperatures; ii) the importance of the complete formulation increases with the temperature; iii) at low temperature regimes, the assumption of constant heat capacity gives accurate values, but for high temperatures, such as Venus or Jupiter atmospheres, the polynomial description of the heat capacity is needed. For those situations where the temperature and pressure are similar to Earth's values, the use of the "Classical" equation provides values close enough to the real ones, and the simplicity of the expression justifies its use below 350-400 K. The approximation of constant heat capacity has a wider range of validity, but becomes incorrect beyond 700 K, as for example be the case of the Venus atmosphere.

Table 2. Gibbs Energy of formation for different compunds. Values of Δ G (kJ mol^{-1}) on Earth and Mars conditions using Eq. 1, 5 and 6 .

Compound	$\Delta G_{f,\mathrm{Earth}}$	$\Delta G_{f,\mathrm{Mars}}$ Eq. 5	$\Delta G_{f,\mathrm{Mars}}$ Eq. 6
CO_2	-394400	-394653	-394673
H_2O	-228600	-232511	-232517
O_2	0	-404	-411
CH_4	- 50500	-57273	-57297

3. Gibbs free energy in the present day Mars

The calculation of the Gibbs free energy could be a measurement of abiotic sources of disequilibrium in present day Mars; and could be useful to identify zones of biological activity, if life is currently present on Mars. In this section, we determine the Gibbs free energy of the near-surface Martian atmosphere.

The Gibbs free energy depends on molar fraction, pressure and temperature. For our calculations, we have used the lower Martian atmospheric species provided by the Laboratoire de Météorologie Dynamique (LMD) GCM (*Forget et al.* [2013], *Lefevre and Forget* [2009]). The pressure and temperature variations during a Martian day are based on the measurements by the REMS instrument.

In order to calculate the available Gibbs free energy in the lower Martian atmosphere, we compute the chemical potential of the atmospheric species as function of time and, using these values of the Gibbs energy of formation, we calculate the Gibbs free energy of the most relevant reactions in the atmosphere. The calculations in this section are performed using the data provided by REMS. Given that REMS is located near the equator on crater Gale (4.49° S, 137.42°E), the computed values could be considered as an upper limit, computed from purely thermodynamic arguments, of the amount of energy that can be used by living beings on present-day Mars.

Table 3. Gibbs free energy of the most relevant reactions at the lower atmosphere of Mars. The second and third columns show the values calculated with the "Classic" and the "C_p constant" formulations. In the last column, their relative difference is shown.

reaction	$\Delta G_{classic}$	$\Delta G_{C_pconstant}$	Difference
1	57668.6	74598.0	-29.4 %
2	-337231.4	-319616.5	5.2 %
3	-394900.0	-394214.5	0.2 %
4	0.0	0.0	0.0 %
5	65284.0	66038.7	-1.2 %
6	5592.0	6003.8	-7.3 %
7	0.0	0.0	0.0 %
8	-394900.0	-394214.5	0.2 %
9	-57668.6	-74598.0	-29.4 %
10	892.0	1992.3	-123.4 %
11	-29939.8	-13591.4	54.6 %
12	-283652.0	-283928.7	-0.1 %
13	-220108.0	-220351.7	-0.1 %
14	-62792.0	-64070.7	-2.0 %
15	-332108.0	-330143.8	0.6 %
16	-157316.0	-156280.9	0.6 %
17	-225700.0	-226355.4	-0.3 %
18	-222600.0	-222319.6	0.1 %
19	-285392.0	-286390.4	-0.4 %
20	-150700.0	-152069.8	-0.9 %
21	-134692.0	-134320.6	0.3 %
22	-59692.0	-60034.9	-0.6 %
23	-54331.5	-35194.1	35.2 %
24	-69408.0	-68281.9	1.6 %
25	-65284.0	-66038.7	-1.2 %
26	-174792.0	-173862.9	0.5 %
27	-304570.0	-294949.7	3.2 %
28	-150700.0	-152069.8	-0.9 %
29	-47715.5	-30982.9	35.0 %
30	-280031.4	-261549.5	6.6 %
31	-231700.0	-194613.8	16.0 %
32	-163200.0	-199600.7	-22.3 %
33	-24708.0	-25737.9	-4.2 %
34	-88292.0	-91139.5	-3.2 %
35	-362731.5	-346685.3	4.4 %
Total	-5237419.0	-5124576	2.2 %

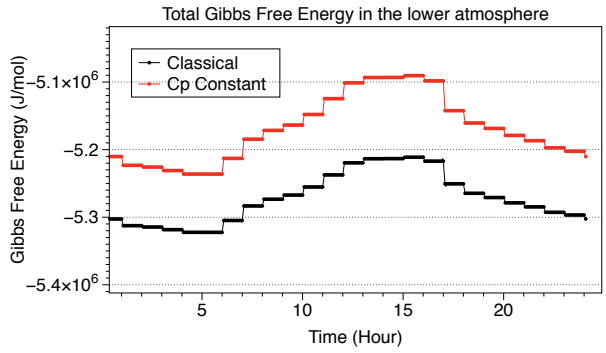

Figure 4. Daily evolution of the total Gibbs Free Energy in the lower atmosphere calculated with the "Classical" equation and the "C_p constant" expressions.

3.1. Gibbs free energy of formation on Mars

In the theoretical framework developed in Section 2, we deduced Equation 5 as an approximation of the complete chemical potential, i.e., Equation 6. We can assume that the heat capacity, C_p, can be approximated as a constant at the temperature range on Mars, being able to use Eq. 5 to determine the chemical potential. In order to compare both equations, we determine, using both equations, the chemical potential of the major components of the Martian atmosphere. From the values in Table 2 we conclude that Eq. 5 (assuming constant heat capacity), as expected, is acceptable under the Martian environment.

As has been seen in Figure 2, the importance of a correct calculation of the Gibbs free energy increases with temperature and pressure, and for the Martian environment Eq. 5 represents a very good approximation. Note that Mars (due to its low T and p) is a special case compared with other planets where the use of Eq. 6 is relevant (as shown in Figure 2).

Within a Martian day, the diurnal thermal and pressure ranges are around 60 K and 60 Pa. Figure 3 shows the chemical potential of formation of the CO_2 during a Martian day for different seasons, characterized for a particular solar longitude (Ls=180°, Ls=270° , Ls=360° and Ls=90°). The solar longitude is the Mars-Sun angle, measured from the Northern Hemisphere, being the spring equinox Ls=0. It can be seen in the Figure 3 that the Gibbs free energy of formation of the compounds changes during the day, and it is important to determine it correctly in order to determine of the total Gibbs free energy of the atmosphere.

Table 4. Enthalpy for the most relevant reactions in Mars lower atmosphere in Table 5 (Ls =180°, noon).

reaction	$\Delta H_{classic}$	$\Delta H_{C_pconstant}$	Difference
1	-106480.0	-105812.7	0.6 %
2	-498360.0	-497565.8	0.2 %
3	-391880.0	-391753.2	0.0 %
4	0.0	0.0	0.0 %
5	70646.0	70408.9	0.3 %
6	7818.0	7818.0	0.0 %
7	0.0	0.0	0.0 %
8	-391880.0	-391753.2	0.0 %
9	106480.0	105812.7	0.6 %
10	10120.0	9513.3	6.0 %
11	60154.0	59837.4	0.5 %
12	-283180.0	-283544.0	-0.1 %
13	-220680.0	-220817.9	-0.1 %
14	-70182.0	-70093.8	0.1 %
15	-321698.0	-321659.4	0.0 %
16	-150498.0	-150724.1	-0.1 %
17	-228498.0	-228635.9	-0.1 %
18	-221144.0	-221133.0	0.0 %
19	-291326.0	-291226.8	0.0 %
20	-157300.0	-157448.9	-0.1 %
21	-134026.0	-133777.8	0.2 %
22	-62828.0	-62590.9	0.4 %
23	-207498.0	-206654.2	0.4 %
24	-63380.0	-63369.0	0.0 %
25	-70646.0	-70408.9	0.3 %
26	-171200.0	-170935.3	0.2 %
27	-114200.0	-115005.2	-0.7 %
28	-157300.0	-157448.9	-0.1 %
29	-214300.0	-213379.0	0.4 %
30	-435996.0	-435290.1	0.2 %
31	-191090.0	-191101.0	-0.0 %
32	-200790.0	-200652.1	0.1 %
33	-29590.0	-29716.8	-0.4 %
34	-104014.0	-103953.3	0.1 %
35	-532192.0	-531425.4	0.1 %
Total	-5766938.	-5764486.	0.04 %

3.2. Gibbs free energy of reactions on Mars

The values of the Gibbs free energy of formation of each compound allows the calculation of the Gibbs free energy of the atmospheric reactions. We have developed a photochemical model ranging from the surface to 150 km, divided in

131 altitude layers, and consisting of 35 atmospheric species interacting in 35 reactions. The reactions investigated have been used before in Mars atmospheric studies (*Lefevre and Forget* [2009]). The Gibbs free energy of the reactions can be easily calculated once the Gibbs free energy of formation is computed:

$$\mu_{reaction} = \sum \mu_{products} - \mu_{reactants} \quad (7)$$

$$\mu_{total} = \sum \mu_{reactions} \quad (8)$$

The Gibbs free energy of a reaction is:

$$\Delta G = \Delta G^0 + RT \ln(p/p_0) \quad (9)$$

where as explained in Section 2, ΔG^0 is in fact $\Delta G(p_0,T)$ and not $\Delta G(p_0,T_0)$, as usually assumed.

We determine the Gibbs free energy of the reactions of the Martian lower atmosphere using the Equations 8 and 9, assuming constant heat capacity (Eq. 5), and compare the results with the incorrect "Classical" equation.

The initial concentrations of the atmospheric species of the model have been taken from the General Circulation Model developed and maintained by the Laboratoire de Météorologie Dynamique (LMD, Paris) and the sub-Department of Atmospheric, Oceanic and Planetary Physics at Oxford University (*Forget et al.* [2013]).

Table 3 shows the values of the Gibbs free energy for the most relevant reactions in the lower atmosphere of Mars (see Appendix) and the total value of the Gibbs free energy of the atmosphere, and Figure 4 shows the daily evolution of this total Gibbs free energy. The results have been calculated using REMS data for Ls=180° at noon on Mars.

The total Gibbs free energy obtained with our model provides a value of -5124576 J/mol for the near surface Martian atmosphere. Although the total value obtained with the "Classical" equation differs only in a 2.2%, some reactions have a considerable difference, up to 123%, which remarks the importance of use a proper formulation of the Gibbs free energy.

4. Enthalpy

The enthalpy flux at the surface level on Mars should be suitable to propagate through the regolith to the subsurface. This is of importance from an astrobiological point of view (*Weiss et al.* [2000]). The dependence of the enthalpy with temperature and pressure is:

$$h(p,T) = h(p_0,T_0) + \left[\int_{T_0}^{T} C_p dT\right]_{p_0} \quad (10)$$

and the enthalpy of a reaction can be calculated as:

$$\Delta h_{reaction} = \sum h_{products} - h_{reactants} \quad (11)$$

With the photochemical model that we have developed we can estimate the values of the enthalpy for the lower Martian atmosphere. The results are summarized in Table 4, for the enthalpy at standard conditions ("Classic") and including the changes in temperature assuming C_p constant ("C_p constant").

Table 4 shows that the difference in enthalpy is much smaller than the changes in the Gibbs free energy seen in Table 3. The variation between the "Classical" formulation and the "C_p constant" approximation is only 0.04%, and individual reactions change usually less than 1%. The consideration that the enthalpy does not change for the Mars atmosphere is a very good assumption; the use of the "classical" equation provides very accurate values and it is much simpler than the constant heat capacity approximation, which makes its use recommendable for Martian environment. With our model, we obtain a value for the total enthalpy of the Martian near surface of -5744486 J/mol, an order of magnitude larger than previous results where only a couple of reactions were considered (*Weiss et al.* [2000]).

5. Conclusions

The Gibbs free energy is a thermodynamic potential that depends on molar fraction, pressure and temperature, and it determines the disequilibrium of an atmosphere. Previous calculations of the Gibbs free energy are sometimes erroneous because a proper dependence of the variables is not included in the formulation. We have derived the complete equations for the determination of the chemical potential of a particular compound, and some approximations that might be useful in planetary sciences. We have proven the validity of those equations for different environments, such as Mars, Venus or Earth. Although exoplanet atmospheres are beyond the scope of this work, we remark the fact that the complete formulation of the chemical potential is of capital importance when working with hot exoplanets (see Figure 2).

Using a validated photochemical model of Mars, and the measurements of pressure and temperature of the lower Martian atmosphere provided by the REMS instrument, we estimate the disequilibrium of the near surface Martian atmosphere. Our results indicate that the chemical disequilibrium of the atmosphere is about - 5124576 J/mol. The negative sign of the Gibbs free energy shows that the chemistry in present day Martian atmosphere is carried spontaneously, and the flux of Gibbs free energy is suitable to penetrate into the regolith and be used as energy for hypothetical chemolithoautotrophs as primary energy source.

Also, we have determined the atmospheric enthalpy flux near the surface of Mars using a complete photochemical model. Our calculations show that the complete enthalpy flux is larger than previously reported, being the value of -5764486 J/mol. The negative sign in the enthalpy flux means that, in general, the Martian atmosphere is exothermic, providing heat to the surface and subsurface.

Acknowledgments. A.D.B. wants to acknowledge the INTA Grant TD 04/10 at the Spanish Center of Astrobiology (INTA-CSIC) that partially supported this work.

References

Stevenson, K. B., J. Harrington, S. Nymeyer, N. Madhusudhan, S. Seager, W. C. Bowman, R. A. Hardy, D. Deming, E. Rauscher, and N. B. Lust (2010), Possible thermochemical disequilibrium in the atmosphere of the exoplanet GJ 436b, *Nature Letter*, *464*, 1161–1164.

Moses, J. I., C. Visscher, J. J. Fortney, A. P. Showman, N. K. Lewis, C. A. Griffith, S. J. Klippenstein, M. Shabram, A. J. Friedson, M. S. Marley, and R. S. Freedman (2011), Disequilibrium Carbon, Oxygen, and Nitrogen Chemistry in the Atmospheres of HD 189733b and HD 209458b, *The Astrophysical Journal*, *737*, 15.

Griffith, C. A., and R. V. Yelle (1999), Disequilibrium Chemistry in a Brown Dwarf's Atmosphere: Carbon Monoxide in Gliese 229B, *The Astrophysical Journal*, *519*, 85–88.

Jakosky, B. M., and E. L. Shock (1998), The biological potential of Mars, the early Earth and Europa, *Journal of Geophysical Research,103* 8, 19359–19364.

Levine, J. S., and M. E. Summers (2003), Non-Equilibrium Thermodynamic Chemistry and the Composition of the Atmosphere of Mars, *Sixth International Conference on Mars*.

McCollom, T. M. (1999), Methanogenesis as a potential source of chemical energy for primary biomass production by autotrophic organisms in hydrothermal systems on Europa, *Journal of Geophysical Research*, *104*,12,729–742.

McKay, C. P., and H. D. Smith (2005), Possibilities for methanogenic life in liquid methane on the surface of Titan, *Icarus*, *178*, 274–276.

Kleidon, A. (2012), How does the Earth system generate and maintain thermodynamic disequilibrium and what does it imply for the future of the planet?, *Phil. Trans. R. Soc. A*, *370*, 1012–1040.

Mast, C. B., N. Osterman, and D. Braun (2010), Disequilibrium first: the origin of life, *Journal of Cosmology*,*10*, 3305-3314.

Baross, J. A. (2007), The Limits of Organic Life in Planetary Systems ("The Weird Life Report"), *National Academies Press*. ISBN 9780309104845.

Lovelock, J. E. (1965), A physical basis for life detection experiments, *Nature*, *207*.

Krissansen-Totton, J., D. Bergsman, and D. C. Catling (2015), On detecting biospheres from chemical disequilibrium in planetary atmospheres, submitted to *Astrobiology*.

Catling, D. C., and D. S. Bergsman (2010), On detecting exoplanet biospheres from atmospheric chemical disequilibrium, *Astrobiology Science Conference*.

Nicholls, G., and I. Prigogine (1977), Selforganization in Nonequilibrium Systems, *New York: Academic Press*.

Schneider, E. D., and J. J. Kay (1995), Order from Disorder: The Thermodynamics of Complexity in Biology, in Murphy, M. P., and L. A. J. O'Neill (ed), What is Life: The Next Fifty Years. Reflections on the Future of Biology, *Cambridge University Press*, 161–172.

Summers, M. E., B. J. Lieb, E. Chapman, and Y. L. Yung (2002), Atmospheric biomarkers of subsurface life on Mars, *Geophysical Research Letters*, *29*,24, 24.1–24.4.

Pilcher, C.B. (2003), Biosignatures of Early Earths, *Astrobiology*, *3*,3, 471–486.

Hitchcock, D. R., and J. E. Lovelock (1967), Life detection by atmospheric analysis, *Icarus*, *7*,1-3, 149–159.

Sagan, C., W. R. Thompson, R. Carlson, D. Gurnett, and C. Hord (1993), A search for life on Earth from the Galileo spacecraft, *Nature*,*365*, 715–721.

Goody, R. (1995), Principles of Atmospheric Physics and Chemistry, *Oxford University Press*, ISBN-10: 0195093623.

Boxe, C. S., K. P. Handa, K. H. Nealson, Y. L. Yung, and A. Saiz-Lopez (2012), An active nitrogen cycle on Mars sufficient to support a subsurface biosphere, *International Journal of Astrobiology*, *11*,2, 109–115.

Tierney L. L., and B. M. Jakosky (2008), Assessing the habitability of Meridiani Planum, Mars, based on thermodynamic energy requirements, *Lunar and Planetary Science*, *XXXIX*, 1396.

Forget, F., R. Wordsworth, E. Millour, J.-B. Madeleine, L. Kerber, J. Leconte, E. Marcq, and R. M. Haberle (2013), 3D modelling of the early martian climate under a denser CO2 atmosphere: Temperatures and CO2 ice clouds, *Icarus*, *222*,1, 81–99.

Lefevre, F., and F. Forget (2009), Observed variations of methane on Mars unexplained by known atmospheric chemistry and physics, *Nature*, *460*.

Gómez-Elvira, J., C. Armiens, L. Castaner, M. Domínguez, M., Genzer, F. Gómez, R. Haberle, A.-M. Harri, V. Jimenez, H. Kahanpää, L. Kowalski, A. Lepinette, J. Martínez-Frías, J. Martín, I. McEwan, L. Mora, J. Moreno, S. Navarro, M. A. de Pablo, V. Peinado, A. Pena, J. Polkko, M. Ramos, N. O. Renno, J. Ricart, M. Richardson, J. A. Rodríguez-Manfredi, J. Romeral, E. Sebastián, J. Serrano, M. de la Torre Juárez, J. Torres, F. Torrero, R. Urqui, T. Velasco, J. Verdasca, M.-P Zorzano, and F. J. Martín-Torres (2012), REMS: an Environmental Sensor Suite for the Mars Science Laboratory, *Space Science Reviews*, *170*, 5–56.

Gómez-Elvira, J., C. Armiens, I. Carrasco, M. Genzer, F. Gómez, R. Haberle, V. E. Hamilton, A.-M. Harri, H. Kahanpää, O. Kemppinen, A. Lepinette, J. Martín-Soler, F. J. Martń-Torres, J. Martínez-Frías, M. Mischna, L. Mora, S. Navarro, C. Newman, M. A. de Pablo, V. Peinado, J. Polkko, S. C. Rafkin, M. Ramos, N. O. Rennó, M. Richardson, J. A. Rodríguez-Manfredi, J. J. Romeral Planelló, E. Sebastián, M. de la Torre Juárez, J. Torres, R. Urquí, A. R. Vasavada, J. Verdasca, and M.-P. Zorzano (2014), Curiosity's Rover Environmental Monitoring Station: Overview of the First 100 Sols, *Journal of Geophysical Research: Planets*, Accepted manuscript, DOI: 10.1002/2013JE004576.

Grotzinger, J. P., J. Crisp, A. R. Vasavada, R. C. Anderson, C. J. Baker, R. Barry, D. F. Blake, P. Conrad, K. S. Edgett, B. Ferdowski, R. Gellert, J. B. Gilbert, M. Golombek, J. Gómez-Elvira, D. M. Hassler, L. Jandura, M. Litvak, P. Mahaffy, J. Maki, M. Meyer, M. C. Malin, I. Mitrofanov, J. J. Simmonds, D. Vaniman, R. V. Welch, and R. C. Wiens (2012), Mars Science Laboratory Mission and Science Investigation, *Space Science Reviews*, *170*1-4, 5–56.

Weiss B. P., Y. L. Yung, and K. H. Nealson (2000), Atmospheric energy for subsurface life on Mars?, *PNAS*, *97*, 1395–1399.

Line, M.R., G. Vasisht, P. Chen, D. Angerhausen, and Y. L. Yung (2011), Thermochemical and photochemical kinetics in cooler hydrogen-dominated extrasolar planets: a methane-poor GJ436b?, *The Astrophysical Journal*, *738*,32, 14.

McCollom T. M., and E. L. Shock (1997), Geochemical constraints on chemolithoautotrophic metabolism by microorganisms in seafloor hydrothermal systems, *Geochimicaet Cosmochimica Acta*, *61*,20, 4375–4391.

Simoncini, E., N. Vigo, and A. Kleidon (2013), Quantifying drivers of chemical disequilibrium: theory and application to methane in the Earths atmosphere, *Earth Syst. Dynam.*, *4*, 317–331.

Seager, S. (2010), Exoplanet Atmospheres, *Princeton series in astrophysics*, Princeton.

Kodepudi, D., and I. Prigogine (1998), Modern Thermodynamics: From Heat Engines to. Dissipative Structures, *Wiley: New York*, ISBN 0-471-97339-9.

Corresponding author: A. Delgado-Bonal, Instituto de Física Fundamental y Matemáticas, University of Salamanca, Casas del parque, 37008, Salamanca, Spain. (alfonso_delgado@usal.es)

Appendix A: Derivation of the chemical potential equation

The most complete equation to determine the chemical potential for a compound at a particular pressure and temperature is the expression given in Eq. 4:

$$\mu(p,T) = \frac{T}{T_0}\mu(p_0,T_0) + T\cdot\int_{T_0}^{T}\frac{-H_m(p_0,T')}{T'^2}dT' + RT\ln(p/p_0) \quad \text{(A1)}$$

The molar enthalpy $H_m(p_0,T)$ at an arbitrary temperature T can be obtained from the values of the heat capacity at constant pressure, $C_p(T)$, and the tabulated values of enthalpy at a standard temperature H(p_0,T_0):

$$H(p_0,T) = H(p_0,T_0) + \int_{T_0}^{T} C_p(T)dT \quad \text{(A2)}$$

Using this last relation, the enthalpy integral can be simplified to:

$$\int_{T_0}^{T}\frac{-H_m(p_0,T')}{T'^2}dT' = -\int_{T_0}^{T}\frac{H_m(p_0,T_0)+\int_{T_0}^{T'}C_p(T^*)dT^*}{T'^2}dT' \quad \text{(A3)}$$

For the case of Mars, we can consider the heat capacity as a constant, $C_p = C_p(T)$, being able to extract it from the integral and obtaining (see the discussion for hot exoplanets later):

$$-\int_{T_0}^{T}\frac{H_m(p_0,T_0)+C_p(T'-T_0)}{T'^2}dT' =$$

$$-\int_{T_0}^{T}\frac{H_m(p_0,T_0)-C_pT_0+C_pT'}{T'^2}dT' =$$

$$-(H_m(p_0,T_0)-C_pT_0)\int_{T_0}^{T}\frac{1}{T'^2}dT' - C_p\int_{T_0}^{T}\frac{1}{T'}dT' =$$

$$+(H_m(p_0,T_0)-C_pT_0)\left[\frac{1}{T}-\frac{1}{T_0}\right] - C_p\ln\frac{T}{T_0} \quad \text{(A4)}$$

Using (A4) and (A1), we obtain an useful approximation for the calculation of the chemical potential at the Martian environment

$$\mu(p,T) = \frac{T}{T_0}\mu(p_0,T_0) + T\cdot(H_m(p_0,T_0)-C_pT_0)\left[\frac{1}{T}-\frac{1}{T_0}\right]$$

$$-C_pT\ln(\frac{T}{T_0}) + RT\ln(p/p_0) \quad \text{(A5)}$$

When the temperature is T=T_0, the above expression is reduced to the more familiar equation:

$$\mu(p,T_0) = \mu(p_0,T_0) + RT_0\ln(p/p_0) \quad \text{(A6)}$$

However, as has been explained in Section 2, this expression is only useful for situations where the temperature is close to the standard temperature of reference (usually 298 K), i.e., the Earth environment. When the temperatures are different, the complete expression for the chemical potential is needed.

Equation A5 represents an useful approximation for those environments where the temperature variations are not large and the heat capacity can be considered as constant. For Venus and hot exoplanets a more detailed expression might be needed.

The temperature dependence of the heat capacity is usually expressed as a polynomial function with tabulated constants:

$$C_p(T) = a + bT + cT^2 \quad \text{(A7)}$$

and the molar enthalpy at an arbitrary temperature reads now:

$$H(p_0,T) = H(p_0,T_0) + \int_{T_0}^{T} a + bT + cT^2dT$$

$$H(p_0,T) = H(p_0,T_0) - (aT_0 + \frac{b}{2}T_0^2 + \frac{c}{3}T_0^3) + (aT' + \frac{b}{2}T'^2 + \frac{c}{3}T'^3) \quad \text{(A8)}$$

The enthalpy integral in Eq. A1 becomes:

$$\begin{aligned}&\int_{T_0}^{T}\frac{-H_m(p_0,T')}{T'^2}dT' = \\ &-\left(H(p_0,T_0)-(aT_0+\frac{b}{2}T_0^2+\frac{c}{3}T_0^3)\right)\int_{T_0}^{T}\frac{1}{T'^2}dT' \\ &-\int_{T_0}^{T}\frac{(aT'+\frac{b}{2}T'^2+\frac{c}{3}T'^3)}{T'^2}dT' = \\ &+\left(H(p_0,T_0)-(aT_0+\frac{b}{2}T_0^2+\frac{c}{3}T_0^3)\right)\left[\frac{1}{T}-\frac{1}{T_0}\right] \\ &-a\ln\left(\frac{T}{T_0}\right)-\frac{b}{2}(T-T_0)-\frac{c}{6}(T^2-T_0^2)\end{aligned} \quad \text{(A9)}$$

Note that when we consider C_p = constant, i.e., b and c = zero and C_p = a, the expression A9 is reduced to A4.

We can use A9 into the chemical potential formula detailed in A1 and obtain a general equation for the chemical potential for an arbitrary pressure and temperature, useful for any planetary atmosphere:

$$\mu(p,T) = \frac{T}{T_0}\mu(p_0,T_0) + T\cdot\int_{T_0}^{T}\frac{-H_m(p_0,T')}{T'^2}dT' + RT\ln(p/p_0)$$

$$\begin{aligned}\mu(p,T) =& \frac{T}{T_0}\mu(p_0,T_0) + RT\ln(p/p_0) + \\ &-T\left(H(p_0,T_0)-(aT_0+\frac{b}{2}T_0^2+\frac{c}{3}T_0^3)\right)\left[\frac{1}{T}-\frac{1}{T_0}\right] \\ &-aT\ln\left(\frac{T}{T_0}\right)-\frac{b}{2}T(T-T_0)-\frac{c}{6}T(T^2-T_0^2)\end{aligned} \quad \text{(A10)}$$

Although these equations have been obtained by direct integration of the chemical potential equation, it is important to remark that it is possible to obtain the same equations by Legendre transformations. By definition, the Gibbs potential function is given as:

$$G = H - TS \quad \text{(A11)}$$

The G function is called chemical potential in the case of one mol, and including the proper dependence of pressure and temperature in the equation, we can write:

$$\mu(p,T) = h(p,T) - T\cdot s(p,T) \quad \text{(A12)}$$

The determination of the enthalpy and entropy at different (p,T) can be done using:

$$h(p,T) = h(p_0,T_0) + \left[\int_{T_0}^{T}C_pdT\right]_{p_0} + \left[\int_{p_0}^{p}-\mu_{JT}C_pdp\right]_{T}$$

$$s(p_0,T) = s(p_0,T_0) + \left[\int_{T_0}^{T} \frac{C_p}{T} dT\right]_{p_0} - \left[\int_{p_0}^{p} \left(\frac{\partial V}{\partial T}\right)_p dp\right]_T$$

where μ_{JT} is the Joule-Thompson coefficient

$$\mu_{JT} = \left(\frac{\partial T}{\partial P}\right)_H = \frac{V}{C_p}(\alpha T - 1)$$

and α is the volumetric thermal expansion coefficient, $\frac{1}{V}\left(\frac{\partial V}{\partial T}\right)_p$; for an ideal gas is easy to prove that $\alpha = \frac{1}{T}$, and therefore $\mu_{JT} = 0$.

If we consider the first step in Figure 1, i.e., the variation in temperature without any changes in the pressure, and knowing the enthalpy and entropy variations on temperature (considering C_p as constant):

$$\mu(p_0,T) = h(p_0,T_0) + C_p(T-T_0) - T\cdot s(p_0,T_0) - C_pT\ln(\frac{T}{T_0}) \quad \text{(A13)}$$

We consider now the second step in Figure 1, the pressure variation. The Joule-Thompson coefficient is zero for an ideal gas and therefore the pressure term in the enthalpy becomes zero, being the pressure dependence due to the entropy expression. The final equation for the chemical potential reads:

$$\mu(p,T) = h(p_0,T_0) - T\cdot s(p_0,T_0) + C_p(T-T_0) - C_pT\ln(\frac{T}{T_0}) + RT\ln(\frac{p}{p_0}) \quad \text{(A14)}$$

It is trivial to prove that Equation A6 and Equation A14 are in fact the same equation where $\mu(p_0,T_0) = h(p_0,T_0) - T_0\cdot s(p_0,T_0)$.

Appendix B: Reaction list

In Table 5 we show the chemical reactions considered in this work.

Table 5. List of reactions in the photochemical model

1	$O + O_2 + CO_2$	$\rightleftarrows$	$O_3 + CO_2$
2	$O + O + CO_2$	$\rightleftarrows$	$O_2 + CO_2$
3	$O + O_3$	$\rightleftarrows$	$O_2 + O_2$
4	$O(1d) + CO_2$	$\rightleftarrows$	$O + CO_2$
5	$O(1d) + H_2O$	$\rightleftarrows$	$OH + OH$
6	$O(1d) + H_2$	$\rightleftarrows$	$OH + H$
7	$O(1d) + O_2$	$\rightleftarrows$	$O + O_2$
8	$O(1d) + O_3$	$\rightleftarrows$	$O_2 + O_2$
9	$O(1d) + O_3$	$\rightleftarrows$	$O_2 + O + O$
10	$O(1d) + CH_4$	$\rightleftarrows$	$CH_3 + OH$
11	$O(1d) + CH_4$	$\rightleftarrows$	$CH_3O + H$
12	$O(1d) + CH_4$	$\rightleftarrows$	$CH_2O + H_2$
13	$O + HO_2$	$\rightleftarrows$	$OH + O_2$
14	$O + OH$	$\rightleftarrows$	$O_2 + H$
15	$H + O_3$	$\rightleftarrows$	$OH + O_2$
16	$H + HO_2$	$\rightleftarrows$	$OH + OH$
17	$H + HO_2$	$\rightleftarrows$	$H_2 + O_2$
18	$H + HO_2$	$\rightleftarrows$	$H_2O + O$
19	$OH + HO_2$	$\rightleftarrows$	$H_2O + O_2$
20	$HO_2 + HO_2$	$\rightleftarrows$	$H_2O_2 + O_2$
21	$OH + H_2O_2$	$\rightleftarrows$	$H_2O + HO_2$
22	$OH + H_2$	$\rightleftarrows$	$H_2O + H$
23	$H + O_2 + CO_2$	$\rightleftarrows$	$HO_2 + CO_2$
24	$O + H_2O_2$	$\rightleftarrows$	$OH + HO_2$
25	$OH + OH$	$\rightleftarrows$	$H_2O + O$
26	$OH + O_3$	$\rightleftarrows$	$HO_2 + O_2$
27	$HO_2 + O_3$	$\rightleftarrows$	$OH + O_2 + O_2$
28	$HO_2 + HO_2 + CO_2$	$\rightleftarrows$	$H_2O_2 + O_2 + CO_2$
29	$OH + OH + CO_2$	$\rightleftarrows$	$H_2O_2 + CO_2$
30	$H + H + CO_2$	$\rightleftarrows$	$H_2 + CO_2$
31	$NO_2 + O$	$\rightleftarrows$	$NO + O_2$
32	$NO + O_3$	$\rightleftarrows$	$NO_2 + O_2$
33	$NO + HO_2$	$\rightleftarrows$	$NO_2 + OH$
34	$OH + CO$	$\rightleftarrows$	$CO_2 + H$
35	$O + CO + M$	$\rightleftarrows$	$CO_2 + M$

5

Evaluation of the Mars atmospheric chemical entropy production

Para poder mantener la biosfera terrestre se necesitan tanto energía como una situación de desequilibrio termodinámico que permitan crear y mantener estructuras complejas emergentes.

Las condiciones de desequilibrio para la existencia de vida no tienen por qué ser particulares de la Tierra, y pueden extenderse a Marte. En este capítulo, he desarrollado un modelo termoquímico de la atmósfera marciana y he estudiado el desequilibrio causado por reacciones químicas. Para ello, he analizado la producción de entropía de las principales reacciones en su atmósfera y he comparado sus valores cerca de la superficie con los de la Tierra. De esta comparación se deduce que la cantidad de entropía producida por tan solo la reacción de recombinación de O_3 ($O + O_2 + M \rightleftharpoons O_3 + M$) en la atmósfera de la Tierra es más grande que la entropía producida por todas las reacciones químicas dominantes consideradas para la atmósfera de Marte. Este resultado es consecuencia de la baja densidad y la pobre variedad de especies de la atmósfera marciana.

Si se necesita desequilibrio para crear y mantener estructuras complejas en un sistema, en este capítulo se concluye que las reacciones químicas atmosféricas en Marte no permiten mantenerlas como ocurre en la Tierra, aunque no excluye que pueda haber otras fuentes de desequilibrio termodinámico en el planeta.

6

Martian top of the atmosphere 10-to 420 nm spectral irradiance database and forecast for solar cycle 24

La cuantificación de la radiación que llega a lo alto de la atmósfera (TOA, por sus siglas en inglés) de Marte es de interés en una variedad amplia de campos como estudios de habitabilidad, la exploración espacial, la modelización del clima, y el diseño de naves espaciales. Tiene impacto en la física y la química de la atmósfera y el suelo. A pesar de la existencia de bases de datos de la radiación UV que llega a la atmósfera de la Tierra, basadas en los datos recogidos por instrumentos espaciales que orbitan nuestro planeta, no existe información similar para Marte.

En este capítulo presento una base de datos de la irradiancia espectral en la capa superior de la atmósfera de Marte para el ciclo solar 24 (periodo comprendido entre los años 2008 y 2019), que contiene los valores diarios de irradiancia entre 10 y 420 nm. Puesto que la radiación procedente del Sol no es completamente isotrópica, con el fin de eliminar las características geométricas de la posición de la Tierra pero ser capaces de capturar las características generales de la etapa del ciclo solar, en esta base de datos damos valores promedios de 3, 7 y 15 días para cada longitud de onda.

Martian Top of the Atmosphere 10-to 420 nm spectral irradiance database and forecast for solar cycle 24

Alfonso Delgado-Bonal[a,b,*], María-Paz Zorzano[c], F. Javier Martín-Torres[b,d]

[a] *Institute of Fundamental Physics and Mathematics, University of Salamanca, Pza de la Merced s/n, 37008, Spain*
[b] *Division of Space Technology, Department of Computer Science, Electrical and Space Engineering, Luleå University of Technology, Kiruna, Sweden*
[c] *Centro de Astrobiología (INTA-CSIC), Ctra. Ajalvir km.4, Torrejón de Ardoz, 28850, Madrid, Spain*
[d] *Instituto Andaluz de Ciencias de la Tierra (CSIC-UGR), Avda. de Las Palmeras n 4, Armilla, 18100, Granada, Spain*

Abstract

Ultraviolet radiation from 10- to 420-nm reaching Mars top of the atmosphere (TOA) and surface is important in a wide variety of fields such as space exploration, climate modeling, and spacecraft design, as it has impact in the physics and chemistry of the atmosphere and soil. Despite the existence of databases for UV radiation reaching Earth TOA, based in space borne instrumentation orbiting our planet, there is no similar information for Mars. Here we present a Mars TOA UV spectral irradiance database for solar cycle 24 (years 2008-2019), containing daily values from 10- to 420-nm. The values in this database have been computed using a model that is fed by the Earth-orbiting Solar Radiation and Climate Experiment (SORCE) data. As the radiation coming from the Sun is not completely isotropic, in order to eliminate the geometrically related features but being able to capture the general characteristics of the solar cycle stage, we provide 3-, 7- and 15- days averaged values at each wavelength. Our database is of interest for atmospheric modeling and spectrally dependent experiments on Mars, the analysis of current and upcoming surface missions (rovers and landers) and orbiters in Mars. Daily values for the TOA UV conditions at the rover Curiosity location, as well as for the NASA Insight mission in 2016, and ESA/Russia ExoMars mission in 2018 are provided.

Keywords:
Mars TOA, UV radiation, REMS, Space exploration

1. Introduction

Ultraviolet (UV) radiation covers the range from 10- to 400-nm of the electromagnetic spectrum and is usually divided into different channels with different implications for atmospheric sciences and engineering. The determination of the solar UV radiation reaching the planets is of importance in a range of scientific and engineering disciplines, and it is a driving force of chemical, organic and biological evolution, being a key factor in climate modeling.

Although UV radiation energy is less than 3% of all solar radiation reaching the Earth, and the total solar irradiance varies by about 0.1% during the course of the solar cycle, the spectral features change in the course of a solar cycle and these variations are highly significant in terms of its effects on climate modeling or biological responses. For example, photochemistry in the atmosphere is very sensitive to small changes in UV radiation, being this radiation the driver of ozone chemistry on Earth [1] and one of the potential triggers of methane on Mars [2].

The solar cycle is the periodic change in the Sun's activity with an average duration of about 11 years. During the cycle, the levels of solar radiation and ejection of solar material change, with visible manifestations such as the number of sunspots or flares. Those changes have implications in space weather, and on Earth's and other planets weather and climate. Figure 1 shows the 11 years variability of the Sun measured by the Solar Radiation and Climate Experiment (SORCE) mission. The Total Solar Irradiance (TSI) is represented in W/m^2 from 2003 to 2014, showing the change in the irradiation from the Sun that reaches the Earth. The changes in the TSI are also accompanied by changes in individual wavelengths or spectral regions. Besides the 11 years cycle, aperiodic fluctuations are also a component of solar variation. Solar variability in the UV is a result of the growth and decay of active regions and other features on the Sun and are distributed unevenly over the surface of the Sun.

As the radiation reaching a planet is a dynamical feature, it is important to know the most precise values possible. The UV radiation has been monitored on Earth's surface and Top of the Atmosphere (TOA) extensively and treated as a key environmental and health parameter [3]. One of the most complete Earth's TOA UV radiation databases available has been provided by the NASA Solar Radiation and Climate Experiment (SORCE) experiment [4]. SORCE was launched in January 2003 and is still operating and measuring the total solar irradiance (TSI) and solar spectral irradiance from 1 nm to 2000 nm, accounting for 95% of the spectral contribution to the TSI.

*Corresponding author:
Email address: alfonso.delgado-bonal@ltu.se (Alfonso Delgado-Bonal)

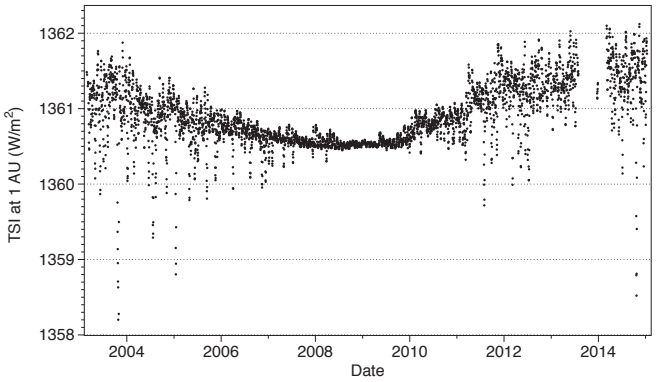

Figure 1: Total Solar Irradiance (TSI) data in W/m^2 since 2003 to 2014 from SORCE mission at 1 AU.

Despite the existence of this and other databases for Earth, there are not available UV radiation databases for other planets, particularly Mars. To solve this lack of data, standard radiation spectra scaled for Mars have been used in atmospheric and engineering research, such as the Thuillier spectra [5], but these spectra do not allow to study cyclic variations in spectral irradiance on Mars.

On Mars, photochemistry is mainly driven by wavelengths lower than 200 nm, involving CO_2 and H_2O of the atmosphere. The martian atmosphere is composed by 98% of CO_2, which has absorption bands between 210 -190 nm, and also between 180 - 135 nm and 125 - 120 nm. H_2O is also present in the martian atmosphere and its photolysis is the driver of ozone photochemistry for example. H_2O has absorption bands in 166.5 nm and 125 nm, although the 200 nm and 266 nm bands are also important; even lower wavelengths such as the 56 nm absorption band are important for photochemistry on Mars.

Wavelengths from 200- to 400 nm are also important in the study of other atmospheric compounds such as ozone, or to the analysis of dust and biology responses on Mars. The increment of UV-B (280-320 nm) is known to impair essential biological processes [6][7]. The UV-C (200-280 nm) radiation is specially harmful for living beings, causing high damage even in low doses [8]. This radiation is blocked in Earth's atmosphere mainly by oxygen and ozone, blocking the radiation at different wavelengths (the Hartley bands between 200 and 300 nm, the Huggins bands between 320 and 360 nm and the Chappuis bands between 375 and 650 nm). UV-B and UV-A (320-400 nm) radiation cause also damage to cells, and they are also biologically interesting because of their effects as photosynthesis inhibitors and their relation with carbon fixation [9], among others.

The aim of this paper is to provide a daily UV radiation database for Mars TOA for Solar Cycle 24 (2008-2019) representative of the solar stage in the solar cycle and orbital position of the planet. For this purpose we have used the data from the SORCE mission and the UV model developed by Woods and Rottman (W-R) [10] to compute the radiation reaching Mars TOA for solar cycle 24 (2008 - 2019) in the spectral range 10 - 420 nm with an step of $\Delta\lambda$ = 1 nm interval.

In Section 2 we explain the procedure followed to generate the UV database reaching the martian Top of the Atmosphere. The database is divided in two different sections for the solar cycle 24. In the first section, covering the years from 2008 to 2013, we have used the SORCE mission data to calculate the radiation reaching Mars TOA. Although the SORCE mission is one of the most complete databases containing UV radiation, there are some gaps in the wavelengths and the mission has been turned off during some days. To complete the database, we have compared the SORCE mission data with the W-R model and analysed the standard deviation of the model, which allows us to improve the W-R model and fill the gaps in the database.

The second section of the database covers the years from 2014 to 2019. Using the improved version of the W-R model, and the predicted values of the solar radio flux at 10.7 cm index (F10.7) [11], we generate a database containing daily UV radiation from 10- to 420 nm for Mars TOA. The aim of this prediction is to generate a database that can be used as reference for the data analysis of the Curiosity rover (currently on Mars) and the upcoming missions Insight (2016) and Exomars (2018).

In Section 3 we present the main results of the model for the maximum and the minimum of the Solar Cycle, as average values within 10 nm intervals and also as integrated values for UV-C, UV-B and UV-A. The radiation coming from the Sun is not exactly isotropic and has daily variations. The presence of aperiodic events such as sunspots or solar storms generates variations in the emission. Those emissions can reach the Earth and be measured by satellites, but not necessarily reach Mars. In order to eliminate those daily features in the first section of our database, we provide not only extrapolated values of each wavelength but also averaged values of 3-, 7-, and 15- days, with the intention to modulate the daily variations but capture the cyclic stages of the Sun. We compare the results of our model with the widely used Thuillier spectra [5] to show the importance of taking into account the solar cycle in UV radiation reaching Mars TOA.

Using our generated values of UV radiation, in Section 3.1 we compare the modelled Mars TOA spectral irradiance with UV in-situ measurements taken during the period 2011-2013 by the instrument REMS (Rover Environmental Meteorological Station) onboard the Curiosity rover in Mars [12][13], being able to provide values of the opacity of the atmosphere. In Section 3.2 we provide values for locations of the upcoming surface missions to Mars, to be used as a tool in the design and test of the instruments on-board. Other applications can be derived from our database, as for example the use of UV radiation to produce solar energy in the planet. Although UV solar cells are not widely spread on Earth due to the presence of strong absorbers in the atmosphere, it could be an interesting alternative for martian environment.

Finally, in Section 4 we summarize the results and explain the range of applicability and the structure of the data of our database. It contains values of the martian TOA UV radiation in a daily basis, and 3-, 7- and 15- days averaged values, for different latitudes from 2008 to 2019, and is freely available at the site www.planetarysci.com/UV_Irradiance/Mars/.

2. The model

The Solar Radiation and Climate Experiment (SORCE) mission was launched in 2003 to enable solar-terrestrial studies by providing precise daily measurements of the total solar irradiance (TSI) and the solar spectral irradiance (SSI) at wavelengths extending from the UV to the near infrared (1-2000 nm) [14]. The SORCE mission is still operating and is managed by the Laboratory for Atmospheric and Space Physics (LASP), University of colorado. The SORCE database is publicly accessible at `http://lasp.colorado.edu/lisird/sorce/` .

The spectral range measured by the SORCE (1-2000 nm) includes UV radiation with an excellent precision ([4],[15]), and it has been used to validate models [16] and evaluate the effect of UV radiation variations on climate modeling [17].

There are no similar missions orbiting Mars, so we have developed a model to provide values of the Mars TOA UV spectral irradiance for solar cycle 24 (2008 - 2019), between 10 and 420 nm. As solar cycle 24 is currently on-going, we have separated our database in two parts: the first part is based in SORCE data and provides values of past UV radiation on Mars from 2008 to 2013, and the second part is based on W-R model along with the predicted solar radio flux at 10.7 cm (F10.7 index) and covers the years 2014-2019.

The first section of the database is based on the extrapolation of the SORCE data to Mars TOA. Despite the fact that the SORCE database contains spectral irradiance values at 1 AU for almost every wavelength from 2008 to 2013, there are some gaps. These gaps include missing wavelengths in particular days, or the fact that SORCE mission has been deactivated during some days for maintenance. As our intention is to provide a complete database for Mars, we have filled those gaps in the database with values from the Woods-Rottman (W-R) model.

The Woods-Rottman model feeds with the daily and monthly F10.7 index, and its calculations are very precise. The solar radio flux at 10.7 cm (2800 MHz) has been used since 1947 and is an excellent indicator of solar activity. The F10.7 radio emissions are features of the chromosphere and the corona of the solar atmosphere, and it is correlated with the sunspot number as well as a number of ultraviolet and visible solar irradiance records. Measured in a day-to-day basis from the Earths surface, the F10.7 index has proven very valuable in specifying and forecasting space weather, and provides climatology of solar activity over the last six solar cycles.

Although W-R model gives very approximate values, when we compare the SORCE database with the results of the model, we obtain slight differences between them. In order to fill the gaps in the SORCE database, we have compared the values in the SORCE database with the values of the Woods-Rottman model during the period 2008-2013, and computed the mean deviation of the model at each wavelength.

Those mean deviations were used to correct the values of the W-R model and fill the gaps for those days in which the SORCE database lacks data, being able to reproduce the expected behaviour of the curve. In the occasional cases where a value of the spectral irradiance is missing in all the SORCE database for a given wavelength, the mean deviation of the closest wavelength was used to correct the model. In this way, we obtain a complete database that can be extrapolated to Mars. In Figure 2 we show an example of the integrated UV radiation between 220-280 nm computed with SORCE data (black line) and with the W-R model (blue line). It is possible to see that the SORCE database contains gaps in specific days and the line is dashed. Using the W-R model and the mean deviation, our database (red line) is able to reproduce the expected behaviour and fill those gaps to have a continuous and smooth curve.

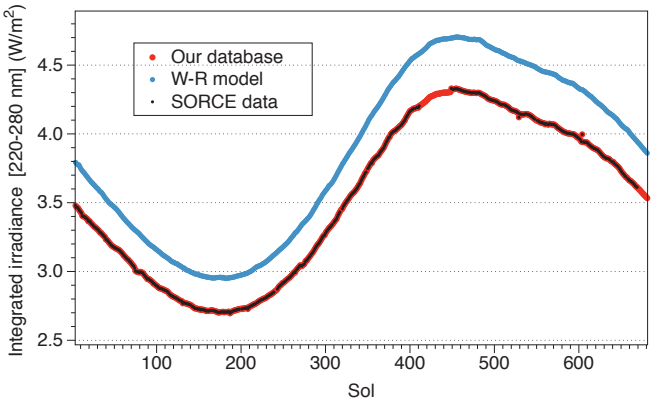

Figure 2: UV integration between 220 - 280 nm using the SORCE data (black line), W-R model (blue line) and our database (red line). It is possible to see a gap in the SORCE data that is filled in out database using the W-R model and the mean deviation of the previous days.

We have modelled the orbit of Mars to calculate its distance from the Sun as a function of Solar Longitude, the angle between Mars-Sun measured from the Northern Hemisphere (being the summer solstice Ls=90, the autumn equinox Ls=180, the winter solstice Ls=270 and the spring equinox Ls=360). One of the main parameters determining the spectral irradiance on Mars TOA is the position of the planet in the orbit. Unlike the Earth, Mars orbit is not close to a circular orbit (eccentricity 5.58 times greater), which implies a change in the TSI between Mars aphelion and perihelion of about 45%. This implies that the relative differences of the radiation reaching the planet during an orbit are larger than on Earth, creating a larger difference among season temperatures.

Once the distance is determined, the spectral irradiance reaching it is extrapolated as:

$$I_\lambda = I_{\lambda,0} \cdot \frac{1}{R^2_{Mars}} \tag{1}$$

where $I_{\lambda,0}$ is the spectral irradiance at 1 AU measured by SORCE and R^2_{Mars} is the instantaneous Sun-Mars distance expressed in AU. The instantaneous position of Mars in its orbit can be determined using its semi-major axis and eccentricity [18]. The irradiance at a particular position on Mars TOA is calculated as:

$$I_{\phi,\lambda} = I_\lambda \cdot \cos(z) \tag{2}$$

where ϕ is the latitude and z is the zenith angle of the incident solar radiation. The radiation reaching the martian TOA

will depend on the latitude of the selected location and on the position of the planet in the orbit. These dependences are implicit in the zenith angle, which is calculated as:

$$Cos(z) = \sin(\phi)\sin(\delta) + \cos(\phi)\cos(\delta)\cos(h) \quad (3)$$

where δ is the declination, calculated as:

$$\delta = Arcsin(\sin(e) \cdot \sin(Ls)) \quad (4)$$

In summary, for the first section of the database (2008-2013) we have followed the following steps: 1) to model the orbit of Mars from 2008 to 2013; 2) to calculate the daily distance between Mars and the Sun; 3) to compute the spectral irradiance at 1 AU using the Woods-Rottman model with measured F10.7 data; 4) to estimate the mean deviation of the spectral irradiance between the model and SORCE data at each wavelength; 5) to use the Woods-Rottman values corrected by the mean deviation to fill the gaps in the SORCE database; 6) to compute the spectral irradiance reaching Mars TOA.

In addition to our calculations of the spectral irradiance for the period 2008-2013, we provide a prediction of the solar spectral irradiance reaching Mars TOA until 2019, based in the prediction of the solar flux and the position of the planet in its orbit. For that we use the accepted monthly average and daily F10.7 radio flux available at the NOAA Space Weather Prediction Center (SWPC) website [11]. The prediction of the F10.7 for solar cycle 24 is provided by the Solar Cycle Prediction Panel representing the National Oceanic and Atmospheric Administration (NOAA), the International Space Environmental Services (ISES), and NASA.

The results of these calculations constitute the second part of our database, which has the intention to be a tool for current and future missions to Mars and for scientific studies of the planet. For the calculations of this second part (2013-2019), we have used the mean deviation between real data and the results of the code computed in the 2008-2013 interval to correct the values of the W-R model. The algorithm used for the second par of the database is: 1) to model the orbit of Mars from 2013 to 2019; 2) to calculate the daily distance between Mars and the Sun; 3) to compute the spectral irradiance at 1 AU using the Wood-Rottman model with predicted F10.7 data; 4) to correct the Wood-Rottman values with the mean deviation at each wavelength obtained in the first section of the database; 5) to compute the spectral irradiance reaching Mars TOA.

As a result of the model the UV spectral irradiance (10-420 nm) reaching Mars Top of the Atmosphere has been calculated in a daily basis for Solar Cycle 24 (years 2008-2019). A summary of the results and some examples of its application are presented in Section 3.

Solar radiation is not totally isotropic and contains daily features that are dependent on the geometrical location of the observer, such as solar storms or sunspots. These daily variations were measured by SORCE at the Earth's position, but not necessarily reached the martian atmosphere. In order to eliminate those daily variations but capture the global solar features at a particular stage of the solar cycle, we provide values not only

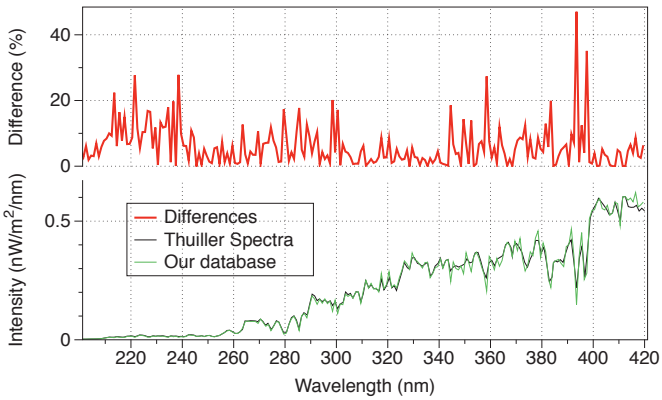

Figure 3: Bottom: Comparison between Thuiller's generic spectra geometrically scaled to Mars position (red) and the spectra from our model (green) for Ls = 0° (2012/03/29). Top: Relative differences in % between our model and Thuiller Spectra calculated as $\left(\frac{Our\ model - Thuiller}{Our\ model} \cdot 100\right)$. Note the intensity differences at wavelengths 393 nm and 397 nm due to the Ca II and K lines.

of the daily extrapolated spectral irradiance, but also the averaged values of 3-, 7- and 15- days. In this way, the user is able to choose those values that better fit their research interest, and obtain, in general, better results than using standard spectra.

3. Applications

In this section, we show the results of the model and examples of the use of the database. The radiation reaching the TOA is dependent on the position of the planet in the orbit, the latitude of the observer, and also depends on the stage of the Sun in the solar cycle. A summary of the results of the model for Ls 90, Ls 180, Ls 270 and Ls 360 for the maximum and the minimum of the solar cycle is presented in Tables 1, 2 and 3. The starting point of the Solar Cycle 24 has been taken as the minimum value, the Martian year 29 (2008/2009), and we use the Martian year 31 (2012/2013) as maximum of this cycle.

The knowledge of the spectral irradiance allows the integration in spectral ranges. Tables 1 and 2 show the spectral integration of channels UV-C (200-280 nm), UV-B (280-320 nm) and UV-A (320-400 nm) for different Ls. The differences between the maximum and the minimum in UV radiation are relatively small over the year. These differences can be seen in Table 3.

To solve the lack of a martian UV database, Thuiller proposed two different generic spectra to be used in martian research, for the maximum and minimum of the solar cycle. With this database, we pretend to go further and expand the availability of data for the community. In Figure 3 we compare the spectra generated with our model versus the generic Thuillier spectra. This figure underlines the need of using a database for different stages of the solar cycle instead of using generic spectra. Although the shapes of the spectra are quite similar, the spectral differences can be up to 50% of the intensity as a consequence of the Ca II and K solar lines at 393 and 397 nm for example. These lines have a strong variability over the 11-years solar cycle and must be considered in atmospheric sciences and

Wavelength	Ls 90	Ls 180	Ls 270	Ls 360
UV-C	2.0284	2.9864	3.1008	2.6390
UV-B	6.2971	9.2463	9.6242	8.1594
UV-A	25.8183	37.9033	39.567	33.6188

Table 1: Total daily irradiances in the UVC, UVB and UVA spectral ranges for the solar cycle 24 maximum (2012/2013) in W m^{-2}

Wavelength	Ls 90	Ls 180	Ls 270	Ls 360
UV-C	2.0100	2.9573	3.0789	2.6178
UV-B	6.2911	9.2736	9.6488	8.1984
UV-A	25.715	37.7878	39.4229	33.4826

Table 2: otal daily irradiances in the UVC, UVB and UVA spectral ranges for the solar cycle 24 minimum (2008/2009) in W m^{-2}

Wavelength	Ls 90	Ls 180	Ls 270	Ls 360
UV-C	0.9080%	0.9761 %	0.7042%	0.8036%
UV-B	0.0956%	-0.2958 %	-0.2555%	-0.4773 %
UV-A	0.3973%	0.3048 %	0.3652%	0.4052%

Table 3: Spectral irradiance daily differences between maximum and minimum for Solar Cycle 24, calculated as $\frac{max - min}{max} \cdot 100$

engineering research. In general, the variations are smaller than that, usually between 5-10%, but still important to be taken into account. These variations on UV radiation have, for example, the potential to produce changes on ozone chemistry [1], which in turn has implications in water vapor and methane amount in the atmosphere of Mars. This database provides a tool to analyze those changes on Mars atmosphere that cannot be anaysed using generic spectra.

3.1. Calculation of opacity after REMS/Curiosity data

The REMS UV sensor consists of one SiC photodiode dedicated to the UV spectrum 200-380 nm together with 5 filtered photodiodes for narrower band channels [12][13]. During the day, as the Sun moves in the sky, the measured UV spectral irradiance varies from diffuse irradiance in the morning, to global irradiance close to noon (when the direct Sun beam is within the field of view of the photodiodes), and diffuse irradiance again in the afternoon. The downwelling solar UV irradiance interacts with the atmospheric molecules and dust as it goes from the top of the atmosphere to the surface. Variations in the downwelling irradiance can be used to characterize the properties of the atmosphere and for this a precise knowledge of the UV irradiance at TOA is critical. In particular the aerosol content of the atmosphere can be retrieved by measuring the opacity at a given wavelength (when this parameter is evaluated at visible wavelengths is usually referred to as optical depth):

$$\tau(\lambda) \cdot Cos(SZA) = -\ln \frac{I_{dir}(\lambda)}{I^S_{TOA}(\lambda)} \quad (5)$$

Here SZA is the Solar Zenith Angle at the moment of observation. The above expression describes the exponential decay of the solar incident radiation at the Top Of the Atmosphere (TOA), $I^S_{TOA}(\lambda)$. Here $I_{dir}(\lambda)$ is the direct component of irradiance, i.e. the radiation that reaches the surface in the direct path from the Sun. Photons of the direct component have passed straightly through the atmosphere. The remaining photons, after interacting with the atmospheric constituents, have been either scattered away from the direct path (and thus form part of the diffuse irradiance) or have been absorbed.

TOA (220-380) nm [W/m2]	40,78
Global UV-ABC_{max} at Gale [W/m2]	19,45
Diffuse UV-ABC_{max} at Gale [W/m2]	3,28
SZA at Maximum global irradiance	13
Estimated UV opacity	0,86

Table 4: TOA irradiance with REMS UV-ABC 220-380 nm surface measurements: Mars UV atmospheric absorption in the ABC band integrated range of 220-380 nm at Gale on Ls=180 (sol 55 of MSL operation on Mars). (Per second???)

Table 4 shows an example of the UV radiative transfer properties of the atmosphere on Mars at the beginning local Spring (Ls 180) where the TOA ABC irradiance is compared with the surface measured value global (i.e. direct plus diffuse) and diffuse UV irradiance.

With the knowledge of the radiation reaching the Top of the Atmosphere, it is possible to calculate the opacity of the atmosphere of Mars with an excellent precision. The estimated UV opacity for this sol is consistent with the reported visible opacity provided by the Mastcam solar observation of the Curiosity rover for this Ls, tau=0.79-0.69, as well as the observed by the Opportunity rover [19].

3.2. Application to current and future surface missions to Mars

Here we present values for locations of special interest for present or future space exploration landing sites, including a prediction up to 2019, but values for other latitudes are located in the planetarysci.com web server. We have computed radiation values at the surface assuming an exponential attenuation

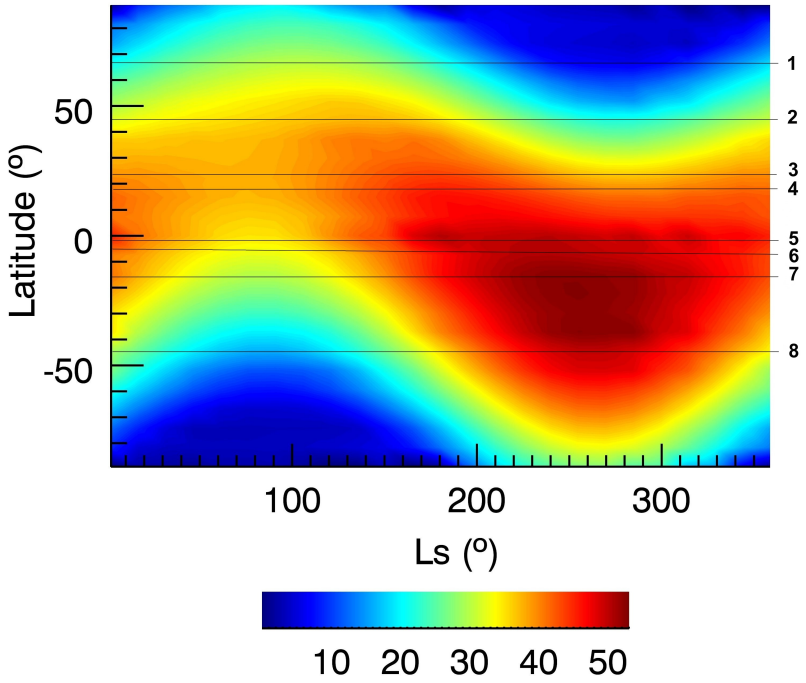

Figure 4: Integrated UV radiation between 200-400 nm (W/m^2) map on Mars TOA for the 2011/2013 complete orbit based on SORCE data geometrically scaled to Mars position. Marked in the figure are Mars mission landing latitudes 1: Phoenix (68N), 2: Viking 2 (48N), 3: Viking 1 (23N), 4: Pathfinder (19.30N), 5: Opportunity (-1.9S), 6: Curiosity (-4.5S), 7: Spirit (-14.5) and 8: Mars 3(45S).

with index $\tau = 0.3$, which is consistent with the minimum diode opacity (660-nm) measured by Vikings in a clear scenario (this gives a value of the upper bound dose reaching the surface) [20].

Gale crater (Curiosity Landing Site)

Tables 5 and 6 show the daily spectral irradiance average every 10 nm during the maximum (2012-2013) and the minimum (2008-2009) of the present solar cycle. The results in tables 5 and 6 were calculated for the Gale Crater location (4.49° S, 137.42°E), the Curiosity rover landing site. Although the differences between the integrated spectral irradiance during the maximum and the minimum are of the order of 1%, those small variations could be very important in planetary sciences [21]. These differences should be larger under high solar activity conditions. During a solar cycle, the total solar spectral irradiance variation is about 0.1%, but individual wavelengths could change their irradiance up to 60% [22], as can be seen in Figure 3.

Elysium Planitia (Insight landing site)

Table 7 shows the averaged spectral irradiance for the Martian year 34 (2017/2018) in the Elysium Planitia area every 10 nm (from 2.5 degrees South to 4 degrees North). This is the selected landing site for NASA's Insight mission in 2016. Table 7 represents a useful tool to predict the spectral irradiance on the area, important for scientific and engineering studies. More information about the landing site could be find in [23].

Figure 4 shows the UV radiation on Mars TOA in the 200 - 400 nm spectral region for a complete orbit at the Martian year 31 (2011/2013). The maximum value of the integrated radiation on Mars is 50 W/m^{-2}. During the summer, assuming clear sky conditions on Earth, the UV dosage for 12 hours ascends to 10 kJ/m^{-2}, which corresponds to 0.23 W/m^{-2} [24]. The almost complete absorption of UV-C radiation by oxygen and ozone limits the radiation reaching the Earth's surface, and its value is very low compared with the radiation on Mars surface. This radiation map of Mars TOA is correlated with the radiation reaching the surface. The knowledge of the UV radiation at TOA along with the absorbers in the atmosphere allows the study of the radiation field at surface.

4. Conclusions

UV radiation reaching Mars TOA has been computed for solar cycle 24 (2008-2019), based on real data provided by the SORCE mission and predicted values of solar radio flux F10.7 in a modified version of the Woods-Rottmann model. We present a database divided in two sections: with real data extrapolated to Mars (2008-2013) and predicted values based on the F10.7 index (2014-2019).

This database allows to take into account the effects of the solar cycle in the UV radiation. The changes in particular wavelengths could be up to 50%, and variations are usually between 5-20%.

Using the computed TOA values and the UV radiation measured by the REMS instrument on the Curiosity rover we have computed, as an academic example, the UV opacity for a particular day of REMS measurements. We obtain a value of the UV opacity (0.89) consistent with other measurements in Mars.

The Solar radiation is not completely isotropic. In order to eliminate the perturbations derived from a particular location, we present averaged values of 3-, 7- and 15- days, which provides a much better representation to the current stage in the solar cycle than generic spectra used nowadays.

The knowledge of UV radiation on Mars TOA allows the study of surface and atmospheric events on Mars. This database provides a tool for scientific and engineering investigations on Mars based on real data instead of temporally static tabulated spectra. The full daily database between 10 and 420-nm every 1-nm at different latitudes is available at www.planetarysci.com/UV_Irradiances/Mars/, as well as the averaged 3-,7-, and 15- days databases.

Acknowledgements

The first author wants to acknowledge the Luleå University of Technology in Kiruna, Sweden, for the scholarship award that partially funded this investigation. We also thanks to Tom Woods for providing the W-R model and to him and Jeffrey Harder for their comments about the gaps and status of the SORCE data.

5. References

[1] Merkel, A.W., Harder, J.W., Marsh, D.R., Smith, A.K., Fontenla, J.M., Woods, T.N., 2011. The impact of solar spectral irradiance variability on middle atmospheric ozone. Geophysical Research Letters 38, L13802, doi:10.1029/2011GL047561.

[2] Keppler, F., Vigano, I., McLeod, A., Ott, U., Frchtl, M., Rckmann, T., 2012. Ultraviolet-radiation-induced methane emissions from meteorites and the Martian atmosphere. Nature 486, 93-96.

[3] Ghetti, F., Checcucci, G., Bornman, J.F., 2006. Environmental UV Radiation: Impact on Ecosystems and Human Health and Predictive Models. Nato Science Series 57, 288.

[4] Rottman, G.J., Woods, T.N., McClintock, W., 2006. SORCE solar UV irradiance results. Advances in Space Research 37, 201-208.

[5] Thuillier, G., Hersé, M., Labs, D., Foujols, T., Peetermans, W., Gillotay, D., Simon, P.C., Mandel, H., 2003. The Solar Spectral Irradiance from 200 to 2400 nm as Measured by the SOLSPEC Spectrometer from the Atlas and Eureca Missions. Solar Physics 214, 1-22.

[6] Häder, D.P., Kumar, H.D., Smithc, R.C., Worrestd,R.C., 2007. Effects of solar UV radiation on aquatic ecosystems and interactions with climate change. Photochemical & Photobiological Sciences 6, 267-285.

[7] Häder, D.P., Helbling, E.W., Williamson, C.E, Worrest, R.C., 2011. Effects of UV radiation on aquatic ecosystems and interactions with climate change. Photochemical & Photobiological Sciences 10, 242-60.

[8] Lindberg, C., Horneck, G., 1991. Action spectra for survival and spore photoproduct formation of Bacillus subtilis irradiated with short-wavelength (200-300 nm) UV at atmospheric pressure and in vacuo. Journal of Photochemistry and Photobiology B: Biology 11, 69-80.

[9] Boucher, N., Prezelin, B.B., Evens, T., Jovine, R., Kroon, B., Moline, M.A., Schofield, O., 1994. Icecolors '93: Biological weighting function for the ultraviolet inhibition of carbon fixation in a natural antarctic phytoplankton community. Antarctic Journal Review 1994, 272-275.

[10] http://lasp.colorado.edu/rocket/rocket_results.html

[11] http://www.swpc.noaa.gov/ftpdir/weekly/Predict.txt

[12] Gómez-Elvira, J., Armiens, C., Castaner, L., Domínguez, M., Genzer, M., Gómez, F., Haberle, R., Harri, A-M., Jimenez, V., Kahanpää, H., Kowalski, L., Lepinette, A., Martínez-Frías, J., Martín, J., McEwan, I., Mora, L., Moreno, J., Navarro, S., de Pablo, M.A., Peinado, V., Pena, A., Polkko, J., Ramos, M., Renno, N.O., Ricart, J., Richardson, M., Rodríguez-Manfredi, J., Romeral, J., Sebastián, E., Serrano, J., de la Torre Juárez, M., Torres, J., Torrero, F., Urqui, R., Velasco, T., Verdasca, J., Zorzano, M.-P., Martín-Torres, F. J., 2012. REMS: an Environmental Sensor Suite for the Mars Science Laboratory. Space Science Reviews 170, 556.

[13] Gómez-Elvira, J., Armiens, C., Carrasco, I., Genzer, M., Gómez, F., Haberle, R., Hamilton, V.E., Harri, A-M., Kahanpää, H., Kemppinen, O., Lepinette, A., Martín-Soler, J., Martń-Torres, J., Martínez-Frías, J., Mischna, M., Mora, L., Navarro, S., Newman, C., de Pablo, M.A., Peinado, V., Polkko, J., Rafkin, S.C.R., Ramos, M., Rennó, N.O., Richardson, M., Rodríguez-Manfredi, J.A., Romeral Planelló, J.J., Sebastián, E., de la Torre Juárez, M.,Torres, J., Urquí, R., Vasavada, A.R., Verdasca, J., Zorzano, M.-P. 2014. Curiosity's Rover Environmental Monitoring Station: Overview of the First 100 Sols. Journal of Geophysical Research: Planets. Accepted manuscript, DOI: 10.1002/2013JE004576.

[14] Rottman, G., 2005. The SORCE Mission. In: Rottman, G., Woods, T. and George, V. (Eds.) The Solar Radiation and Climate Experiment (SORCE). Springer New York, pp. 7-25.

[15] Pankratz, C.K., Knapp, B.G., Fontenla, J.M. , Rottman, G.J., Woods, T.N., Harder, J.W., Kopp, G., McClintock, W.E., Snow, M., 2005. SORCE Solar Irradiance Data Products. AGU Spring Meeting Abstracts, B3

[16] Ball, W.T., Unruh, Y.C., Krivova, N.A., Solanki, S., Harder, J.W., 2011. Solar irradiance variability: a six-year comparison between SORCE observations and the SATIRE model. Astronomy & Astrophysics 530, A71.

[17] Ermolli, I., Matthes, K., Dudok de Wit, T., Krivova, N.A., Tourpali, K., Weber, M., Unruh, Y.C., Gray, L., Langematz, U., Pilewskie, P., Rozanov, E., Schmutz, W., Shapiro, A., Solanki, S.K., Thuillier, G., Woods, T.N., 2012. Recent variability of the solar spectral irradiance and its impact on climate modelling. Atmospheric Chemistry and Physics Discussions 12, 24557-24642.

[18] Levine, J.S., Kraemer, D.R., Kuhn, W.R., 1977. Solar radiation incident on Mars and the outer planets: Latitudinal, seasonal, and atmospheric effects. Icarus, 31, 136-145

[19] Lemmon, M.T., 2014. The Mars Science Laboratory optical depth record. Eighth International Conference on Mars. 1338 (abstract)

[20] http://atmos.pds.nasa.gov

[21] McKenzie, R. L., Bjorn, L. O., Bais, A., Ilyasd, M., 2003. Changes in biologically active ultraviolet radiation reaching the Earth's surface. Photochemical & Photobiological Sciences 2, 5-15.

[22] Krivova, N.A., Solanki, S.K., Floyd, L., 2006. Reconstruction of solar UV irradiance in cycle 23. Astronomy & Astrophysics 452, 631-639.

[23] Golombek, M., Redmond, L., Gengl, H., Schwartz, C., Warner, N., Banerdt, B., Smrekar, S., 2013. Selection of the Insight landing site: constrains, plans, and progress. 44th Lunar and Planetary Science Conference. 1691 (abstract)

[24] http://www.gse-promote.org/gallery/UV/dwd_forecast.htm

Wavelength (nm)	**Ls 90**	**Ls 180**	**Ls 270**	Ls **360**
1 - 10	1.1957×10^{-5}	2.3491×10^{-5}	1.2937×10^{-6}	1.6628×10^{-6}
10 - 20	2.1831×10^{-5}	3.6505×10^{-5}	5.4338×10^{-7}	1.1432×10^{-6}
20 - 30	2.2751×10^{-5}	4.0115×10^{-5}	4.7430×10^{-7}	8.2409×10^{-7}
30 - 40	2.4781×10^{-5}	4.0966×10^{-5}	7.0083×10^{-7}	1.1541×10^{-6}
40 - 50	5.1947×10^{-6}	8.3710×10^{-6}	4.0434×10^{-6}	3.6640×10^{-6}
50 - 60	4.1800×10^{-6}	6.5532×10^{-6}	5.7888×10^{-6}	5.1476×10^{-6}
60 - 70	3.7637×10^{-6}	5.9337×10^{-6}	5.4652×10^{-6}	4.8875×10^{-6}
70 - 80	4.0540×10^{-6}	6.3690×10^{-6}	5.9352×10^{-6}	5.2944×10^{-6}
80 - 90	9.5321×10^{-6}	1.4914×10^{-5}	1.4001×10^{-5}	1.2451×10^{-5}
90 - 100	1.1422×10^{-5}	1.7814×10^{-5}	1.6817×10^{-5}	1.4919×10^{-5}
100 - 110	1.0314×10^{-5}	1.6081×10^{-5}	1.5188×10^{-5}	1.3471×10^{-5}
110 - 120	8.0661×10^{-6}	1.2741×10^{-5}	1.1827×10^{-5}	1.0662×10^{-5}
120 - 130	2.4648×10^{-4}	3.8861×10^{-4}	3.5153×10^{-4}	3.2427×10^{-4}
130 - 140	4.2134×10^{-5}	6.6236×10^{-5}	6.0618×10^{-5}	5.5612×10^{-5}
140 - 150	2.0618×10^{-5}	3.1626×10^{-5}	3.0258×10^{-5}	2.6930×10^{-5}
150 - 160	4.4041×10^{-5}	6.7145×10^{-5}	6.4838×10^{-5}	5.7736×10^{-5}
160 - 170	9.5672×10^{-5}	1.4364×10^{-4}	1.4194×10^{-4}	1.2479×10^{-4}
170 - 180	2.8915×10^{-4}	4.3112×10^{-4}	4.3443×10^{-4}	3.7424×10^{-4}
180 - 190	7.9319×10^{-4}	1.1849×10^{-3}	1.1953×10^{-3}	1.0311×10^{-3}
190 - 200	1.5640×10^{-3}	2.3306×10^{-3}	2.3754×10^{-3}	2.0332×10^{-3}
200 - 210	3.1216×10^{-3}	4.6459×10^{-3}	4.7525×10^{-3}	4.0598×10^{-3}
210 - 220	9.8404×10^{-3}	1.4515×10^{-2}	1.5002×10^{-2}	1.2805×10^{-2}
220 - 230	1.4102×10^{-2}	2.0818×10^{-2}	2.1533×10^{-2}	1.8360×10^{-2}
230 - 240	1.3892×10^{-2}	2.0478×10^{-2}	2.1191×10^{-2}	1.8055×10^{-2}
240 - 250	1.5746×10^{-2}	2.3191×10^{-2}	2.4015×10^{-2}	2.0439×10^{-2}
250 - 260	2.2838×10^{-2}	3.3646×10^{-2}	3.4943×10^{-2}	2.9765×10^{-2}
260 - 270	5.4632×10^{-2}	8.0357×10^{-2}	8.3612×10^{-2}	7.1145×10^{-2}
270 - 280	6.3161×10^{-2}	9.2841×10^{-2}	9.6634×10^{-2}	8.2097×10^{-2}
280 - 290	7.6375×10^{-2}	0.1122	0.1166	9.9025×10^{-2}
290 - 300	0.1515	0.2224	0.2313	0.1959
300 - 310	0.1710	0.2512	0.2609	0.2208
310 - 320	0.2073	0.3044	0.3176	0.2698
320 - 330	0.2551	0.3744	0.3910	0.3321
330 - 340	0.2878	0.4225	0.4412	0.3748
340 - 350	0.2963	0.4349	0.4541	0.3858
350 - 360	0.3094	0.4543	0.4742	0.4029
360 - 370	0.3488	0.5119	0.5346	0.4542
370 - 380	0.3575	0.5248	0.5479	0.4655
380 - 390	0.3175	0.4664	0.4865	0.4135
390 - 400	0.3537	0.5196	0.5420	0.4606
400 - 410	0.5243	0.7694	0.8037	0.6827
410 - 420	0.5601	0.8220	0.8586	0.7293

Table 5: Daily irradiances in W m^{-2} nm^{-1} for solar cycle 24 maximum (2012/2013) at Gale.

Wavelength (nm)	**Ls 90**	**Ls 180**	**Ls 270**	Ls **360**
1 - 10	4.0728×10^{-6}	6.2646×10^{-6}	6.9435×10^{-6}	6.0578×10^{-6}
10 - 20	1.5558×10^{-5}	2.3035×10^{-5}	2.4378×10^{-5}	2.0794×10^{-5}
20 - 30	1.3195×10^{-5}	1.9675×10^{-5}	2.1043×10^{-5}	1.8021×10^{-5}
30 - 40	1.8349×10^{-5}	2.7143×10^{-5}	2.8676×10^{-5}	2.4452×10^{-5}
40 - 50	3.8860×10^{-6}	5.7577×10^{-6}	6.0942×10^{-6}	5.2234×10^{-6}
50 - 60	3.3885×10^{-6}	5.0180×10^{-6}	5.3005×10^{-6}	4.5510×10^{-6}
60 - 70	3.0317×10^{-6}	4.4965×10^{-6}	4.7554×10^{-6}	4.0921×10^{-6}
70 - 80	3.3289×10^{-6}	4.9339×10^{-6}	5.2127×10^{-6}	4.4819×10^{-6}
80 - 90	7.7400×10^{-6}	1.1465×10^{-5}	1.2114×10^{-5}	1.0409×10^{-5}
90 - 100	9.4749×10^{-6}	1.4026×10^{-5}	1.4803×10^{-5}	1.2708×10^{-5}
100 - 110	8.5557×10^{-6}	1.2664×10^{-5}	1.3366×10^{-5}	1.1474×10^{-5}
110 - 120	7.2429×10^{-6}	1.0868×10^{-5}	1.1211×10^{-5}	9.6939×10^{-6}
120 - 130	1.9776×10^{-4}	2.9122×10^{-4}	3.1113×10^{-4}	2.6709×10^{-4}
130 - 140	3.5155×10^{-5}	5.1873×10^{-5}	5.4895×10^{-5}	4.7264×10^{-5}
140 - 150	1.8758×10^{-5}	2.7998×10^{-5}	2.9094×10^{-5}	2.4881×10^{-5}
150 - 160	4.0296×10^{-5}	5.9741×10^{-5}	6.2091×10^{-5}	5.3475×10^{-5}
160 - 170	8.9947×10^{-5}	1.3292×10^{-4}	1.3851×10^{-4}	1.1870×10^{-4}
170 - 180	2.8147×10^{-4}	4.1383×10^{-4}	4.3165×10^{-4}	3.6680×10^{-4}
180 - 190	7.6224×10^{-4}	1.1172×10^{-3}	1.1730×10^{-3}	1.0000×10^{-3}
190 - 200	1.5131×10^{-3}	2.2226×10^{-3}	2.3213×10^{-3}	1.9752×10^{-3}
200 - 210	3.0230×10^{-3}	4.4491×10^{-3}	4.6440×10^{-3}	3.9500×10^{-3}
210 - 220	9.6697×10^{-3}	1.4219×10^{-2}	1.4824×10^{-2}	1.2604×10^{-2}
220 - 230	1.3886×10^{-2}	2.0440×10^{-2}	2.1299×10^{-2}	1.8117×10^{-2}
230 - 240	1.3722×10^{-2}	2.0189×10^{-2}	2.1019×10^{-2}	1.7871×10^{-2}
240 - 250	1.5635×10^{-2}	2.2984×10^{-2}	2.3920×10^{-2}	2.0323×10^{-2}
250 - 260	2.2480×10^{-2}	3.3100×10^{-2}	3.4487×10^{-2}	2.9354×10^{-2}
260 - 270	5.4213×10^{-2}	7.9758×10^{-2}	8.3016×10^{-2}	7.0605×10^{-2}
270 - 280	6.2931×10^{-2}	9.2586×10^{-2}	9.6358×10^{-2}	8.1864×10^{-2}
280 - 290	7.6470×10^{-2}	0.1125	0.1170	9.9431×10^{-2}
290 - 300	0.1522	0.2242	0.2331	0.1979
300 - 310	0.1711	0.2531	0.2627	0.2232
310 - 320	0.2060	0.3032	0.3162	0.2688
320 - 330	0.2535	0.3731	0.3890	0.3305
330 - 340	0.2863	0.4211	0.4388	0.3730
340 - 350	0.2946	0.4333	0.4520	0.3839
350 - 360	0.3076	0.4523	0.4719	0.4010
360 - 370	0.3474	0.5105	0.5327	0.4523
370 - 380	0.3560	0.5229	0.5458	0.4635
380 - 390	0.3167	0.4650	0.4855	0.4121
390 - 400	0.3535	0.5188	0.5414	0.4595
400 - 410	0.5234	0.7681	0.8016	0.6807
410 - 420	0.5590	0.8204	0.8561	0.7270

Table 6: Daily irradiances in W m^{-2} nm^{-1} for solar cycle 24 minimum (2008/2009) at Gale.

Wavelength (nm)	**Ls 90**	**Ls 180**	**Ls 270**	Ls **360**
1 - 10	6.5763×10^{-6}	4.9452×10^{-6}	5.9300×10^{-6}	5.7179×10^{-6}
10 - 20	2.3931×10^{-5}	1.8530×10^{-5}	2.4881×10^{-5}	2.4537×10^{-5}
20 - 30	1.9097×10^{-5}	1.4675×10^{-5}	1.8375×10^{-5}	1.8007×10^{-5}
30 - 40	3.3905×10^{-5}	2.6371×10^{-5}	3.4462×10^{-5}	3.4061×10^{-5}
40 - 50	6.3460×10^{-6}	4.9513×10^{-6}	6.5544×10^{-6}	6.4917×10^{-6}
50 - 60	4.8357×10^{-6}	3.7965×10^{-6}	5.1708×10^{-6}	5.1421×10^{-6}
60 - 70	4.2881×10^{-6}	3.3589×10^{-6}	4.5843×10^{-6}	4.5529×10^{-6}
70 - 80	4.6684×10^{-6}	3.6618×10^{-6}	5.0176×10^{-6}	4.9873×10^{-6}
80 - 90	1.0877×10^{-5}	8.5413×10^{-6}	1.1661×10^{-5}	1.1598×10^{-5}
90 - 100	1.3214×10^{-5}	1.0390×10^{-5}	1.4247×10^{-5}	1.4181×10^{-5}
100 - 110	1.1931×10^{-5}	9.3822×10^{-6}	1.2864×10^{-5}	1.2805×10^{-5}
110 - 120	7.2786×10^{-6}	5.7508×10^{-6}	7.9908×10^{-6}	7.9765×10^{-6}
120 - 130	2.7770×10^{-4}	2.1865×10^{-4}	2.9939×10^{-4}	2.9823×10^{-4}
130 - 140	4.8790×10^{-5}	3.8475×10^{-5}	5.3017×10^{-5}	5.2862×10^{-5}
140 - 150	2.5287×10^{-5}	2.0050×10^{-5}	2.7994×10^{-5}	2.8000×10^{-5}
150 - 160	5.4408×10^{-5}	4.3215×10^{-5}	6.0614×10^{-5}	6.0687×10^{-5}
160 - 170	1.2009×10^{-4}	9.5646×10^{-5}	1.3460×10^{-4}	1.3496×10^{-4}
170 - 180	3.6978×10^{-4}	2.9500×10^{-4}	4.1593×10^{-4}	4.1744×10^{-4}
180 - 190	1.0066×10^{-3}	8.0310×10^{-4}	1.1313×10^{-3}	1.1354×10^{-3}
190 - 200	1.9931×10^{-3}	1.5913×10^{-3}	2.2430×10^{-3}	2.2521×10^{-3}
200 - 210	3.9843×10^{-3}	3.1817×10^{-3}	4.4871×10^{-3}	4.5057×10^{-3}
210 - 220	1.2652×10^{-2}	1.0119×10^{-2}	1.4274×10^{-2}	1.4345×10^{-2}
220 - 230	1.8178×10^{-2}	1.4541×10^{-2}	2.0524×10^{-2}	2.0628×10^{-2}
230 - 240	1.7922×10^{-2}	1.4334×10^{-2}	2.0234×10^{-2}	2.0335×10^{-2}
240 - 250	2.0364×10^{-2}	1.6290×10^{-2}	2.2998×10^{-2}	2.3115×10^{-2}
250 - 260	2.9474×10^{-2}	2.3588×10^{-2}	3.3320×10^{-2}	3.3498×10^{-2}
260 - 270	7.0789×10^{-2}	5.6673×10^{-2}	8.0085×10^{-2}	8.0528×10^{-2}
270 - 280	8.1965×10^{-2}	6.5621×10^{-2}	9.2731×10^{-2}	9.3245×10^{-2}
280 - 290	9.9320×10^{-2}	7.9516×10^{-2}	0.1123	0.1129
290 - 300	0.1973	0.1580	0.2233	0.2246
300 - 310	0.2224	0.1781	0.2517	0.2532
310 - 320	0.2728	0.2185	0.3088	0.3105
320 - 330	0.3347	0.2680	0.3788	0.3810
330 - 340	0.3762	0.3013	0.4258	0.4283
340 - 350	0.3787	0.3033	0.4287	0.4311
350 - 360	0.3872	0.3101	0.4383	0.4408
360 - 370	0.4517	0.3617	0.5112	0.5142
370 - 380	0.4685	0.3752	0.5302	0.5333
380 - 390	0.3993	0.3197	0.4519	0.4545
390 - 400	0.4164	0.3335	0.4713	0.4740
400 - 410	0.6771	0.5423	0.7664	0.7708
410 - 420	0.7105	0.5691	0.8042	0.8088

Table 7: Daily irradiances in W m^{-2} nm^{-1} for Mars for Martian year 34 (2017/2018) in Elysium Planitia.

7

Solar cell temperature on Mars

Al igual que sucede en la Tierra, la mayor fuente de energía disponible en Marte es la radiación solar y la habilidad de transformar esa energía solar en otras fuentes de energía nos ha permitido enviar satélites y vehículos rover para explorar el planeta. La energía solar representa hoy en día la fuente de energía más apropiada para colonizar el planeta.

La energía solar se utilizó por primera vez como fuente de energía en Marte en las sondas Vikings y desde entonces se ha utilizado con éxito en otros vehículos rover. Ha demostrado ser una fuente de energía segura y útil. Aunque pueda parecer ciencia ficción, las agencias espaciales, principalmente NASA, planean la exploración de Marte con astronautas en las próximas décadas.

Para estudiar el comportamiento de paneles solares en la superficie marciana es necesario estudiar la temperatura de operación de la célula solar, que determina su eficiencia y rendimiento. Esta temperatura depende de los materiales utilizados para construir la célula y de las variables ambientales que lo rodean (es decir, la radiación, la temperatura ambiente, la velocidad del viento y la humedad). Este tipo de análisis se ha hecho para paneles solares en la Tierra y se han propuesto diferentes ecuaciones para calcular la temperatura de operación en función de estas variables. Las ecuaciones simplificadas que se han desarrollado no son válidas para otras condiciones como puede ser el caso de Marte, donde las condiciones ambientales son muy diferentes.

En este capítulo desarrollamos una ecuación simplificada para calcular la temperatura de una célula solar en condiciones ambientales de Marte, discutiendo el efecto que la latitud y el viento en Marte podrían tener en la temperatura de la célula solar. La determinación correcta de la temperatura de funcionamiento de la célula ayudará a optimizar el diseño de los próximos vehículos rover impulsados con energía solar para la exploración de Marte.

8

Solar exergy and wind energy on Mars

Como he mencionado en el capítulo 7, el uso de la energía solar ha sido fundamental para la exploración espacial. Varias misiones en la superficie de Marte han demostrado la viabilidad y el éxito de los paneles solares como fuente de energía. Sorprendentemente hasta la fecha no hay estudios publicados sobre la eficiencia de la transformación de la energía solar en Marte, aunque estos estudios han sido muy útiles para nuestro planeta.

Para analizar la eficiencia máxima de la transformación hay que analizar la energía obtenible (exergía) de la radiación solar en condiciones marcianas, es decir, la exergía de la radiación solar. En este capítulo presento los cálculos que he realizado de la exergía en Marte utilizando valores de las variables ambientales medidos tanto desde satélite como in-situ en la superficie de Marte. He calculado la exergía de la radiación solar a escala global usando datos orbitales durante un año marciano medidos por el instrumento TES (Thermal Emission Spectrometer) a bordo de la misión espacial MGS (Mars Global Surveyor) de la NASA, y también en una sola ubicación en Marte (el cráter Gale) con una resolución temporal de 1 h medidos por la estación meteorológica REMS (Rover Environmental Monitoring Station) a bordo del rover Curiosity de la NASA.

En este capítulo también he analizado la energía eólica como fuente alternativa de energía para la exploración de Marte.

Al comparar los resultados de la eficiencia de la energía solar y la producción de energía eólica con los obtenidos en la Tierra, llego a la conclusión de que la eficiencia térmica de los paneles solares en Marte es baja debido a la baja densidad de la atmósfera. Esta baja densidad también hace que el uso de la energía eólica sea inadecuado.

Solar exergy and wind energy on Mars

Alfonso Delgado-Bonal[a,b,*], F. Javier Martín-Torres[b,c], Sandra Vázquez-Martín[b,c], María-Paz Zorzano[d]

[a]*Instituto Universitario de Física Fundamental y Matemáticas, Universidad de Salamanca, 37008, Spain*
[b]*Instituto Andaluz de Ciencias de la Tierra (CSIC-UGR), Avda. de Las Palmeras nº 4, Armilla, 18100, Granada, Spain*
[c]*Division of Space Technology, Department of Computer Science, Electrical and Space Engineering, Luleå University of Technology, Kiruna, Sweden*
[d]*Centro de Astrobiología (INTA-CSIC), Ctra. Ajalvir km.4, Torrejón de Ardoz, 28850, Madrid, Spain*

Abstract

Several missions to the surface of Mars have proven the feasibility and success of solar panels as energy source. Analysis of the efficiency of the solar radiation has been carried out successfully on Earth, however, to date, there is not an extensive research regarding the thermodynamic efficiency of in-situ renewable energy sources on Mars. In this paper, we analyze the obtainable energy (exergy) from solar radiation under martian conditions. For this analysis we have used the surface environmental variables on Mars measured in-situ by the Rover Environmental Monitoring Station onboard the Curiosity rover and from satellite by the Thermal Emission Spectrometer instrument onboard the Mars Global Surveyor satellite mission. We evaluate the exergy from solar radiation on a global spatial scale using orbital data for a martian year; and in a one single location in Mars (the Gale crater) with an appreciable temporal resolution (1 h). Also, we analyze the wind energy as an alternative source of energy for Mars exploration and compare the results with those obtained on Earth. We conclude that the low density of the atmosphere of Mars is responsible of the low thermal efficiency of solar panels and also makes the use of wind energy inappropriate.

Keywords:
Second law analysis, Mars, Solar Exergy, Wind Energy, Renewable Energy

1. Introduction

Solar radiation has been a typical source of energy in space missions as a power source for small satellites, for large structures such as the International Space Station, and for Solar System exploration. The success of the solar energy for Mars exploration has been completely demonstrated. It was used in 1976 during the Viking mission and later in several Mars orbiters and rovers. In particular, the Mars Exploration Rover Opportunity was able to exceed the baseline mission duration from the 90 sols scheduled initially to more than 3500 sols, continuing nowadays. However, the complexity of the rovers, and the increasing energy demands of the experiments onboard have increased in the last decades. An example is the Curiosity rover in the NASA's Mars Science Laboratory (MSL) mission [1] currently operating on Mars. As the solar radiation intensity decreases with the square of the distance to the sun, it might become insufficient or inadequate to maintain a complex spacecraft. For these reasons, the rover Curiosity is powered by a Radioisotope Thermoelectric Generator (nuclear power) and it is likely that the next rovers to Mars will use the same kind of energy source.

Although nuclear power could be a partial and temporary solution [2], human colonization of Mars will require a perdurable and renewable source of energy. The transport of nuclear material from Earth to Mars implies large risk and costs. The existence of fossil energy, such as carbon or oil on Earth, seems unlikely on Mars and its transport in spacecrafts is not feasible. Geothermal energy is not feasible on Mars, since no significant geological activity has been recorded on the planet.

Analysis of the efficiency of solar energy on Earth are usually done using the second law of thermodynamics. They can provide clues to improve the process and optimize the resources. Since the origins of the steam engine, thermodynamics principles have been used to analyze and improve the energy conversion processes, trying to minimize the heat lost and maximize the obtainable work. The first law of thermodynamics establishes that energy is a conserved quantity that can be divided into heat and work; and the second law deals with the heat lost in a particular process, which can be used to analyze the efficiency of a process in a determined environment. Exergy combines the two laws of thermodynamics to analyze the source of energy in a particular environment, providing a powerful tool to investigate the performance of a device in a system. The exergy concept has been applied to solar radiation and it is still an ongoing field of research with a large development on the last decades. It has been applied extensively on Earth and has been prove to be a very useful method to evaluate the efficiency of solar energy conversion, applied in studies in Europa, US, India and Turkey for example [3],[4],[5],[6],[7].

Despite the fact that exergetic analysis is an universal tool based on the laws of thermodynamics, the solar exergy on Mars has been poorly studied [2]. In this paper, we evaluate the spa-

*Corresponding author information:
Email address: alfonso.delgado-bonal@ltu.se (Alfonso Delgado-Bonal)

Nomenclature

A	solar cell area (m^2)	T_{cell}	solar cell temperature (K)
C_p	heat capacity at constant pressure (J Kg^{-1} K^{-1})	T_{sun}	temperature of the Sun (K)
C_{pow}	power constant of wind energy	T(D,z)	Pollack transmission coefficient
d	declination (degrees)	u	free-stream velocity of air (m s^{-1})
D	transmission coefficient of radiation	U_L	overall loss coefficient
E	energy from solar radiation (W)	z	zenith angle (degree)
Ex	exergy of solar radiation (W)		
h_w	wind convection heat transfer coeff. (W m^2 K^{-1})		*Greek Symbols*
h_{rad}	radiative heat transfer coeff. (W m^2 K^{-1})	α	solar absorptance of PV layer
I_{TOA}	Irradiance at Top of the Atmosphere (W m^{-2} s^{-1})	β	$1/T_{amb}$ = coefficient of thermal expansion (K^{-1})
I_{surf}	Irradiance at surface (W m^{-2} s^{-1})	η	electric efficiency
L	latitude (degree)	η_{ref}	reference cell electric efficiency
Ls	solar longitude (degree)	ϵ	emissivity
m_a	mass flow rate (kg s^{-1})	ϕ	irradiance (W m^{-2})
P_r	performance ratio (%)	ψ	photovoltaic efficiency
Q_{cell}	thermal power (W)	ρ	density (kg m^{-3})
r	Mars distance (AU)	σ	Stefan's constant (W m^{-2} K^4)
r_{av}	average distance Mars-Sun (AU)	τ	transmittance of glazing
t	time (s)	ν	frequency (s^{-1})
T_{amb}	ambient temperature (K)		

tial and temporal evolution of the exergy on Mars based in satellite and in-situ rover data. The eccentricity of Mars is 0.09331 and the maximum distance to the sun (aphelion) is 1.665861 AU. As the distance increases, the solar flux intensity reaching the surface decreases, reducing the capabilities of the solar powered spacecrafts. Hence, the exergy of radiation will be different at different seasons during a martian orbit. Not only that, the exergy of radiation will change with location; and for a given location, on a daily basis. Using the environmental data provided by the Rover Environmental Monitoring Station (REMS) instrument [8] onboard the Curiosity rover [1] we calculate the exergy and the efficiency of solar radiation on a single location, and different seasons in a daily basis. The knowledge of the temperature, pressure and density of the atmosphere is used along with the radiation reaching the surface of the planet to determine the efficiency at different hours. The Curiosity rover landed at crater Gale (4.49° S, 137.42°E) on Mars. Although Curiosity data are undoubtedly valuable, they are representative of a single location on the planet. In order to analyze the maximum exergy of radiation at different latitudes on the planet, we use the data provided by the Thermal Emission Spectrometer instrument onboard the Mars Global Surveyor spacecraft [9][10] to determine the maximum temperature of the environment through a complete martian year. The results of the exergy efficiency of the solar radiation conversion are shown in Section 2.

Another energetic alternative for Mars exploration and future human colonization of the planet could be wind energy. Wind stations are an excellent alternative on Earth and their use on other planets could be a potential source of renewable energy. We show the results of the wind energy analysis on Section 3.

In Section 4, we summarize the results and provide insights for future work and developments that could help to increase the efficiency of renewable energy sources on Mars.

2. Solar Energy and Exergy

A solar cell cannot convert all the potential energy of the solar radiation in obtainable energy; and every detector will be more or less efficient at particular solar wavelengths. The solar energy reaching a photovoltaic (PV) panel that cannot be converted in "obtainable" energy heats it. For example, in the Mars Exploration Rovers (MER) mission, the solar cells are composed of a GaInP/GaAs/Ge triple junction that collects the photons in different layers depending on their wavelength. In general, the obtainable energy (E) from solar radiation reaching a panel is:

$$E = A \cdot \eta \cdot \phi \cdot P_r \tag{1}$$

where A is the total solar panel area (m^2), η is the solar panel yield (%) and ϕ (W/m^2) is the solar irradiance reaching the panel. In this equation, P_r is the performance ratio, a coefficient accounting for the losses in the conversion process, which is usually between 0.5 and 0.9 [11]. In an ideal process, the performance ratio would be the unity.

Given the solar radiation field, the parameter that determines the obtainable energy of a panel per unit of area is called the solar panel yield, η. This factor is directly determined by the type of solar cell and the fabrication processes, and it is a critical factor. The maximum yield obtained nowadays is about 45 % of the radiation reaching the panel. In our calculations we will determine the maximum obtainable work under the present day conditions, and we consider 0.45 as the yield value in our calculations. The performance ratio is the ratio between the obtained energy and theoretically calculated values. It depends on

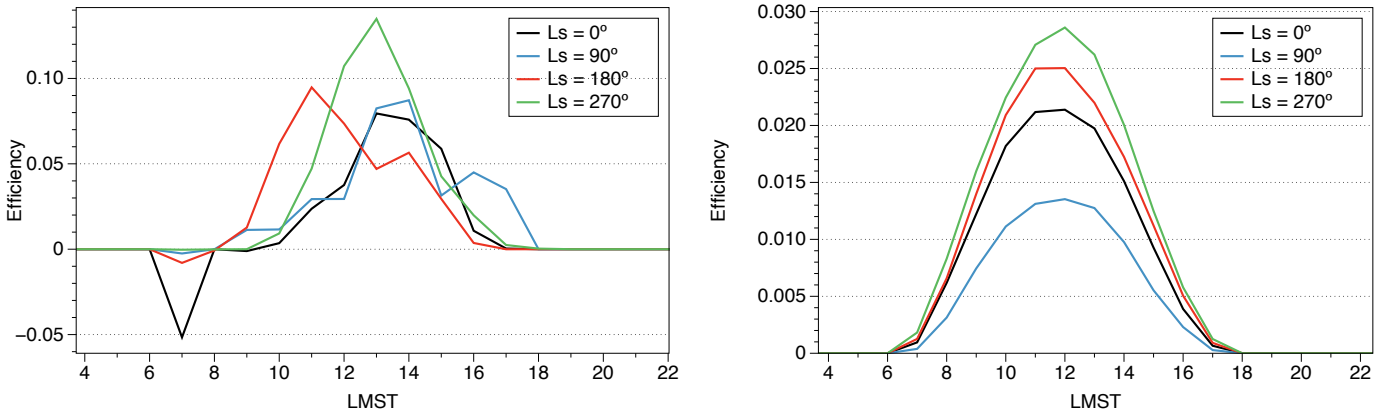

Figure 1: Calculations of daily efficiency for different seasons on Mars considering two solar panel location scenarios: (a) Ground level (Vikings), and (b) 1.6 meters height (Spirit and Opportunity). Note the different scale in the Efficiency axis.

the orientation of the panel, incident solar radiation, electronics, and thermal and conduction energy losses. We consider a nominal value of 0.75 for the calculations performed in this paper.

The obtainable work from energy, i.e., in our case that part of the incident solar radiation that could be used to generate other forms of energy is called exergy, and has been used on Earth under the name of second law analysis to determine the efficiency of solar energy conversion [12].

In order to determine the exergy of radiation, several equations have been proposed. Those proposed by Petela and Spanner in 1964 [13] were confirmed later by other researchers [14][15], and although other authors, like Jeter [16], proposed different equations arguing that the maximum obtainable work is established by a Carnot expression. Candau [17], based on thermodynamical arguments, demonstrated theoretically that the expression for the conversion of solar radiation into work is the one proposed by Petela [13]:

$$Ex = \sigma T_{sun}^4 \left(1 - \frac{4}{3}\frac{T_{amb}}{T_{sun}} + \frac{1}{3}\frac{T_{amb}^4}{T_{sun}^4}\right) \tag{2}$$

The efficiency of a PV cell can be analyzed using the exergy of radiation. The exergy content can be divided in two parts: a electrical part, Ex_e, that depends on the fabrication process and is determined by the yield η (electric efficiency), and the thermal part, Ex_{th},which depends on the interaction between the cell and the environment [3]. Hence, the expression to determine the total efficiency reads:

$$\psi = \frac{Ex_e + Ex_{th}}{Ex} = \eta_{cell} + \frac{\left(1 - \frac{4}{3}\frac{T_{amb}}{T_{cell}} + \frac{1}{3}\frac{T_{amb}^4}{T_{cell}^4}\right) Q_{cell}}{\left(1 - \frac{4}{3}\frac{T_{amb}}{T_{sun}} + \frac{1}{3}\frac{T_{amb}^4}{T_{sun}^4}\right) \cdot \phi_s A_{cell}} \tag{3}$$

The second term of this expression is determined by the interaction between the cell and the environment. The thermal power, Q_{cell} is calculated as [18]:

$$Q_{cell} = m_a \cdot Cp_a \cdot (T_{cell} - T_{amb}) \tag{4}$$

where $\dot{m}_a = \rho v A$ is the mass flow. As can be seen in the latest expressions the thermal efficiency of the conversion depends on the heat lost by the panel in a particular environment, while the electrical part depends only on the fabrication process. For a given panel, the parameters that determine the efficiency of the transformation are the density of the atmosphere (ρ), its composition (Cp_a) and the refrigeration processes ($v, \Delta T$), which will determine ultimately the operating temperature of the cell and the thermal power.

The current martian atmosphere is composed mainly by CO_2 (98% of the total composition). We assume in our calculations that the atmosphere is only composed by CO_2, with a heat capacity varying from C_p = 0.709 ($m^2\ s^{-2}\ K^{-1}$) at 175 K to C_p = 0.791 ($m^2\ s^{-2}\ K^{-1}$) at 250 K. In comparison with our atmosphere, the martian atmosphere is extremely thin, with a density of about ρ = 0.020 kg m^{-3} compared with 1.225 kg m^{-3} on Earth. In this work, we assume that the martian atmosphere behaves as an ideal gas when we determine the value of the density as a function of the temperature and pressure.

The temperature of the cell (T_{cell}) is usually different than the ambient temperature (T_a). For the martian environment, the refrigeration is produced by forced convection and radiation, and its importance depends on the configuration of the solar panel. We consider two cases: a solar cell lying on the ground, as those in the Viking landers; and a flat panel at 1.6 m above the surface, as those mounted on the Mars Exploration Rovers (Spirit and Opportunity). For the first case, we consider T_{cell} as the surface temperature measured by REMS; and for the second case, the temperature is evaluated with the following expression [19]:

$$T_c = \frac{T_a + \left(\frac{\phi_s}{\phi_{s,N}}\right)\frac{U_{L,N}}{U_L}(T_{c,N} - T_{a,N})\left[1 - \frac{\eta_{ref}}{(\tau\alpha)}(1 + \beta_{ref} T_{ref})\right]}{1 - \frac{\beta_{ref}\eta_{ref}}{(\tau\alpha)}\left(\frac{\phi_T}{\phi_N}\right)\frac{h_{w,N}}{h_w}(T_{c,N} - T_{a,N})} \tag{5}$$

u_{NOCT}	1m/s
$T_{a,NOCT}$	20°C
$\phi_{T,NOCT}$	800 W
$T_{c,NOCT}$	47°C
η_{ref}	0.12
β_{ref}	0.004°C^{-1}
T_{ref}	25°C
$\tau\alpha$	0.9

Table 1: NOCT reference values

where T_a is the ambient temperature measured by REMS at 1.6 m above the ground, u is the wind velocity and ϕ_T is the irradiance on the panel. The determination of the operating temperature depends on the solar irradiance heating the panel and the refrigeration processes that release heat to the environment. The overall loss coefficient include the heat released by wind convection (h_w) and by radiation (h_{rad}), $U_L = h_w + h_{rad}$ [20].

In this paper we will use the Nominal Operating Cell Temperature (NOCT) and reference values cited in [19], summarized in Table 1.

Using an iterative process until convergence (6 steps), it is possible to approximate Equation 5 into a linear equation for the martian environment, depending on the ambient temperature (T_a), solar irradiance (ϕ) and wind velocity (v) [21]:

$$T_c = 1.00116 \cdot T_a + 0.0313174 \cdot \phi_s - 0.108832 \cdot u \quad (6)$$

The radiation reaching Mars Top of the Atmosphere (TOA) is calculated in W m^{-2} according to the equation [22]:

$$I_{TOA} = 592\left(\frac{r}{r_{av}}\right)^2 = 592\left(\frac{1 + 0.0934 \cdot \cos(L_s - 250°)}{0.9913}\right)^2 \quad (7)$$

where r_{av} is the average distance Mars-Sun (1.52 AU), and L_s is the solar longitude, which is $L_s = 0°$ in vernal equinox.

The intensity reaching the surface without considering the atmospheric absorption could be calculated as $I_{surf} = I_{TOA} \cdot \cos(z)$, where z is called zenith angle and can be calculated as:

$$\cos(z) = \sin(d) \cdot \sin(L) + \cos(d) \cdot \cos(L) \cdot \cos(2\pi t/24.6) \quad (8)$$

with d the declination angle, L the observational latitude and t the time of day (from -12.3 to +12.3, being noon equal to zero). The declination angle can be easily related with the Ls as $\sin(d) = \sin(25.2°)\sin(L_s)$, where 25.2° is the eccentricity of the planet.

The radiation is scattered and absorbed in its pass through the atmosphere, and those effects must be considered for a correct calculation of the irradiance. The Beer's Law is usually used to calculate the direct component of the irradiance at ground level, being $I_{surf} = I_{TOA} \cdot exp(-D/\cos(z))$, where D is the transmission coefficient for the direct component. However, the Mars atmosphere is very rich in dust and the scattering becomes an important physical process in the radiative transfer on the atmosphere. The diffuse energy can be also used to generate electricity in the solar cells [23], and a precise treatment of the radiation should be consider. In this paper, we will use the Pollack transmission coefficients [24] for an optical depth of D = 0.3, which is consistent with the latest measurements by the cameras on the rover Curiosity [25] . Considering all these processes, the radiation on the surface can be calculated as:

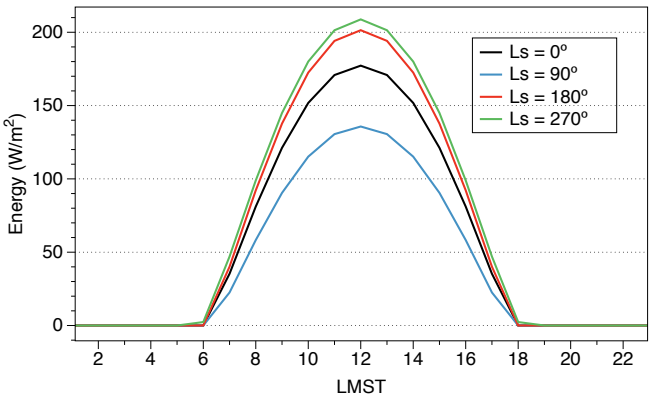

Figure 2: Obtainable solar energy in Gale as a function of Local Mean Solar Time (LMST), and season.

$$I_{surf} = I_{TOA} \cdot \cos(z) \cdot T(D, z) \quad (9)$$

where T(D,z) is the Transmission Coefficient that is a function of optical depth and solar zenith angle [22].

2.1. *Daily and seasonal solar exergy efficiency at a location on Mars: the Gale crater*

The thermal efficiency depends on the mass flow rate, which depends itself on the atmospheric density and wind velocity. The atmospheric density for the different seasons was calculated using REMS measurements and considering the ideal gas approximation. REMS is located on crater Gale (4.49° S, 137.42°E), and contains sensors to determine the ground and air temperature of the environment. The Atmospheric Thermal Sensor (ATS) is located at 1.6 meters over the ground and provides measurements on the air temperature. The Ground Temperature Sensor (GTS) measures the temperature values of the ground (note that given the thermodynamical properties of the ground and the air, $T_g > T_a$ during the daytime and $T_a > T_g$ at nighttime).

The temperature of the solar panel results on the competition of the heating by solar radiation and the heat losses (cooling) by wind convection and radiation. The heat loss by radiation depends itself on the temperature of the radiating body (the panel), and in order to compute it, we have determined the temperature of the body at each hour using an iterative method in Equation 5 until convergence, starting with a temperature 30K over the ground temperature [21]. The heat loss by wind convection is directly proportional to the wind velocity. The best estimations of the wind on Mars predict wind speeds between 10 m s^{-1} and 4 m s^{-1} [26]. During extreme events such as dust devils, the

wind speed could increase until 25 m s^{-1} , with an average of 12 m s^{-1} [27]. However, in those events the dust storm would block the majority of the radiation and the obtainable energy would be very low. Performing a sensitivity analysis of Equation 5 we determine that the effect of the wind speed is much less important than the radiation reaching the panel. At 20 m s^{-1} the refrigeration on the solar panel is only about 2 K, and these wind speeds are not expected on the planetary boundary layer on Mars. In this paper, we use 5 m s^{-1} in our calculations of the exergy of solar radiation.

Figure 1 shows the thermal efficiency of solar radiation on Mars for a square solar panel of 1m length in two different scenarios. In Figure 1 (a) we assume that the solar panel is at the same temperature than the ground, i.e., the measurements provided by the GTS on REMS. This situation will occur when the panel is directly lying on the ground, as for example in the case of the Viking landers. In Figure 1 (b) we determine the temperature of the panel using Equation 5 and the ambient temperature provided by the ATS on REMS at 1.6 meters, i.e., the case of the Spirit and Opportunity rovers for example. In both cases, the efficiency of the radiation is calculated for different orbital positions on Mars. The maximum of the efficiency occurs at different hours as a consequence of the thermal inertia of the ground, being the maximum of the ambient temperature at noon and measured on the next hour on the ground. The radiation reaching the surface has been calculated with the equations presented above and is represented in Figure 2.

The thermal efficiency of the panel on the ground (Vikings) is larger than the case of the panels standing at 1.6 meters (Spirit and Opportunity). When the panel is lying on the ground, the temperature difference between the temperature of the cell and the ambient temperature is larger, increasing the thermal power. This implies an increase in the exergy and in the efficiency coefficient. Figure 1 (a) shows negative values of the efficiency during the first hour in the morning (i.e., the panel is giving energy to the atmosphere). This is because, after the photons reach the panel, this is at lower temperature than its environment. It is heated by the solar photons and after 1 hour the temperature of the cell is higher than the air temperature, and it can obtain energy from radiation instead of give it.

2.2. Seasonal solar exergy efficiency as a function of location on Mars

In the previous section we have analyzed the exergy efficiency of solar energy in a particular location on Mars, the Crater Gale, that is located near the equator of the planet. In this place is expected that its temperatures are higher than the average temperature on Mars. In order to determine the maximum efficiency of solar radiation on Mars as function of location and season, we use the values of surface temperature provided by the Thermal Emission Spectrometer (TES) instrument on board Mars Global Surveyor (MGS). We have organized the temperatures of Mars for different latitudes on the planet at different orbital positions, and selected the maximum temperature for our analysis, which usually correspond to noon, in order to determine the maximum efficiency of the radiation on the planet. Figure 3 (a) shows data from the TES instrument and Figure 3 (b) the efficiency of radiation calculated using the model explained above. The results are shown for a wind velocity of 5 m s^{-1}.

The values of the thermal efficiency on Mars are as low as 0.012 for the situation where the panels are located at 1.6 meters of altitude, and the maximum values are about 0.1 in the case of the panels laying on the ground. In general, the efficiency of solar conversion on Mars is between 0 and 0.02, as represented in Figure 3, and it is higher if the panels are lying directly on the ground. As we explained above, the efficiency has electric and thermal components. The maximum electric efficiency obtained nowadays is about 45% with typical values of 15%. The values obtained on Mars for the thermal efficiency is almost zero and on Earth, the calculations of the thermal efficiency are about 20-30% [3].

Looking at Equations 3 and 4 we identify the atmospheric density as the parameter responsible of the low efficiency on the solar radiation conversion. Typical values of the Earth's atmospheric density at sea level at 15° is approximately 1.225 kg m^{-3}. On Mars, the typical values are about 0.020 kg m^{-3}, i.e., three orders of magnitude lower. The lack of atmospheric density is a critical factor on the analysis of thermal efficiencies on Mars. The rest of the variables included in the equations have similar values than on Earth.

3. Wind Energy

Another renewable source of energy used extensively on Earth is the wind power or wind energy. The ability to extract electrical energy using the wind has been used on Earth since more than a century, and its use is growing around the world. Wind energy is a renewable source of energy which consumes little land, is relatively unexpensive and is free of greenhouse gases and it could be an alternative for the exploration of the Solar System.

The obtainable electrical energy from wind can be expressed as:

$$E = \frac{1}{2}\rho A t u^3 \tag{10}$$

By applying momentum theory to windmills, it can be found that there is an upper limit in the conversion, and the maximum power that an ideal windmill could extract is 0.593, which is called Betz's Law [28]. This law is independent on the atmosphere, and applies also to Mars. The extractable power from wind can be calculated as:

$$P = \frac{1}{2}\rho A u^3 C_{pow} \tag{11}$$

where C_{pow} is the power coefficient with the upper limit of 0.593. For the windmills available nowadays the typical value is between 0.3 and 0.45. The power curve is dependent on the cross-sectional area perpendicular to the flow, A, the velocity of wind, u, and the density of the atmosphere, ρ.

Figure 4 represents the power curve for an hypothetical 100kW wind turbine with a 18m diameter rotor and a hub heigh

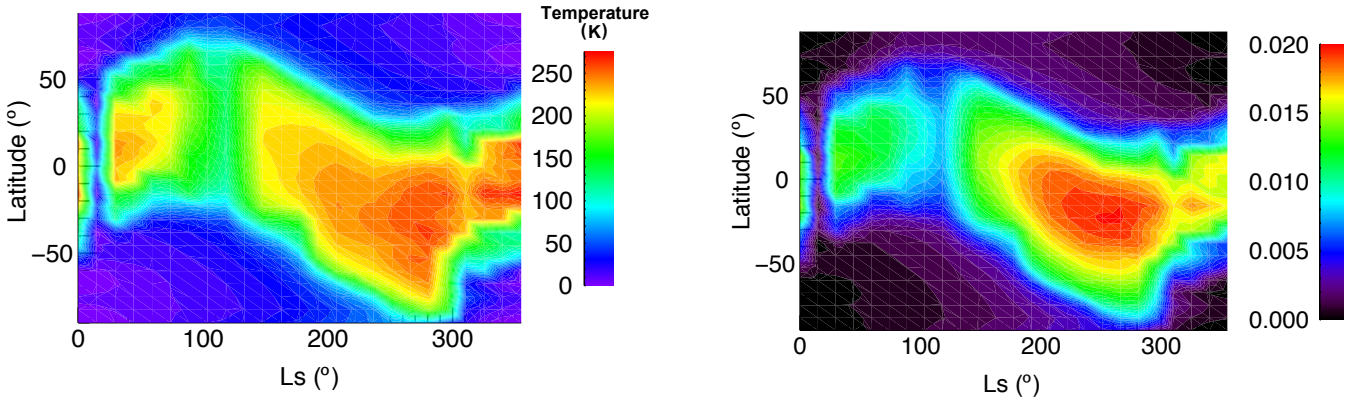

Figure 3: (a) Martian map of maximum temperature for year 24 (left) and (b) solar conversion efficiency in a martian orbit (right).

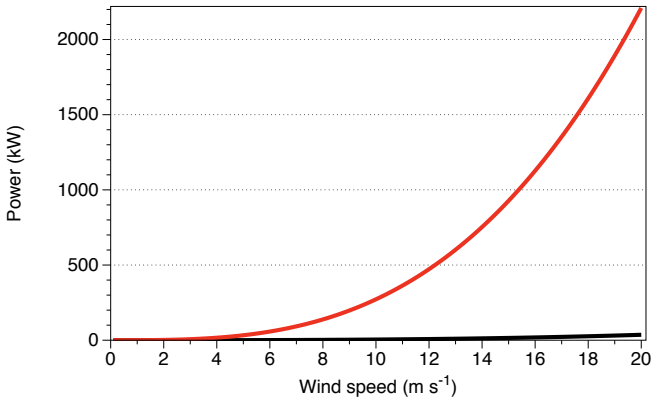

Figure 4: Wind power on Earth (red line) and Mars (black line).

of 30m on Earth and Mars. We have selected this kind of windmill to be able to compare our results with those available in the literature [29] [30]. In our calculations, we assume a power constant of C_{pow} = 0.45 to provide maximum power values that nowadays windmills can generate.

At an altitude of 30 meters, the wind velocities on Mars are expected to be higher than in the planetary boundary layer, and these might reach values of around 20 m s^{-1}. Even in that case, the power produced on Mars would be less than 35 kW, compared with the 2200 kW generated on Earth with the same kind of windchill. Also, at those altitudes, the martian density will be lower (scaling exponenctially) and also the power produced.

The low density of the martian atmosphere is not able to move the windchill strongly to be used a a realistic source of energy. Generation of energy during dust storms, where winds are as fast as 20 m/s and the density increases in a factor of 10, could provide a power of 366 kW. However, these dust storms are not frequent - not a convenient way- to maintain a spacecraft or human beings. Also the winds are very turbulent and could damage the installation.

4. Discussion

Further steps in human exploration and colonization of Mars will require a perdurable and renewable source of energy. Although it may look like a science fiction idea, NASA plans to start human colonization on the planet in 2035. If so, the future colonies will require energy. We discuss here the efficiency of solar and wind stations on Mars. The maximum energy provided by the current solar panels and windmills is presented in Tables 2 and 3. For solar energy, we assume an efficiency of η = 44.7% for the solar cells, with a performance ratio of 0.75 and a panel area of 1 m^2. For wind energy, we assume a C_{pow} = 0.45 and a density an atmospheric density 0.02 kg m^{-3}. Note that these values are proportional to the area of the panel.

From Tables 2 and 3 can be concluded that solar energy on Mars is a much better choice than windmills. Besides the fact that wind energy production is very low on Mars, solar devices present several benefits against windmills. In general, solar panels do not contain moving parts, and the size of the device is considerable smaller than windmills, which is translated into less payload in the spacecraft being therefore cheaper.

The REMS instrument onboard Curiosity has a power consumption of 10.08 W when all sensors are measuring (with ASIC heating) [8]. From our calculations, a windmill of 2.5 meters of diameter rotor could provide 11 W with a constant wind speed of 5 m/s. Meteorological stations on Mars will be, however, more probably constructed based on solar energy. The difficulties of constructing a 2.5 meters of diameter rotor windmill are numerous. To accomplish that power, one would require a square flat panel of 0.30 m of length with a battery, which could provides provides 12.7 W.

The use of solar energy as power source on Solar System exploration has demonstrated to be an excellent choice. It provides enough energy to maintain rovers on Mars and it allows to expand the mission lifetimes, without the need of maintenance. Based on the second law of thermodynamics, the analysis of the efficiency of solar energy conversion has been done success-

	-60°	-45°	-30°	-15°	0°	15°	30°	45°	60°
Ls = 0°	578.3	877.4	1108.0	1253.5	1296.3	1253.5	1108.0	877.4	578.3
Ls = 90°	18.2	221.2	505.9	793.8	1034.0	1220.2	1326.2	1357.8	1335.8
Ls = 180°	657.2	997.0	1259.1	1424.4	1278.3	1424.4	1259.1	997.0	657.2
Ls = 270°	1899.4	1930.5	1885.8	1735.0	1470.2	1128.7	719.3	314.6	25.8

Table 2: Daily solar power (W) production for a 1 m^2 panel (η = 0.447; Pr = 0.75) as a function of latitude and season.

	1m	5m	10m	15m
3 m/s	0.38	9.54	38.15	85.84
5 m/s	1.77	44.16	176.63	397.41
10 m/s	14.13	353.25	1413.00	3179.25
15 m/s	47.69	1192.22	4768.88	10730.00
20 m/s	113.04	2826.00	11304.00	25434.00
25 m/s	220.78	5519.53	22078.10	49675.80

Table 3: Wind power (W) as a function of velocities and rotor diameters on Mars (C_{pow} = 0.45).

fully on Earth, determining the locations where the conversion is optimal. This second law analysis is carried using the exergy concept, which determines the maximum obtainable work from incoming radiation.

The efficiency of solar energy conversion can be divided in two terms: an electric component, dealing with the manufacture process and the technology; and a thermal component, which is determined by the interaction of the solar panel with its environment. The analysis on Earth gives values around 30% of efficiency in the thermal term, while on Mars the typical values are near zero. This implies that there are not thermodynamical arguments to decide the locations of the panels on Mars, and the choice should be done following those places where the irradiance is maximum, i.e., the equator. In order to increase the efficiency of the conversion, efforts should done in order to increase the electrical term, since the thermal part is extremely low to be considered.

In order to increase the thermal efficiency, the thermal power term should be improved. The low density of the martian atmosphere is responsible of the low thermal efficiency, but it might be counteracted increasing the thermal power. The thermal power is a linear function of the differences of temperatures between the ambient and cell. As the ambient temperature is fixed, it is necessary to maintain a low operating cell temperature to increase the efficiency of the transformation. In order to achieve those low temperatures, efforts should be focused in refrigerating systems optimized for the martian environment.

Other renewable source of energy used on Earth is wind power. The low density of the martian atmosphere and the low wind speeds make the wind energy an inappropriate power source. The size of the structures needed to generate enough energy to maintain spacecrafts or human beings on Mars requires a capability to transport which do not have nowadays. Also, the construction should be done with materials supporting the dust interaction and the corrosion, since the presence of chlorine or other elements could damage the structures [31].

5. References

[1] J. P. Grotzinger, J. Crisp, A. R. Vasavada, R. C. Anderson, C. J. Baker, R. Barry, D. F. Blake, P. Conrad, K. S. Edgett, B. Ferdowski, R. Gellert, J. B. Gilbert, M. Golombek, J. Gómez-Elvira, D. M. Hassler, L. Jandura, M. Litvak, P. Mahaffy, J. Maki, M. Meyer, M. C. Malin, I. Mitrofanov, J. J. Simmonds, D. Vaniman, R. V. Welch, R. C. Wiens, Mars science laboratory mission and science investigation, Space Science Reviews 170 (1-4) (2012) 5–56.

[2] V. Badescu, Mars: Prospective Energy and Material Resources, 1st Edition, Springer, Berlin, 2010.

[3] O. Le Corre, J. Broc, I. Dincer, Energetic and exergetic assessment of solar and wind potentials in europe, Int. J. of Exergy 13 (2) (2013) 175–200.

[4] M. Neri, D. Luscietti, M. Pilotelli, Computing the exergy of solar radiation from real radiation data on the italian area, 12th Joint European Thermodynamics Conference 2013.

[5] A. Sahin, E. Mokheimer, H. Bahaidarah, M. Antar, P. Gandhidasan, R. Ben-Mansour, S. Al-Dini, S. Rehman, A. Bejan, M. Al-Nimr, H. Oztop, L. Chen, A. Midilli, J. Lawrence, Special issue: Thermodynamic optimization, exergy analysis, and constructal design, Arabian Journal for Science and Engineering Section B: Engineering 38 (2) (2013) 219.

[6] D. Alta, C. Ertekin, F. Evrendilek, Quantifying spatio-temporal dynamics of solar radiation exergy over turkey, Renewable Energy (2010) 2821–2828.

[7] K. Ranjan, S. Kaushik, N. Panwar, Energy and exergy analyses of solar ponds in the indian climatic conditions, Int. J. of Exergy 15 (2) (2014) 121–151.

[8] J. Gómez-Elvira, C. Armiens, L. Castaner, M. Domínguez, M. Genzer, F. Gómez, R. Haberle, A.-M. Harri, V. Jimenez, H. Kahanpää, L. Kowalski, A. Lepinette, J. Martínez-Frías, J. Martín, I. McEwan, L. Mora, J. Moreno, S. Navarro, M. de Pablo, V. Peinado, A. Pena, J. Polkko, M. Ramos, N. Renno, J. Ricart, M. Richardson, J. Rodríguez-Manfredi, J. Romeral, E. Sebastián, J. Serrano, M. de la Torre Juárez, J. Torres, F. Torrero, R. Urqui, T. Velasco, J. Verdasca, M.-P. Zorzano, F. J. Martín-Torres, REMS: an environmental sensor suite for the mars science laboratory rover, Space Science Reviews 170 (1-4) (2012) 583–640.

[9] B. Conrath, J. Pearl, M. Smith, W. Maguire, P. Christensen, S. Dason, M. Kaelberer, Mars global surveyor thermal emission spectrometer (tes) observations: Atmospheric temperatures during aerobraking and science phasing, J. Geophys. Res 105 (4) (2000) 9509–9515.

[10] P. R. Christensen, J. L. Bandfield, V. E. Hamilton, S. W. Ruff, H. H. Kieffer, T. N. Titus, M. C. Malin, R. V. Morris, M. D. Lane, R. L. Clark, B. M. Jakosky, M. T. Mellon, J. C. Pearl, B. J. Conrath, M. D. Smith, R. T. Clancy, R. O. Kuzmin, T. Roush, G. L. Mehall, N. Gorelick, K. Bender, K. Murray, S. Dason, E. Greene, S. Silverman, M. Greenfield, Mars global surveyor thermal emission spectrometer experiment: Investigation

description and surface science results, J. Geophys Res. Planets 106 (E10) (2001) 23823–23871.
[11] W. v. Sark, N. Reich, B. Muller, A. Armbruster, K. Kiefer, C. Reise, Review of pv performance ratio development, American Solar Energy Society, Boulder/Colo.: World Renewable Energy Forum, WREF 6 (2012) 4795–4800.
[12] R. Petela, Engineering Thermodynamics of Thermal Radiation: for Solar Power Utilization, 1st Edition, McGraw-Hill Professional, 2010.
[13] R. Petela, Exergy of heat radiation, J. Heat Transfer 86 (2) (1964) 187–192.
[14] W. Press, Theoretical maximum for energy from direct and diffuse sunlight, Nature 264 (1976) 735.
[15] J. Parrot, Theoretical upper limit to the conversion efficiency of solar energy, Solar Energy 21 (1978) 227.
[16] S. Jeter, Maximum conversion efficiency for the utilization of direct solar radiation, Solar Energy 26 (1981) 231–236.
[17] Y. Candau, On the exergy of radiation, Solar Energy 75 (2003) 241–247.
[18] A. Joshi, I. Dincer, B. Reddy, Development of new solar exergy maps, Int. J. of Energy Research 33 (8) (2009) 709–718.
[19] E. Skoplaki, A. Boudouvis, J. Palyvos, A simple correlation for the operating temperature of photovoltaic modules of arbitrary mounting, Solar Energy Materials and Solar Cells 92 (11) (2008) 1393–1402.
[20] J. H. Eckstein, Engineering Thermodynamics of Thermal Radiation: for Solar Power Utilization, 1st Edition, University of Wisconsin-Madison, 1990.
[21] A. Delgado-Bonal, F. Martín-Torres, Solar cell temperature on mars, Solar Energy 2015, in press.
[22] D. Rapp, Solar energy on mars, QSS Group, Inc. in affiliation with JPL JPL D-31342-Vol.1.
[23] P. Landsberg, G. Tongue, Thermodynamics of the conversion of diluted radiation, J. Phys.A: Math.Gen. 12 (1979) 551–562.
[24] J. B. Pollack, R. M. Haberle, J. Schaffer, H. Lee, Simulations of the general circulation of the martian atmosphere. polar processes., J. Geophys. Res. 95 (1990) 1447–1473.
[25] M. T. Lemmon, The Mars Science Laboratory optical depth record, Eighth International Conference on Mars.
[26] J. Gómez-Elvira, C. Armiens, I. Carrasco, M. Genzer, G. Gómez, R. Haberle, V. Hamilton, A.-M. Harri, K. Kahanpaa, O. Kemppinen, A. Lepinette, J. Martín-Soler, F. Martín-Torres, J. Martínez-Frias, M. Mischna, L. Mora, C. e. a. Newman, Curiosity's rover environmental monitoring station: The first 100 sols, J. Geo. Research: Planets 119 (7) (2014) 1680–1688.
[27] D. Reiss, A. Spiga, G. Erkeling, The horizontal motion of dust devils on mars derived from {CRISM} and ctx/hirise observations, Icarus 227 (0) (2014) 8 – 20.
[28] E. W. Golding, The Generation of Electricity by Wind Power, 1st Edition, E&F. N. Spon Ltd, London, England, 1955.
[29] T. Pedersen, S. Petersen, U. Paulsen, O. Fabian, B. Pedersen, P. Velk, M. Brink, J. Gjerding, S. Frandsen, J. Olesen, L. Budtz, M. Nielsen, H. Stiesdal, K. Petersen, P. Danwin, L. Danwin, P. Friis, Recommendation for wind turbine power curve measurements to be used for type approval of wind turbines in relation to technical requirements for type approval and certification of wind turbines in denmark, Danish Energy Agency September 1992 (1).
[30] S. Ahmet Duran, I. Dincer, M. Rosen, Thermodynamic analysis of wind energy, Int. J. Energy Res. 30 (2006) 553–566.
[31] F. Martín-Torres, et al., Transient liquid water and water activity at Gale crater on Mars, Nature 2015, in press.

9
Conclusiones

Aunque la empresa sea difícil, sin embargo, ayudado por los que me inducen a a cometerla, espero llevarla a punto de que a cualquier otro quede breve camino para realizarla por completo.

Nicolás Maquiavelo

Discursos sobre la primera década de Tito Livio.

La energía y la entropía son magnitudes termodinámicas que están íntimamente relacionadas con la evolución de la vida. Los seres vivos utilizan la energía en varias formas y maneras; la segunda ley de la termodinámica aparece de forma natural en la naturaleza, limitando las posibilidades de cambio y gobernando la evolución de los sistemas.

La vida apareció en la Tierra relativamente poco después de la formación del planeta. Durante las primeras etapas, la energía utilizada por los organismos vivos era química, lo que limitaba las posibilidades de expansión en el planeta. Una de las conclusiones de esta tesis en el **Capítulo 2** es que los seres vivos no fueron capaces de fijar el nitrógeno necesario para sobrevivir y necesitaban nitrógeno que se fijaba por procesos abióticos hasta la explosión del Cámbrico.

Más tarde, los organismos evolucionaron y fueron capaces de utilizar la radiación solar como fuente de energía a través de la fotosíntesis. Sin embargo, no toda la energía que llega a la superficie del planeta puede ser transformada en otras formas de energía. Durante el paso de la radiación a través de la atmósfera, el contenido de entropía aumenta y ello implica una disminución en la exergía, la máxima cantidad de energía útil para producir trabajo. Este cambio de entropía y exergía depende de la composición y la estructura atmosférica.

En el **Capítulo 3** he analizado el máximo rendimiento de la transformación de energía solar que se puede obtener a diferentes alturas dadas las actuales condiciones de la atmósfera de la Tierra, proporcionando un valor máximo para la eficiencia de los procesos fotosintéticos y células fotovoltaicas. En este capítulo concluyo que la eficiencia es menor que la calculada anteriormente y casi toda la disminución se produce en la troposfera, al contrario que en investigaciones anteriores.

Aparentemente, el planeta más cercano que podría ser adecuado para mantener vida es Marte, aunque el ambiente actual es duro y muy seco. Es poco probable que la vida está presente en la superficie pero podría encontrarse en el subsuelo, siendo por lo tanto no fotosintética y mantenida con energía química.

Al igual que en las primeras etapas de la vida en la Tierra, las fuentes de energía química en Marte hoy en día podrían ser un impedimento para la propagación de la vida en el planeta, si es que existe. En el **Capítulo 4** analizo el medio ambiente marciano actual y calculo la energía química útil, es decir, la energía libre de Gibbs que está presente en la capa atmosférica cercana a la superficie de Marte, y concluyo que hay suficiente energía disponible para mantener una biosfera.

Además de los requerimientos energéticos, se deben cumplir otros requisitos con el fin de mantener la vida en el planeta. Citando a Boltzmann, "la vida no es una lucha por energía ni por alimentos, sino más bien una lucha por entropía". En el **Capítulo 5** analizo el desequilibrio químico atmosférico de la atmósfera de Marte y concluyo que la cantidad de entropía química producida en la atmósfera es significativamente más baja que la entropía producida en la atmósfera de la Tierra. Si se necesita desequilibrio para crear estructuras emergentes auto-organizadas, llego a la conclusión de que Marte no puede soportar grandes estructuras como las que se encuentran en la Tierra.

La atmósfera marciana es extremadamente delgada en comparación con la atmósfera de la Tierra. Su química es mantenida por reacciones fotoquímicas, y esas reacciones dependen de la radiación que llega al planeta. Con el fin de conocer el campo de radiación en el rango de 10 a 420 nm (UV), en el **Capítulo 6** presento una base de datos de la irradiación solar para el ciclo solar 24 (2008-2019) que proporciona valores más exactos que los espectros genéricos utilizados hoy en día.

Debido a la baja densidad de la atmósfera de Marte, la radiación ultravioleta que llega a la superficie podría ser utilizada para producir energía solar utilizando células solares en el planeta. En general, el principal problema relacionado con el uso de la energía solar para la exploración del planeta es la baja eficiencia de la transformación. Con el fin de conocer la eficiencia de la transformación, he desarrollado las ecuaciones necesarias para determinar la temperatura de funcionamiento de una célula solar en Marte. En el **Capítulo**

7 proporciono una ecuación para determinar la temperatura de funcionamiento de una célula solar en Marte en función de la temperatura ambiente, el campo de radiación y la velocidad del viento. Esta ecuación se asemeja a la que se utiliza en la Tierra pero además incluye un término para tener en cuenta el efecto de la velocidad del viento.

Una vez que se conoce la temperatura de funcionamiento es posible determinar la eficiencia de la transformación y calcular la energía máxima obtenible a partir de la radiación solar en Marte. Utilizando esta metodología, denominada análisis del segundo principio, varios países de la Tierra han determinado las mejores ubicaciones para instalar paneles solares con la intención de maximizar la eficiencia transformación. En el **Capítulo 8** he desarrollado estos cálculos para Marte, proporcionando mapas de eficiencia que serán de utilidad para el futuro, en la exploración y colonización del planeta. La energía eólica podría ser otra fuente de energía en Marte por lo que en este capítulo analizo también esa posibilidad, y concluyo que la baja densidad de la atmósfera hace que su uso sea poco realista para la exploración del planeta.

9
Conclusions

And although the undertaking is difficult, yet, aided by those who have encouraged me in this attempt, I hope to carry it sufficiently far, so that but little may remain for others to carry it to its destined end.

Niccolo Machiavelli
Discourses on Livy.

Energy and entropy are thermodynamic magnitudes that are intimately related to the evolution of life. While living beings use energy in several forms and ways, the second law of thermodynamics appears naturally in nature, constraining the possibilities of change and governing the evolution of the systems.

Life appeared on Earth relatively soon after the formation of the planet. During the first stages, the energy used by living organisms was chemical. This limited the possibilities of expansion in the planet. One of the conclusions of this thesis in **Chapter 2** is that living beings were not able to fix the required nitrogen to survive and they needed nitrogen that was fixed by abiotic processes until the Cambrian explosion.

Later, organisms evolved and were able to use the solar radiation as a source of energy though photosynthesis. However, not all the energy that reaches the surface of the planet is available to be transformed into other forms of energy. During the passage of radiation through the atmosphere, the entropy content increases leading to a decrease in the exergy, the maximum amount of energy useful to produce work. This entropy and exergy change depends on the atmospheric composition and structure.

In **Chapter 3** I have analysed the maximum obtainable solar energy for the current conditions of the atmosphere of the Earth at different heights, providing a maximum value for the efficiency of photosynthetic processes and solar cells. I conclude that the efficiency is smaller than previously calculated and almost all the decrease occurs in the troposphere, in disagreement with previous investigations.

Apparently, the closest planet that could host life is Mars, although the current environment is harsh and dry. It is unlikely that life is present on the surface but it could be present in the subsurface, being therefore not photosynthetic but maintained with chemical energy. In **Chapter 4** I analyse the current martian environment and calculate the useful chemical energy, i.e., the Gibbs free energy that is present in the near-surface layer of the atmosphere

on Mars, and conclude that there is enough available energy to maintain a biosphere.

Besides the energetic requirements, other requirements must be fulfilled in order to maintain life in the planet. Quoting Boltzmann, "life is not a struggle for energy or food but rather for entropy". In **Chapter 5** I analyse the atmospheric chemical disequilibrium of the atmosphere of Mars concluding that the amount of chemical entropy produced in the atmosphere is significantly lower than the entropy produced in the atmosphere of the Earth. If disequilibrium is needed to create self-organized emergent structures, I conclude that Mars cannot support big structures as those found on Earth.

The martian atmosphere is extremely thin when compared with the Earth's atmosphere. Its chemistry is driven by photochemical reactions, and they depend on the radiation field reaching the atmosphere. In order to know this radiation field in the 10 to 420 nm range (UV), in **Chapter 6** I present a database of the irradiance for solar cycle 24 (years 2008 - 2019) and prove that it provides more accurate values than the generic spectra nowadays used generic spectra.

Due to the low dense atmosphere of Mars, the ultraviolet radiation that reaches the surface could be used to produce solar energy using solar cells in the planet. In general, the main problem related to the use of solar energy for the exploration of the planet is the low efficiency of the transformation.

In order to know the efficiency of the transformation, I have developed the equations to determine the operating temperature of a standalone solar cell on Mars. In **Chapter 7** I provide an equation to determine the operating temperature of a solar cell on Mars as a function of the ambient temperature, the radiation field and the velocity of the wind. This equation resembles the one that is being used on Earth but includes a term accounting for the wind speed on the planet.

Once the operating temperature is known, it is possible to determine the efficiency of the transformation and calculate the maximum obtainable energy

from solar radiation in the present day Mars. Using this methodology, called second law analysis, several countries on Earth have determined the best locations to install solar panels with the intention to maximize the efficiency of the transformation. In **Chapter 8** I have developed such calculations for the martian environment providing efficiency maps that will be useful for future designs in the exploration and colonization of the planet. Wind energy could be another source of energy on Mars. In this chapter I analyse that possibility as well and conclude that the low density of the atmosphere makes its use unrealistic for Mars exploration.